The Bioenergetics of a Low-power, Phenazine-dependent Maintenance Metabolism in *Pseudomonas aeruginosa*

Thesis by

John Alan Ciemniecki

In Partial Fulfillment of the Requirements for

the degree of

Doctor of Philosophy in Microbiology

CALIFORNIA INSTITUTE OF TECHNOLOGY

Pasadena, California

2024

(Defended March 7th, 2024)

John Alan Ciemniecki
ORCID: 0000-0003-2789-6700

ACKNOWLEDGEMENTS

While I have some suspicions, I cannot remember exactly who first told me that “Caltech is like a monastery to Science.” While that designation could be a turn-off for some, when I heard it for the first time the equivalence was exciting—it evoked images of monk-like devotion to shedding light on the deep mysteries of the universe and life, and the reputation of Caltech made me believe that I, by association, may one day be involved in the grand illumination. Clearly, I had a very romanticized view of science prior to graduate school. Anyone who has been through the challenge will tell you that the journey of graduate school is truly about the journey just as much as the discoveries. I expected intellectual development, I expected good science, but as I look back, the most staggering growth to me is the expansive amount of personal development I have undergone during my time in Pasadena. Part of that has arisen organically from me struggling and then falling in love with the most difficult intellectual work I’ve ever faced, but a much, much larger part has come from the people who have mentored, helped, and accompanied me along the way. It seems only right to acknowledge their contribution to my development, the true grand product of this PhD.

To my family on the East Coast, and now Midwest: Dad, Mom, Lauren, Rick, and Marie, thank you for your support, understanding, and love through it all; it was the strong foundation I needed to grow, even from afar. You already know how excited I am that the next phase of my life will be back east.

To the bio-crew including Lev Tsypin, Aditi Narayanan, Tom Naragon, Julian Wagner, and David Miller, thank you for being such a kind and supportive friend group throughout graduate school, but especially in the beginning when we were frantically working on classwork and hadn’t settled into permanent labs. Having you guys around made that time much easier, as well as fun and adventurous. We went on trips, published a podcast together, and had movie nights that forever improved my taste in cinema. I will appreciate and savor Scotch for the rest of my life because of our tasting club, especially because of the unforgettable drams we shared stuffed under a table during one of the larger earthquakes of Summer 2019. Thank you all for everything.

To Tomás Aquino for being the best roommate I’ve ever had, for being a wise peer a few years ahead of me with useful insights into the grad school process and life, and for teaching me all the Portuguese I ever really need to know, thank you. It is so rare to meet people with such similar types of intellectually curiosity, and somehow, we not only met but became roommates even before we understood how much we had in common. Our late-night philosophy chats spanning science, politics, art, music, and love were one of the highlights of my time here, and I look forward to more.

To my local Pasadena friend and mentor Jon Pedersen, for teaching me how to see myself more clearly, for introducing me to the fascinating study of the human mind and spirit, and for instilling in me the tools necessary to be my best and whole self, thank you. You taught me the fine art of how to balance life with work in such a way as to love both sustainably, and what I have learned through your mentorship is undoubtedly even more important to my personal life than the PhD. Nonetheless, I’m certain it has enhanced my thesis is countless, nameless ways.

To Rob Phillips and Justin Bois, who together probably set the gold standard for quantitative biology education and do it all selflessly and tirelessly for their students, thank you so much. You give us Biology students the true “Caltech Experience”. You are both role models to me and as you know you have strongly influenced my scientific style. Because of you, I will always bring a pen to meals with colleagues; in lieu of envelopes, there are always napkins.

To Aki Okamoto and Tracy Ho, for providing me and the Newman lab with the tools, collaboration, and guidance necessary to do some of the most interesting measurements of my PhD. Your instrumentation and expertise helped me achieve my dream of measuring the minimum energy required for survival and thereby enabled the most important results of my work. Thank you for your generosity and friendship.

To Vamsi Mootha, for teaching me how to work Clark electrodes, get some last-minute data that helped support my short-circuiting theory, and generously spending your valuable time troubleshooting in the lab with us over some long afternoons, with mitochondrial stories in between sets of experiments—it was a lot of fun.

To the Newman Lab members who have overlapped with me, each of you is part of my intellectual family, and as they say, it takes a village. Thank you for your thoughtfulness, generosity, your very constructive feedback over the years, and for generally just being a fun group of people to hang out with. There are people in the group that deserve special mention, in no specific order:

To Lev Tsypin, my brother through all of this from the time we met as randomly-assigned roommates during Caltech's recruitment weekend, to the time we both joined the Newman Lab and shared a bay there as we got our footing—you are an indelible part of my intellectual journey. Your encyclopedic biological knowledge coupled with your heart and goofy sense of humor make you an unforgettable and generous friend. I hope that I brought as much joy to your journey as you did to mine.

To Megan Bergkessel, Lisa Racki, and David Basta for inspiring me to join you all in the investigation of non- and slow-growth physiology and guiding me to carve out my own niche within it. Your open and friendly discussions on the topic were part of what convinced me to join the Newman Lab, and for that I am very grateful.

To Lucas Meirelles, for connecting me with Tomás and for your mentorship and advice as I navigated the awkward middle-stages of graduate school, you have lent a hand and ear whenever you could for me and we naturally became friends because of it. Your smile was infectious both in the lab and outside of it, thank you for modeling how to stay focused and happy amidst a pandemic that was a struggle for all of us.

To Darcy McRose and Avi Flamholz, for your incisive engagement during lab meetings that improved my science and inspired my own lab meeting engagement style down the road, and for your sincere and kind appreciation of my work.

To Kurt Dahlstrom, for your very early friendship when I began my rotation in the lab that has continued through to today, and for introducing me to and making me the best Maple Manhattans ever.

To Mel Spero, for your friendly warmth, down-to-earth advice, for engaging with me over my hobby of niche perfumery, and most importantly, thank you for matching my dark sense of humor and making me feel at home by doing so.

To Ranjani Murali and Inês Trindade, for kindly sharing your expertise, ideas, and encouragement when I began working on *gasp* membrane proteins and the oxidant pulse assay.

To Roxy Shafiee, my friend from across the pond, thank you for being the friend I needed during the middle of the PhD while still coming out of the pandemic doldrums. You were always the one willing to throw a party, get a drink, ask the deep questions, think differently and independently, and spill some tea. Your time here made my time so much more fun.

To Steven Wilbert, for convincing me to apply to Caltech! It still baffles me how we met beforehand and then ended up joining the same graduate school *and* lab; I guess I have only you to blame! But after all that, thank you so much for teaching me the value of collaboration, how two people with different interests and ways of thinking about a problem can solve it in half the time or less. It was a blast working with you and I hope I get to again someday. Also, thank you for teaching me how to properly care for and maintain beautiful houseplants.

To Rei Alcalde, thank you for being the perfect bay-mate. I know my obnoxious desk chair is annoying but you never complained once, and instead for some reason blessed me with friendship and good conversation. I have great memories of jerry-rigging contraptions together with you to solve some issue or other in the lab, and we (almost) always made it work. Our science is very different but that didn't stop you from having multiple constructive thoughts for me, and I hope mine were at least half as valuable to you.

To Georgia Squyres and Sean Wilson, for introducing me to games that have given me hours of relaxation and the taco truck that has fueled many days in the lab, for openly and critically discussing issues with the academic system, for helping me multiple times with careful experimental design and data analysis, and most of all for generally making me feel appreciated in the lab. I know I returned the favor because Georgia told me how much she felt appreciated by me about once a quarter, which is just one example of the way you two have a considerate way of making everyone you work with feel special.

To Korbi Thalhammer, Richard Horak, and Elin Larsson, my students in microbial metabolism then labmates then friends and collaborators, thank you for helping me to find my footing teaching in class and for placing your trust in me to continue to teach you afterwards. Every scholarly question you came to me with was a compliment, and by the end I was coming to you with questions! You all brought a playfulness to the lab that was sorely lacking after the pandemic, and I have had more laughs with you during work than anyone else. Thank you also for including me in trips and events during the tail end of my time—the thoughtfulness behind each invitation wasn't taken for granted.

And the two people who deserve the most credit:

To Dianne Newman, for taking a risk on me given I had zero microbiology background before graduate school, for continually believing in me even when I didn't, for giving me opportunities left and right to shine and advance my career, for wisely guiding me to the right questions and the right projects at the right time, for encouraging my leadership in the lab when I was hesitant, and most importantly, for knowing precisely when to give me intellectual control and when to give me guiderails, you have more than anyone else nurtured my growth in science. I was a paradox of both overconfidence and insecurity when I began the PhD and everything you did as my mentor helped to gently temper both down into a burgeoning self-reliance. While any professor could have taught me science, I doubt many could have done all that you did for me in terms of mentorship; I am so unbelievably lucky to have been your mentee. By having me TA your class you helped me discover my passion for bioenergetics and, being one of your passions as well, it opened the door to us having

a lot of fun together over the years. I will never forget the thrill of formulating the bc_1 hypothesis and pursuing it with your guidance, and what a beautifully humbling scientific experience it was to falsify. Many more thrilling hypotheses arose from our conversations and private reflections, and many of them thankfully bore sweeter fruit. Through it all you let me be myself and lead my project with an independence that I never took for granted, because it gave me an ownership that I hadn't experienced before that embedded *me* into my work. The ultimate result of everything you did is that by the end my science blossomed into a form of self-expression, which I think is the greatest gift any mentor can bestow.

And finally, to Chelsey VanDrisse: what can I say? You are, simply, the best match I could ever ask for. Your contributions to my life pile excessively outside the scope of this acknowledgement section. That we specifically found each other while I was in the middle of the PhD was to my great fortune for multiple reasons. You helped me to realize that I wanted to study molecular physiology early on while my interests were still opaque to me. You helped me to see and let go of my paralyzing perfectionism (most of it, anyway). You taught me that it was ok to ask for a lot of help and sometimes even beneficial to those you ask. You questioned the prevailing models in the lab and thereby influenced my lines of inquiry and expanded my perspective. You taught me everything I know about cloning and shared with me all your "lazy lab tricks" (which I will continually insist are in fact clever tricks). Perhaps the wisest thing you ever shared with me during the PhD was the line that became my mantra: *Trust in the process.* And beyond all of that, thank you for the absorbing late-night chats about both of our science (even though they cost you some sleep). While I could go on, suffice it to say: Thank you for being my best friend, you made the difficult parts of the PhD tolerable and the happy parts euphoric. I love you, and I would not be where I am today without you.

And now that the work is contextualized by the people who contributed, on to it…

ABSTRACT

A common feature of all life is the metabolic transformation of energy from the environment to biochemical energy in the organism. While this process is well-characterized in molecular detail for fast-growing or otherwise fast-metabolizing organisms such as humans, many microorganisms subsist in the environment around us with little to no exogenous energy for extended periods, and we have only vague ideas how. Questions about the metabolic mechanisms and rates underpinning these astounding survival capabilities speak to the fundamental question of the lower energetic limits of life. Motivated by this big-picture question in biology, this thesis represents one line of physiological inquiry into a specific anaerobic survival metabolism of *Pseudomonas aeruginosa*, an opportunistic bacterial pathogen. *Pseudomonas* is perhaps best known for its characteristic production of colorful, redox-active, secondary metabolites called phenazines that allow a metabolic process called extracellular electron transfer. Phenazine extracellular electron transfer has been previously shown to unlock a slow, anaerobic glucose catabolism that facilitates the survival of energy-limited populations of cells. My thesis work has elucidated the predominant membrane-bound protein complexes involved in phenazine reduction and the predominant subcellular location of reduction for each of the main phenazines produced by *Pseudomonas*. I show that the survival metabolism powered by these phenazines places them in a true maintenance state where there is no detectable growth in the population at the single-cell level. The metabolic rate of this maintenance was measured and found to be 1,000 times slower than when the cells are growing in aerobic culture, 100 times slower than estimates of maintenance rates made in continuous culture, and 10 times slower than the mean basal metabolic rate estimated across all life on the planet. These results open the door to investigations of metabolic attenuation, a physiological state that underpins microbial survival in nature and disease. In pursuit of these discoveries, various new experimental assays that allow further investigation into the bioenergetics and biochemistry of phenazine metabolism were developed. Finally, intellectual frameworks are presented that, in conjunction with the discoveries made and methods developed, collectively bring us steps closer to understanding the bioenergetic basis of microbial resiliency.

PUBLISHED CONTENT AND CONTRIBUTIONS

Ciemniecki JA, Ho CL, Okimoto A, Newman DK. 2024. *Anaerobic phenazine cycling powers* Pseudomonas aeruginosa *maintenance at extremely low metabolic rates.* In prep.

J.A.C. contributed to the conceptualization and carried out the experiments, data analysis, and manuscript preparation. This work was adapted into Chapter 5.

Horak R, **Ciemniecki JA**, Newman DK. 2024. *Bioenergetic suppression by redox-active toxins promotes antibiotic tolerance in* Pseudomonas aeruginosa*.* In prep.

J.A.C. designed and carried out experiments and analyzed data regarding redox-active metabolite inhibition of respiratory H^+ translocation. This assay and the results are detailed in Chapter 4.

Ciemniecki JA, Newman DK. 2023. *NADH dehydrogenases are the predominant phenazine reductases in the electron transport chain of* Pseudomonas aeruginosa*,* Mol Microbiol. *119*(5), 560-73. DOI: 10.1111/mmi.15049.

J.A.C. contributed to the conceptualization and carried out the experiments, data analysis, and manuscript preparation. This work was adapted into Chapter 3.

Ciemniecki JA, Newman DK. 2020. *The Potential for Redox-Active Metabolites To Enhance or Unlock Anaerobic Survival Metabolisms in Aerobes.* J Bact. *202*(11), e00797-19. DOI: 10.1128/JB.00797-19.

J.A.C. contributed to the conceptualization, performed all literature review, and prepared the manuscript. This work was adapted into Chapter 2.

TABLE OF CONTENTS

LIST OF FIGURES

UNCOMMON NOMENCLATURE USED

Δ***phz1/2***. A mutant of *Pseudomonas aeruginosa* strain PA14 that has clean-deletions of both phenazine biosynthesis gene clusters, *phzA1-G1* and *phzA2-G2*. As a result, the strain cannot synthesize phenazines and is therefore useful for phenazine-based experiments.

Extracellular electron shuttle (EES). A soluble, redox-active molecule that can accept reducing equivalents from a cell and transfer them to a distal oxidant via diffusion or electron-hopping.

Extracellular electron transfer (EET). The process of transferring electrons from intracellular reducing equivalents to an extracellular oxidant. This can be achieved via direct physical contact with the extracellular oxidant, use of an EES, or the production of proteinaceous, conductive filaments called "nanowires" that connect cells and oxidant.

Facilitated fermentation. A hybrid form of metabolism that conserves energy via substrate-level phosphorylation and generates organic acid byproducts like a fermentation, but that uses an exogenous oxidant (e.g. an EES) to achieve redox-balance, like a respiration.

Pyocyanin (PYO) / phenazine-1-carboxamide (PCN) / phenazine-1-carboxylic acid (PCA). The predominant phenazine derivatives secreted by *Pseudomonas aeruginosa* strain PA14. Each is an EES that can promote EET via redox-cycling and power a facilitated fermentation. Their chemical structures can be found in Chapter 3, Figure 1: Schematic of *P. aeruginosa* phenazine biosynthesis and electron transport chain.

Metabolic attenuation. Alternative nomenclature to describe what is commonly referred to in microbiological literature as dormancy, or a state of reduced metabolic activity. Metabolic attenuation is preferred because it clearly implies continued metabolic activity (which thermodynamically must occur for the cell to remain viable) that is otherwise ambiguous in the term dormant.

Redox-active secondary metabolite (RAM). Redox-active small molecules produced and secreted after rapid cell growth has ceased. They may or may not function as extracellular electron shuttles.

Redox-cycling. When an EES's redox state is fully reversible and the molecule is thereby used multiple times (recycled) by the cell during EET.

Slow growth. The physiological state associated with growth that is significantly slower than typically observed in the lab (i.e. in rich medium) and that approaches estimated doubling times in nature of a few days to years. It is sometimes also used loosely to describe states of non-growth.

C h a p t e r 1

PREFACE AND OUTLINE

Any philosophically inclined student of biology will eventually come to wonder, what is life? The answer (1) is that life is a reproducing, out-of-equilibrium system powered by the transformation of energy from the environment into order within an organism. But taken one step further, one comes to ask: what is life's lower power limit? If the conditions are defined, is there a threshold below which even the simplest of cells lose their viability?

This is the broad biological curiosity that drove this thesis. What became clear over time is that beyond curiosity, understanding the minimal energy requirements and physiology of cells in a non- or slow-growth state is a highly practical pursuit. This is evident because in natural systems, microbes rarely double anywhere near the rates commonly elicited in the lab. Modern methods using stable isotopes estimate that soil microbe doubling times *in situ* range anywhere from a few days to a few years (2–4). In the ocean water column, heterotrophic bacteria are estimated to double at an average rate of once every 13 days, and even more slowly in many regions (5). Meanwhile, most microbial physiology studies in pure culture have been conducted using model species grown with doubling times under an hour. The consequences of this lab-to-nature growth rate mismatch is manifested in multiple fields of study. In the clinic, we struggle to eradicate slow- or non-growing subpopulations of pathogens (6). Bioengineers have no clear way to design microbes that catalyze desirable changes in natural settings long-term (7,8). Perhaps most pressing, climate scientists' predictions of the net contribution of microbial metabolism to the global carbon cycle

struggles to produce well constrained values, in part because environmental rates of metabolism are not well constrained (9). In all such applications, a basic understanding of metabolism and physiology "in the slow lane" is needed (10).

Toward this end, over a decade ago the Newman lab discovered that the redox-cycling of phenazine secondary metabolites (metabolites made *after* growth as opposed to during it) could help cells achieve redox homeostasis and stabilize survival when oxygen was limited or absent (11,12). Later, it was found that this phenazine-enhanced survival was due to an "unlocking" of a substrate-level phosphorylation pathway that became redox-balanced only during active phenazine redox-cycling (13). This was a consequential discovery because it is a rare instance of a tractable, pure-culture system where the consequences of energy conservation were demonstrable and *not* tied to growth of the cell population. It appeared it might be a dedicated maintenance metabolism, an alternative to the species' growth metabolism. My thesis is the direct continuation of investigations into this unique mode of energy conservation and survival.

In Chapter 2, I introduce the field of microbial slow growth and survival, explain the specific challenges aerobes like *P. aeruginosa* face in anoxic environments, and provide a detailed analysis of what we understood about the phenazine-dependent anaerobic survival metabolism in *P. aeruginosa* prior to my thesis work. One of the key questions to come out of this analysis was which enzymes are the predominant phenazine reductases necessary to power anaerobic survival?

Chapter 3 details a joint biochemical and genetic study I carried out to answer where and how phenazine reduction occurs. I show that within the isolated electron transport chain of *P. aeruginosa* the NADH dehydrogenases Nuo and Nqr couple phenazine reduction to

NADH oxidation, the key redox-balancing step of the metabolism powering anaerobic survival. I confirm that in whole cells the reduction of phenazine-1-carboxamide (the phenazine made in the highest quantity by *P. aeruginosa* biofilms) is strongly attenuated by knocking out these enzymes.

The NADH dehydrogenases Nuo and Nqr, during their normal aerobic function, couple the oxidation of NADH to the pumping of protons across the membrane to contribute to a chemiosmotic gradient. Chapter 4 details studies made to determine how the presence of phenazines affects this normal bioenergetic coupling. Using a classic oxidant pulse assay, I show that all phenazines lower the H^+/O ratio to varying degrees correlating with their reduction rate. Respirometry studies revealed phenazines shuttle electrons to oxygen even when the electron transport chain is blocked by azide. I present a new concept called metabolic short-circuiting as a model to explain these observations.

Returning to anaerobic survival conditions, in Chapter 5, I show that the NADH dehydrogenases Nuo and Nqr are required for the full anaerobic survival of *P. aeruginosa* while redox-cycling phenazine-1-carboxamide, confirming their involvement in the metabolism of interest. I go on to show that this survival has an extremely low metabolic rate of 1.6×10^3 electrons sec^{-1} $cell^{-1}$, about 1,000 times slower than when *P. aeruginosa* is growing aerobically and 10 times slower than the average basal metabolic rate across all life on the planet. Using a 96-well plate potentiostat developed by the Okimoto lab from NIMS in Japan, I confirm this metabolism is energy-limited by the amount of phenazine reduced and that cells are surviving near their minimum maintenance power requirement. This work constitutes, to my knowledge, the first direct measurement of a bacterial maintenance

metabolic rate in the lab and corresponds to an ATP production rate of about 800 ATP sec^{-1} $cell^{-1}$, around 100 times lower than estimates made in chemostat systems.

In Chapter 6, I briefly summarize the conclusions of this thesis and discuss the future directions I foresee being fruitful continuations. There were many observations that I made during the completion of this work that resulted in the formulation of new, unproven principles and hypotheses—my thoughts on these and other open questions are explained.

Along with the many scientists that I interacted with who helped me during the progress of this work, there were many I could not meet who nonetheless helped me through their writing. I share two of these people below, in their own words, and hope that I may write in a way that approaches their clarity, candidness, and passion.

> *"For me, encountering the bacterial growth curve was a transforming experience. As my partner and I took samples of the culture at intervals to measure optical density and plotted the results on semilogarithmic paper, we saw, after the lag period, a straight line developing…beautiful in precision and remarkable in speed. As the line extended itself straight-edge true, I imagined what was happening in the flask—living protoplasm being made from glucose and salts as the initial cells… grew and divided. The liquid in the flask progressed from having a barely discernible haze to a milky whiteness thick with the stuff of life, all within a very brief Boston winter afternoon. Mutably specific autocatalysis, the physicist Erwin Schrödinger had declared a few years earlier, was the defining characteristic of living systems, and I had just witnessed [it]."*
>
> - Frederick C. Neidhardt, Ph.D. (14)

> *"Envisage a steady flux of energy through the metabolic web, coupled to that of matter, … a device for generating dynamic order at the molecular level. What is it about all these reactions, which seem ordinary enough from the chemical viewpoint, that endows them with the mystical quality of generating order? … This capacity ultimately stems from the enzymes … refined by millennia of mutation and selection for a fitter organism. In the last analysis, the meaning of metabolic work lies in the production of a particular constellation of complex molecules, a unique order that is assigned by the historical forces that have shaped the organism as a whole."*
>
> - Franklin M. Harold, Ph.D. (15)

References

1. Schrödinger E. What Is Life? The Physical Aspect of the Living Cell. Dublin Institute for Advanced Studies, Dublin; 1944.

2. Blazewicz SJ, Hungate BA, Koch BJ, Nuccio EE, Morrissey E, Brodie EL, et al. Taxon-specific microbial growth and mortality patterns reveal distinct temporal population responses to rewetting in a California grassland soil. ISME J. 2020 Jun;14(6):1520–32.

3. Caro TA, McFarlin J, Jech S, Fierer N, Kopf S. Hydrogen stable isotope probing of lipids demonstrates slow rates of microbial growth in soil. Proc Natl Acad Sci USA. 2023 Apr 18;120(16):e2211625120.

4. Coskun ÖK, Özen V, Wankel SD, Orsi WD. Quantifying population-specific growth in benthic bacterial communities under low oxygen using H218O. ISME J. 2019 Jun;13(6):1546–59.

5. Kirchman DL. Growth rates of microbes in the oceans. Ann Rev Mar Sci. 2016;8:285–309.

6. Balaban NQ, Helaine S, Lewis K, Ackermann M, Aldridge B, Andersson DI, et al. Definitions and guidelines for research on antibiotic persistence. Nat Rev Microbiol. 2019 Jul;17(7):441–8.

7. Boo A, Ellis T, Stan G-B. Host-Aware Synthetic Biology. Current Opinion in Systems Biology. 2019 Mar;14:66–72.

8. Jones EM, Marken JP, Silver PA. Synthetic microbiology in sustainability applications. Nat Rev Microbiol. 2024 Jan 22;

9. Shi Z, Crowell S, Luo Y, Moore B. Model structures amplify uncertainty in predicted soil carbon responses to climate change. Nat Commun. 2018 Jun 4;9(1):2171.

10. Walker RM, Sanabria VC, Youk H. Microbial life in slow and stopped lanes. Trends Microbiol. 2023 Dec 19;

11. Price-Whelan A, Dietrich LEP, Newman DK. Pyocyanin alters redox homeostasis and carbon flux through central metabolic pathways in *Pseudomonas aeruginosa* PA14. J Bacteriol. 2007 Sep;189(17):6372–81.

12. Wang Y, Kern SE, Newman DK. Endogenous phenazine antibiotics promote anaerobic survival of *Pseudomonas aeruginosa* via extracellular electron transfer. J Bacteriol. 2010 Jan;192(1):365–9.

13. Glasser NR, Kern SE, Newman DK. Phenazine redox cycling enhances anaerobic survival in *Pseudomonas aeruginosa* by facilitating generation of ATP and a proton-motive force. Mol Microbiol. 2014 Apr;92(2):399–412.

14. Neidhardt FC. Bacterial growth: constant obsession with dN/dt. J Bacteriol. 1999 Dec;181(24):7405–8.

15. Harold FM. The Metabolic Web. The Vital Force: A Study of Bioenergetics. W.H. Freeman and Company; 1986.

C h a p t e r 2

INTRODUCTION - THE POTENTIAL FOR REDOX-ACTIVE METABOLITES TO ENHANCE OR UNLOCK ANAEROBIC SURVIVAL METABOLISMS IN AEROBES

Abstract

Classifying microorganisms as "obligate" aerobes has colloquially implied death without air, leading to the erroneous assumption that without oxygen they are unable to survive. However, over the past few decades, more than a few obligate aerobes have been found to possess anaerobic energy conservation strategies that sustain metabolic activity in the absence of growth or at very slow growth rates. Similarly, studies emphasizing the aerobic prowess of certain facultative aerobes have sometimes led to under-recognition of their anaerobic capabilities. Yet an inescapable consequence of the affinity both obligate and facultative aerobes have for oxygen is that the metabolism of these organisms may drive this substrate to scarcity, making anoxic survival an essential skill. To illustrate this, we highlight the importance of anaerobic survival strategies for *Pseudomonas aeruginosa* and *Streptomyces coelicolor,* representative facultative and obligate aerobes, respectively. Included amongst these strategies we describe a role for redox-active secondary metabolites (RAMs), such as phenazines made by *P. aeruginosa*, in enhancing substrate-level phosphorylation. Importantly, RAMs are made by diverse bacteria, often during stationary phase in the absence of oxygen, and can sustain anoxic survival. We present a hypothesis for how RAMs may enhance or even unlock energy conservation pathways that facilitate the anaerobic survival of both RAM-producers and non-producers.

The human heart pumps approximately three and a half trillion times in the average lifetime. It has evolved to pump dependably, one after the other, because the consistent flow of blood throughout the body is necessary to sustain a human life. Bacteria don't contain a circulatory system, per se. However, like the flow of blood, all cells maintain a flow of electrons through their metabolic pathways and a flow of ions across their membrane to remain alive. Without a redox-balanced cytosol, ATP generation coupled to electron-transfer reactions becomes stalled along with biosynthesis, and without an electrochemical potential at the membrane, the cell can neither power its flagella(1, 2) nor transport nutrients into and waste out of the cytosol(3). Failure to uphold these physiological requirements results in rapid loss of viability in a population as cell after cell struggles to conserve the energy needed to stay alive.

What does being labeled an aerobe imply? Bacteria classified as "obligate" aerobes are defined by their lack of growth in the absence of oxygen. It is important to note that this does not necessarily mean the cells die in the absence of oxygen: indeed, anaerobic survival mechanisms in obligate aerobes are known, though they are understudied relative to their likely relevance in the wild. To survive anoxia, these aerobes are faced with a metabolic dilemma: they must maintain redox balance and the proton motive force (PMF) despite interrupted flux through the electron transport chain (ETC) due to the absence of oxygen. While facultative aerobes are well understood to be able to conserve energy and even grow rapidly in the absence of oxygen, either through the use of alternative electron acceptors or fermentation, aerobic respiration is commonly viewed as their preferred metabolic mode. We contend, however, that this presumed physiological bias may better reflect what fosters fast growth in the laboratory rather than what promotes fitness in nature. The ability to efficiently

survive until nutrients return is essential for any microbe's evolutionary success, and in many natural scenarios may be even more important than growth.

The bioenergetic basis of bacterial survival strategies in the real world is poorly understood. Key to gaining relevant physiological insights is to couple microenvironmental characterization with the design of reductionist laboratory experiments that bear fidelity to those conditions. It is well appreciated that a major form of bacterial life in the wild is within slowly growing biofilms(4) and that cells in the interior of these biofilms are often oxygen-limited because oxygen consumption outpaces its diffusion inwards(5). Yet these cells are very much alive: they are not only able to maintain their viability, but also to mount transcriptional responses(6) and to produce a steady stream of new proteins(7). Furthermore, for any microorganism living in the soil, periods of rainfall are a common stressor because wetted soil quickly becomes depleted in oxygen(8), and even in the human body, counterintuitively, aerobes that infect the lung often become embedded in mucus that is largely hypoxic or anoxic(9, 10). Therefore, researching anaerobic metabolisms in aerobes is to work towards understanding an aspect of bacterial physiology that is important in nature.

Anaerobic metabolisms within the facultative aerobic genera *Pseudomonas*(11) and *Bacillus*(12), and the obligate aerobic genera *Arthrobacter*(13, 14), *Azotobacter*(15), *Streptomyces*(16), and *Mycobacteria*(17, 18) have been studied in some detail; in this review, we will discuss *Pseudomonas aeruginosa* and *Streptomyces coelicolor* as illustrative examples. Even though streptomycetes undergo a spore stage in their lifecycle, we focus our review only on the survival mechanisms of vegetative cells. While *P. aeruginosa* is still sometimes described as an obligate aerobe, it has long been known to be a facultative aerobe capable of denitrification (i.e., utilizing nitrate rather than oxygen as the terminal electron

acceptor for respiration)(19–21). *P. aeruginosa* also grows anaerobically via arginine fermentation(22) and can survive anaerobically via pyruvate fermentation(11); interestingly, anaerobic survival powered by substrate-level phosphorylation can also be achieved by the reduction of self-produced extracellular electron shuttles called phenazines(23). We end this review by discussing the potential for functionally similar redox-active metabolites (RAMs) made by other aerobes to also promote anaerobic survival. Such multi-species use of these secondary metabolites for energy conservation would raise exciting, new interpretations of their producers' impact on microbial communities in soil, infection, and even industrial fermentation settings.

The Relevance of Energy-Limited Survival

While many things can limit bacterial growth, from nutrient scarcity to chemical warfare to predation, from a catabolic perspective, electron donor (*e.g.* carbon) and electron acceptor (*e.g.* oxygen) limitation are the most obvious drivers of energy-stress for heterotrophic aerobes and have been the best studied. There are significant differences in how the cell handles oxygen- and carbon-limitation(24), but they both diminish flux through the ETC by halting the flow of electrons in or out. This lack of flux can threaten survival by interrupting the PMF, ATP synthesis, and cellular redox-balancing systems. Given the paucity of mechanistic research on survival physiology (though this is beginning to be rectified(6, 24, 25)), as a point of departure for our discussion of how oxygen-limitation may be overcome via unconventional catabolic pathways, we first remind the reader of the broader challenges that must be solved by cells that are energy-limited and the ecological relevance of this state.

Irrespective of how energy-limitation is imposed in the lab, a cell that is so challenged must transition from a conventional stationary state to a distinct starvation-survival state, involving a (sometimes dramatic) decrease in cell size(26, 27) often accompanied by sustained changes in lipid content(26, 28), the proteome(26, 29), and the transcriptome(4, 26). Interestingly, the transition from growth into the starvation-survival state seems to require proteolysis(30, 31), presumably to supply the amino acids needed to produce new proteins. This physiological state describes the vast majority of microbes in nature(4, 32, 33), as most bacterial environments are oligotrophic or energy-limited(32). The amount of dissolved organic carbon in soil varies but is estimated to be quite low: as an example, one comprehensive study in the United Kingdom estimated it to range between 1 and 100 mg L^{-1}(34). In fact, the methods used to measure dissolved organic carbon likely release labile carbon from complexes, and therefore the actual bioavailable carbon is probably even lower(32). Nonetheless, isotope tracing experiments made with *Vibrio* environmental isolates demonstrate rapid consumption of labile glutamate added in picomolar concentrations (10^{-12}, the lower detection limit of the method) confirming that microbial carbon consumption can capture exceedingly dilute substrates(35).

These studies and others(32, 33) strongly suggest two things: 1) environments are kept energy-limited by the microbes that inhabit them and 2) nutrient flux and bacterial growth in the wild is quite low relative to growth in the lab. Given natural environmental variability, a cell can be induced into a growth-arrested state for many reasons, and it is often challenging (if not impossible) to know which particular limitation or stress is responsible for growth arrest at any given time. Regardless, division frequency estimates within environmental samples predict soil heterotrophs replicate between less than 1 to 36 times per

year, with the majority of estimates falling below one(36). To put that in perspective, growing one cell in a 5 mL culture to an OD of about 1.0 (~10^{10} cells) takes about 33 generations. This means growth typically made in a day in the lab simulates the equivalent of at least, and likely more than, a years-worth of reproduction in the soil. And while it is not always the case, if these soils become waterlogged, which can quickly render them anoxic(8), it stands to reason that the aerobes in these environments with the ability to survive in the absence of oxygen will have a fitness advantage over those that don't. But what does the ability to survive really mean?

When cells enter growth arrest, the majority of their available energy budget is used for non-growth-related maintenance processes (see Figure 1). The concept of maintenance energy arose from chemostat studies, which revealed that the bacterial growth yield falls below expectations given the ATP yield. This difference implied that a fraction of the ATP energy produced was being diverted away from growth processes. Since then, many studies have quantified this difference as the maintenance energy and found it to vary depending on both the species and conditions(37–39). One can create a linear fit showing how energy consumption changes with the growth rate in a chemostat and extrapolate this line to a hypothetical growth rate of zero in order to estimate the maintenance energy. The line does not pass through the origin, which fits the intuitive expectation that there must be some minimal power consumption necessary to sustain even non-growing biomass against death and degradation.

However, the maintenance energy calculated this way assumes the metabolic state of fast-growing cells is the same as starved cells, when in reality, starving cells have made a large variety of physiological adjustments. Indeed, chemostat-based maintenance energy

inferences are estimated to be about 3 orders of magnitude higher than those measured in environmental samples(38). The interpretation of this discrepancy is difficult, as the processes contributing to chemostat-derived maintenance energy are not well defined. They likely vary by species and growth condition, and may not all be essential to survival.

This all begs the question of what are the actual minimal energy requirements for a cell to survive? To differentiate between the concepts of chemostat-derived maintenance energy and the minimal energy needed to sustain an organism, Hoehler and Jørgensen suggested the term basal power requirement (BPR). The BPR is defined as the minimum energy turnover rate per cell required to sustain a metabolically active state(33). While careful measurements of the BPR are rare, Lever *et al.* made one estimate from bulk oxygen consumption rates in aerobic marine sediments that approached an asymptote with sampling depth(26). They reason this value might reflect the BPR in this environment and estimated it to be between 3×10^{-14} and 3×10^{-13} kJ $cell^{-1}$ yr^{-1}, depending on whether one assumes the average Gibbs free energy yield of those cells' aerobic metabolism to be 100 or 1000 kJ mol O_2^{-1}. For comparison, *E. coli* power consumption during exponential growth (also based on its bulk oxygen consumption rate and the same free energy yields of aerobic metabolism(41)) is extrapolated to be between 8×10^{-9} and 8×10^{-8} kJ $cell^{-1}$ yr^{-1}, 4 to 6 orders of magnitude higher. It is important to note, however, that the BPR for organisms surviving in the absence of oxygen may be even less, as the burden of repairing cellular components damaged by oxidative species generated via aerobic respiration may inflate these values(42).

Metabolic Requirements for Survival

Because there are few mechanistic studies related to energy-limited survival, any description of minimal metabolic requirements is limited to our understanding of metabolism during fast growth. One primary question is: when energy is limited, what are the cell's metabolic priorities? Intuitively, preservation of a minimum PMF would seem essential to transport nutrients in and wastes out(43). This intuition relies on the assumption that active transport of some kind (either powered by the PMF or ATP) is necessary for homeostasis to be achieved, yet that may not always be the case. Intriguingly, recent evidence suggests that some obligate aerobes in their vegetative state, such as *Bacillus subtilis*, may take an entirely different survival strategy, benefiting from attenuation of the PMF(44). An exciting frontier for bacterial physiology lies in determining the level of PMF actually needed to sustain a cell, and what mechanisms underpin its maintenance under different conditions. Innovations in tools that enable quantitative measurement of the PMF in single cells, together with tools that quantitatively measure ATP or other metabolites that permit the assessment of metabolic state, are a priority for development in bacteria.

Putting these existential unknowns and corresponding research opportunities aside, it is helpful to recall some basic facts about energy conservation in bacteria. To start, it is axiomatic that metabolically active, aerobically respiring cells charge the PMF through the electron transport chain (ETC), enabling ATP generation by dissipation of the chemiosmotic gradient through the F_1F_O-ATP(synth)ase. Yet a fact that is perhaps less well-remembered is that when the ETC flux is stalled due to the lack of a terminal electron acceptor, cells have many other options for PMF maintenance. For instance, anaerobic proton extrusion can be accomplished by protonated carbon compound antiport(45), and driving the F_1F_O-

ATP(synth)ase in reverse (which can be regulated(46)) can also charge the PMF(47). Intriguingly, oxygen-limited *P. aeruginosa* cells lower their ATP pools more quickly than carbon-limited cells, and treating such cells with PMF inhibitors reduces the number of survivors(24, 48). These results are consistent with energy limitation being more extreme for oxygen-limited cells due to their dependency on the low-energy-yielding acetate kinase-phosphate acetyltranserase (AckA-Pta) pathway, a pathway that generates ATP via substrate-level phosphorylation(11, 47). It is in this context that we believe much stands to be gained from identifying what constrains flux through substrate-level phosphorylation pathways in aerobes.

Directly related to this challenge is the question: what facilitates maintenance of intracellular redox pools, the homeostasis of which is critical for both catabolism and anabolism? These pools include species such as NADH/NAD^+ (predominantly involved in energy conservation), NADPH/$NADP^+$ (predominantly involved in biomass generation), and glutathione (predominantly involved in protein disulfide bridge homeostasis). When the NAD(P)H/$NAD(P)^+$ balance is disrupted, reactions that rely on electron flow through these pools become stalled, and the growth rate of the cell diminishes. For example, Richardson *et al.* found that when the photoheterotroph *Rhodobacter capsulatus* is grown anaerobically on reduced carbon compounds, it displays a growth deficit in the absence of CO_2. This growth defect can be recovered upon addition of alternative terminal oxidants, suggesting that the Calvin Cycle functions as an electron-sink necessary for proper redox-balance during growth(49). Using C^{13}- metabolic flux analysis, McKinlay *et al.* confirmed that in the photoheterotroph *Rhodopsuedomonas palustris*, the Calvin Cycle indeed functions as a crucial electron sink, accounting for almost 50% of NADH oxidation during conversion of

acetate to biomass(50). Rao *et al.* found that in non-replicating hypoxic *Mycobacterium tuberculosis*, the NADH dehydrogenase NDH-2 is essential to cells' survival because it replenished the NAD^+ pool of cells that were otherwise stalled in a predominantly reduced state(48). The importance of redox-balancing is also well-appreciated in the study of fermentation and metabolic engineering, as shifting the NADH/NAD^+ ratio of the cell, either genetically or through providing differently oxidized carbon sources, can significantly alter not only growth but also the yield of fermentation products(51).

While both the PMF Δp (the potential energy stored across the membrane from differences in ion concentration) and NADH/NAD^+ ratio vary depending on the organism and the environment(52, 53), as discussed above, it seems likely that there are limits to this variation beyond which most cells cannot live. At the extremes, without a PMF, the cell would be relying on passive import of substrates in a likely dilute environment. Without a properly maintained NADH/NAD^+ ratio, flux through key redox enzymes would cease. The result of either is that the flux through ATP-producing pathways would be reduced, along with the BPR processes necessary to maintain metabolic activity. Therefore, the PMF and intracellular redox state are valuable integrative metabolic outputs to track when assessing a survival phenotype, regardless of which stress triggers the growth-arrested state.

Consequences of Life without Oxygen

Focusing on oxygen as a key physiological variable, it is tempting to assume that the net energy available to respiring aerobes is always much greater than that available to fermenting anaerobes. In reality, there are tradeoffs to each metabolic strategy given its respective environmental context. Understanding those tradeoffs provides a framework for

how energy budgets and relative fitness shift in changing conditions. Cells in anoxic conditions may produce energy from the respiration of alternative terminal electron acceptors such as fumarate, sulfate, and nitrate. Each such alternative electron acceptor has a lower redox potential than oxygen, so the amount of energy the cell is capable of acquiring from its reduction is lower than that which would result from the reduction of an equivalent amount of oxygen. Cells can also ferment by maintaining a balance of their $NADH/NAD^+$ pool, permitting flux through pathways that generate ATP by substrate-level phosphorylation. Though the energetic efficiency of fermentation is about an order of magnitude less compared to aerobic respiration (for one mole of glucose, fermentation generates 1-5 moles of ATP depending on the pathway, much less than the approximately 32 moles generated from aerobic respiration), the fitness benefit of efficiency depends on context.

Aerobically respiring cells constantly deal with oxidative stress that consumes significant energy. Oxidative stress is characterized by oxidation of redox pools, interfering with homeostasis between anabolism and catabolism. While oxidative stress generically can be caused by a lack of electron donors relative to acceptors, the generation of superoxide radicals and hydrogen peroxide resulting from oxygen excess adds insult to injury. These toxic, reactive oxygen species are generated when oxygen autoxidizes redox enzymes (especially flavoproteins)(42), making oxidative stress an unavoidable consequence of aerobic metabolism(54). If left unchecked, these species will destroy the metal centers of key metabolic proteins, oxidize the cysteine residues of proteins and warp their optimal structure, and even react with iron in the cell through the Fenton reaction to generate hydroxyl radicals that can cause DNA mutations(42). Cells ameliorate this stress with processes that require energy, including the production of superoxide dismutase and catalase proteins, among

others, and by shunting some of their electrons back onto mis-oxidized proteins through the glutathione and/or thioredoxin pools(42).

Despite the acute challenges presented by transitioning from an oxic to an anoxic environment(55), the energy budget of aerobic cells that settle into an anaerobic survival state contracts as these cells no longer have to pay the costs of repairing oxidative damage. Inefficient fermentations may, under these circumstances, be perfectly adequate, particularly if the flux through these pathways is sufficient to meet metabolic demands. Furthermore, the number of proteins required for fermentation is significantly fewer than for respiration; in *E. coli* the protein cost is estimated to be around half(56), a significant fitness advantage given the high energetic cost of producing and maintaining proteins. From this viewpoint, the relative energetic deficit of fermentation begins to look more like a tradeoff. It is similar conceptually to the proposed tradeoff associated with rRNA copy number, where having multiple copies of the *rrn* operon could allow for increased rRNA production, reduced lag, and increased maximal growth rate, but imposes an energy burden that becomes a detriment to fitness under energy-limited conditions(57, 58). Be that as it may, our ability to assess long-term fitness tradeoffs between aerobic and fermentative metabolism is limited by our lack of understanding of how cells allocate energy when it is limited, which may have more to do with maximizing survival than growth. Indeed, recent modeling suggests that the relative fitness of a respiration vs. fermentation strategy in an oxygen-variable niche is nuanced(59).

Beyond needing to sustain sufficient catabolic output under oxygen-limited growth arrest, there is the issue of rewiring anabolic pathways in the absence of oxygen. For example, in *E. coli*, the aspartate oxidase NadB, an essential enzyme in pyridine nucleotide biosynthesis

(i.e. $NAD(P)^+$) is known to reduce molecular oxygen to redox-cycle its solvent-exposed flavin, but is also capable of using fumarate for this purpose during anaerobic growth(60). A similar example can be found in pyrimidine biosynthesis under anoxic conditions, specifically in the membrane-bound dihydroorotate dehydrogenase PyrD. This enzyme catalyzes a non-NAD(P)H-mediated redox reaction (the oxidation of dihydrooratate to oratate), which, under oxic conditions, proceeds by shuttling electrons into the quinone pool and therefore ultimately onto oxygen(61). Under anoxic conditions, *E. coli* transfers these electrons from the quinol pool onto fumarate through either fumarate reductase or the reverse reaction of succinate dehydrogenase(61). Despite having the ability to anaerobically respire, *Campylobacter jejuni* cannot grow in the absence of at least small amounts of oxygen because its ribonucleotide reductase, which catalyzes the essential conversion of ribonucleotides to deoxyribonucleotides, requires oxygen(62). These examples underscore that energy may not always be the limiting factor for growth when an organism fails to grow anaerobically; essential anabolic pathways can sometimes require oxygen. While we know enough to ask increasingly mechanistic questions about how oxygen-limited cells survive growth arrest, much remains to be learned about both catabolic and anabolic fitness determinants.

Anaerobic Survival Mechanisms in *P. aeruginosa*

P. aeruginosa is a ubiquitous bacterium that can cause devastating chronic lung infections in cystic fibrosis patients and chronic wounds in immunocompromised patients. These infection environments can experience prolonged states of hypoxia or anoxia(9, 10), motivating research into how *P. aeruginosa* survives when oxygen is scarce. Here we focus on

fermentative survival mechanisms rather than denitrification, as denitrification in *P. aeruginosa* has been well-reviewed elsewhere (63, 64). After it was discovered that *P. aeruginosa* could generate ATP anaerobically through arginine catabolism(22), Eschbach *et al.* showed that *P. aeruginosa* can survive, but not grow, in anoxic conditions through a mixed-acid fermentation of pyruvate to lactate, acetate, and succinate (Figure 2A). *P. aeruginosa* was able to survive anoxic conditions in minimal pyruvate medium for up to 18 days before any loss in viability was detected, while those in anoxic conditions without a carbon source began to lose viability within three days(11). These fermentation and survival phenotypes were dependent on the genes *ldhA*, *pta* and *ackA*, which comprise the reductive and oxidative arms of the fermentation. Interestingly, the cells did not survive anoxia when provided with glucose as a carbon source, suggesting the fermentation might be oxidatively limited and therefore unable to support flux through glycolysis under these conditions. Yet survival on glucose is sometimes possible, provided flux through ATP-yielding pathways is sufficiently high(23). How might this be achieved?

Separately, *P. aeruginosa* is known for its production of colorful, redox-active metabolites called phenazines(65). With the exception of early work by Friedheim on the potential for phenazines to serve as accessory respiratory pigments(66), the bulk of the literature has portrayed phenazines as antibiotics(67). This view of their biological activity stems from studies that showed that the phenazine pyocyanin (PYO) reduces oxygen, producing superoxide and hydrogen peroxide *in vitro* and in *E. coli* cultures(68, 69), where an aerobic growth inhibition was observed at concentrations as low as 1 μM PYO. These studies found that phenazines are reduced by *E. coli* and therefore generate a massive amount of oxidative stress in the presence of oxygen.

In contrast, *P. aeruginosa* can tolerate up to at least 100 μM of PYO(70). An early hypothesis by our group was that such an alternative electron acceptor would be most beneficial when access to oxidants is limited, such as in the anoxic core of biofilms(71). To test this hypothesis, Wang *et al.* developed an anoxic survival assay, demonstrating that electrodes poised to oxidize phenazines could facilitate phenazine extracellular electron transfer (EET) that promoted cells' survival(72). Under these conditions, at least 2 orders of magnitude more cells survived in the presence of phenazines after 7 days of anoxia. A prior study found that phenazines significantly re-balance the reduced NADH/NAD^+ pool in the early stationary phase of dense cultures(73). This hinted that the metabolic mechanism behind the survival phenotype might be connected to pyruvate fermentation through fermentative redox balance. Data supporting this hypothesis was provided by Glasser *et al.*, who showed the *ackA* and *pta* genes necessary for pyruvate fermentation were also necessary for phenazine-mediated survival phenotype(23). They further demonstrated that this phenotype was unaffected in a *ldhA* mutant and that the cells could survive by fermenting glucose, overcoming the metabolic limitation identified for this mutant by Eschbach *et al.* and concluding that phenazine-mediated EET was sufficient as the oxidative arm of the fermentation (Figure 2A). Importantly, phenazine-mediated EET enabled the production of a PMF, which correlated with survival (23).

An outstanding question is whether this mechanism enhances survival in the center of a biofilm. Like most secondary metabolites, phenazines are secreted by cells during the transition into stationary phase and afterward(73), a state that would be induced as a biofilm grows and cells are suffocated by their outer neighbors(5, 74). Under such conditions, oxygen would be available at a distance, similar to the electrode at a distance away in the survival

assay, and phenazine-mediated EET could close the gap. This hypothesis is supported by the observation that a Δ*phz* strain that cannot produce phenazines forms highly wrinkled biofilms, which maximizes their access to oxygen(75). Indeed, phenazines and/or the redox-state of the cell are directly linked to biofilm morphogenesis through the regulatory protein RmcA that modulates the production of matrix components responsible for these wrinkles(76, 77). Intriguingly, phenazines are retained in biofilms by binding to extracellular DNA, which helps facilitate the EET system as a whole(78). Deletion of certain membrane-bounded cytochrome oxidases curtails phenazine reduction at depth in the colony biofilm system, impacting both the extracellular redox potential within the colony and its morphology(79). Whether the redox-benefits achieved by recycling phenazine using these enzymes and/or others in the cytosol(80) permit energy-generation via oxidative or substrate-level phosphorylation remains to be determined.

Anaerobic Survival in *Streptomyces coelicolor*

P. aeruginosa is not the only bacterium that might derive a catabolic benefit from its secondary metabolites. Indeed, such metabolites are made by diverse bacterial phyla, many of which reside in the soil(81). Of these, the *Streptomyces* genus is the best studied. Streptomycetes exhibit a three-stage lifecycle, which includes outgrowth as a mycelial mat (which, like a more conventional biofilm, becomes anoxic in deeper layers(82)), development of aerial hyphae, and the release of spores from these hyphae. In the absence of oxygen, streptomycetes must rely on alternative energy conservation strategies besides aerobic respiration to survive. As mentioned above, one such alternative is nitrate. *S. coelicolor* has three distinct nitrate reductase operons (*nar1, nar2,* and *nar3)*, each active in

different stages of its life cycle(83). Interestingly, none of them can sustain growth in the absence of oxygen(83).

While spores are typically assumed to be metabolically inactive, some minimal amount of metabolic activity must be maintained—or at least, the potential for metabolic activity—so as to permit revival. While spore metabolism is outside the scope of this review, we simply note that, in *S. coelicolor,* during the spore stage, the electron transport chain is poised to respire nitrate only when oxygen is absent, as nitrite production by spores is reversibly and rapidly inhibited by the presence of oxygen(84). Notably, this doesn't apply to the other life stages of *S. coelicolor*, where nitrate reduction can occur simultaneously with oxygen(83). While it is unclear why nitrate reduction is insufficient to support anaerobic growth of *S. coelicolor*, it has been inferred that nitrate reduction contributes to charging the PMF and/or redox-balancing the cytosol in the absence of oxygen to contribute to cell survival(85). For a detailed summary and analysis of denitrification in *S. coelicolor*, please see the recent review by Sawers *et al*.(85).

However, nitrate respiration cannot be the only anaerobic energy conserving mechanism for *S. coelicolor*, as a Δ*nar123* mutant has no anoxic survival deficit compared to WT in the presence of nitrate(83). This is in contrast to another actinomycete, *Mycobacterium tuberculosis*, where nitrate respiration enhances survival of non-replicating cells in hypoxic conditions(86). Indeed, even germinated *S. coelicolor* spores can survive at least three weeks of anoxia in nitrate-free media, indicating that anaerobic survival is robust in the absence of nitrate and not limited to the spore state(16). What other metabolic mechanisms could *S. coelicolor* be using to provide the energy needed to survive anoxia?

Acid secretion has been observed in various *Streptomyces* species. As one example, *S. coelicolor* is known to secrete pyruvate and alpha-ketoglutarate during the transition from exponential to stationary phase(87). Acid secretion during aerobic growth often suggests rectifying redox or carbon imbalance and is sometimes referred to as overflow metabolism(56, 88). To our knowledge, only a single report suggests a canonical fermentation via lactate secretion in the species *S. griseus* growing under restricted aeration(89). This is interesting considering the *S. coelicolor* genome codes for a gene whose protein shares 44% amino acid identity to the *E. coli* lactate dehydrogenase (LdhA)(16). Although there are not yet any published studies that tested for evidence of fermentation in *S. coelicolor* under anaerobic survival conditions, these data hint at the possibility.

Furthermore, there are curious correlations between *S. coelicolor*'s secondary metabolites and phenazines. Just as phenazine-null *P. aeruginosa* mutants develop into wrinkled colonies, a similar morphology is observed in *S. coelicolor* colonies when actinorhodin or undecylprodigiosin production is interrupted(76, 90). In *S. coelicolor*, production of actinorhodin and undecylprodigiosin is upregulated by iron-, phosphate-, and also ammonium-limitation(91, 92). While in this review we have focused on phenazines' anaerobic survival benefits, phenazines are also involved in liberating iron from minerals in the form of ferrous iron(93, 94) and phenazine biosynthesis is correspondingly also upregulated by iron-limitation(95) and by phosphate-limitation(96). These correlations loosely hint at the possibility that actinorhodin and undecylprodigiosin may share some of the same physiological functions as phenazines. Consistent with this notion, both phenazines and actinorhodin strongly activate SoxR(97), an iron-sulfur cluster transcription factor specifically activated by redox-cycling compounds(98, 99). Recently, it was demonstrated

that actinorhodin is also a redox-active antibiotic(100), suggesting that actinorhodin might also confer a survival benefit to *S. coelicolor* like phenazines do for *P. aeruginosa.*

A General Hypothesis for RAM-mediated Survival

Phenazines and actinorhodin are examples of a broad class of secreted redox-active small molecules produced by many thousands of microbial species(65). For example, flavins can stimulate EET by *Shewanella oneidensis* and *Listeria monocytogenes* (101, 102). Similarly, diverse quinones can stimulate EET by *Klebsiella pneumonia, Lactococcus lactis, Shewanella oneidensis* and *Sphingomonas xenophaga*(103–106). Bioinformatic analysis indicates that hundreds of species from the phyla *Actinobacteria* and *Proteobacteria* contain phenazine biosynthetic clusters(65, 107). However, not all of these putative molecules are necessarily extracellular electron shuttles. Until they are proven to function as such, we prefer the label "redox-active metabolites", or RAMs, to describe these types of metabolites.

The phylogenetic ubiquity of RAMs makes us wonder whether there could be an underlying unity to their physiological functions, such as helping diverse aerobes achieve redox balance during oxygen-limitation. Many of these bacteria contain the genes needed for fermentative metabolisms, though flux through these energy conserving pathways appears to be limited by the aerobes' ability to balance the $NADH/NAD^+$ pool. RAM reduction presents a potential mechanism by which microbes could relieve themselves of the excess reducing equivalents that would accumulate under oxygen-limited conditions, thereby increasing flux through redox-limited pathways (Figure 2B and C). If flux were stimulated in this way through pathways that were otherwise inactive, we could consider those pathways to be "unlocked". Such unlocking could be achieved by endogenous RAMs, as is the case

for *P. aeruginosa*(23), or by exogenous RAMs for an organism that cannot produce them. Given that this mode of survival would only be possible for a non-RAM-producer in the presence of another organism, what is metabolically possible for a single species may only be fully understood by studying its community.

However, it is well established that to many species, RAMs are toxic in the presence of ambient oxygen. In large part this is due to their ability to divert electrons from the cell and shuttle them in an energetically uncoupled fashion to oxygen, generating toxic superoxide radicals in the process(108). This interpretation is consistent with the fact that phenazines become toxic even to *P. aeruginosa* under certain conditions. Meirelles and Newman recently likened phenazines to a double-edged sword, with the relative dominance of benefit or detriment conferred by phenazines depending on the type of energy-limitation the cell is experiencing. For example, under carbon-limited aerobic conditions, where the cell is predominantly oxidized, phenazines cause up to 75% of *P. aeruginosa* cells to lose viability within 26 hours(70). As discussed earlier, this negative effect contrasts with oxygen-limited conditions, where the cell is predominantly reduced and phenazines contribute to energy conservation by redox-balancing the cytosol (Figure 2A). Our working model is that if the redox pool of the cell is predominantly oxidized, further oxidation by phenazines will be toxic, whereas if the cell is predominantly reduced, oxidation by phenazines will be largely beneficial.

We suspect this “rule” for phenazines holds even for other aerobes. The lack of any species-specific reduction of phenazines is an old observation(66, 109), and we have also observed reduction of phenazines by non-phenazine producing species, including *Staphyloccocus aureus*, *Agrobacterium tumefaciens*, *Burkholderia cepacia*, and

Achromobacter sp. While the metabolic consequences of promiscuous phenazine reduction under anoxic and hypoxic conditions remains incompletely characterized, we have yet to encounter a species that cannot reduce phenazines, which is perhaps not surprising given their broad reactivity with redox-active cofactors in common enzymes(80, 108). For example, the pyruvate and alpha-ketoglutarate dehydrogenases have been implicated *in vitro* as phenazine reductases, which is consistent with studies of other redox-active compounds that can oxidize flavoproteins at rates equal to or faster than their physiological acceptors(110). In *E. coli*, multiple groups have found that synthetic phenazines like PMS and neutral red react with the quinone pool in the inner membrane(99, 111). Genetically, a cytochrome oxidase subunit has been shown to contribute to phenazine reduction in *P. aeruginosa* biofilms(79). Furthermore, phenazines are transported through well-conserved pumps(112), and specifically activate the well-conserved SoxR transcription factor, which contains an iron-sulfur cluster(99, 113). Generalizing from these examples, it stands to reason that RAMs likely react with conserved redox cofactors and therefore have the potential to be coupled to NADH oxidation through multiple pathways.

As mentioned above, exactly how phenazine reduction is accomplished while minimizing damage is not fully understood in *P. aeruginosa*. While phenazines are made intracellularly, they are rapidly pumped out of the cell via conserved efflux pumps(112). Upon phenazine re-entry into the cell, if the cytochrome oxidase subunit previously mentioned(79) were able to reduce them on the periplasmic side of the inner membrane, this would provide a means to spatially circumvent undesirable reactions in the cytosol without sacrificing the benefits of promoting intracellular redox balance. Exploring the mechanisms

and sub-cellular localization of RAM cycling in any species that benefits from RAMs is a priority for future research.

Opportunities for Discovery

Theoretically, all microorganisms must fall somewhere along a continuum of being unable to tolerate any oxygen exposure to being entirely reliant on oxygen for survival. In this minireview, we have shared a few examples of the gray areas along this spectrum to argue that they are the norm in the microbial world and represent opportunities for discovery. We respectfully contend that the classical growth classifications of "obligate" and "facultative" can effectively, albeit unintentionally, skew attention away from and even contradict how these organisms survive when they are not growing. Recognizing that many bacteria, from *P. aeruginosa* to *S. coelicolor*, are still sometimes classified as "obligate" aerobes despite their ability to conserve energy anaerobically(11, 17, 18, 83), exemplifies this problem.

As more discoveries are made of anaerobic metabolisms that support survival or slow growth within aerobes, the physiology underpinning these microbes' ecological success will become clearer. We hope to have convinced the reader that an underappreciated aspect of their success is their ability to endure periods of energetic famine, such as when oxygen is limiting. Some vegetative cells can survive with little energy for years(114, 115), a natural phenomenon whose wonder should not go overlooked. Which genes, metabolic modules, community compositions, and environmental factors determine survival potential? How common are they across species and niches? Exploring the mechanisms of survival physiology will not only fill gaps in our understanding of the minimal energy requirements

of life but may also reveal new targets to combat chronic infections and improve the engineering of metabolism decoupled from growth. On the whole, it will bring us steps closer to understanding the heart of microbial resiliency.

Figures

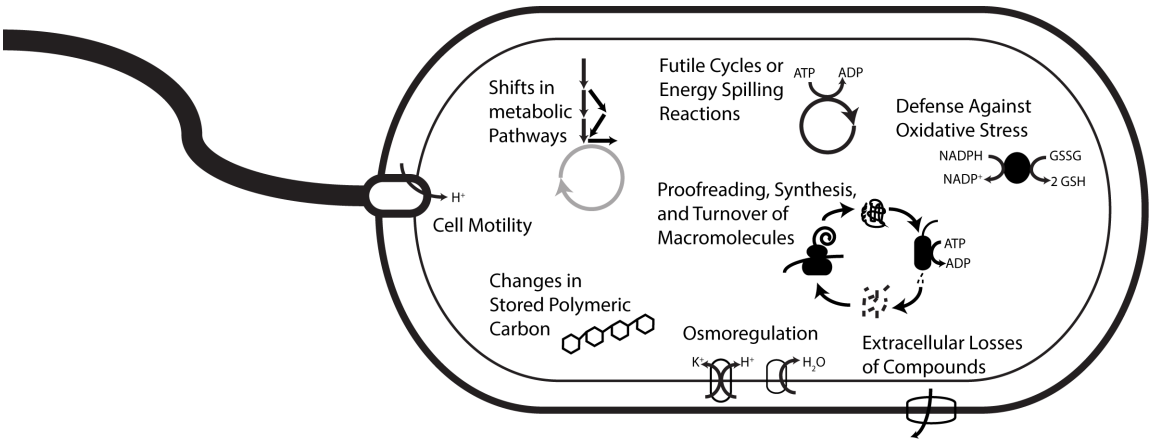

Figure 1. Proposed non-growth components involved in microbial maintenance energy. Adapted from van Bodegom, 2005(40).

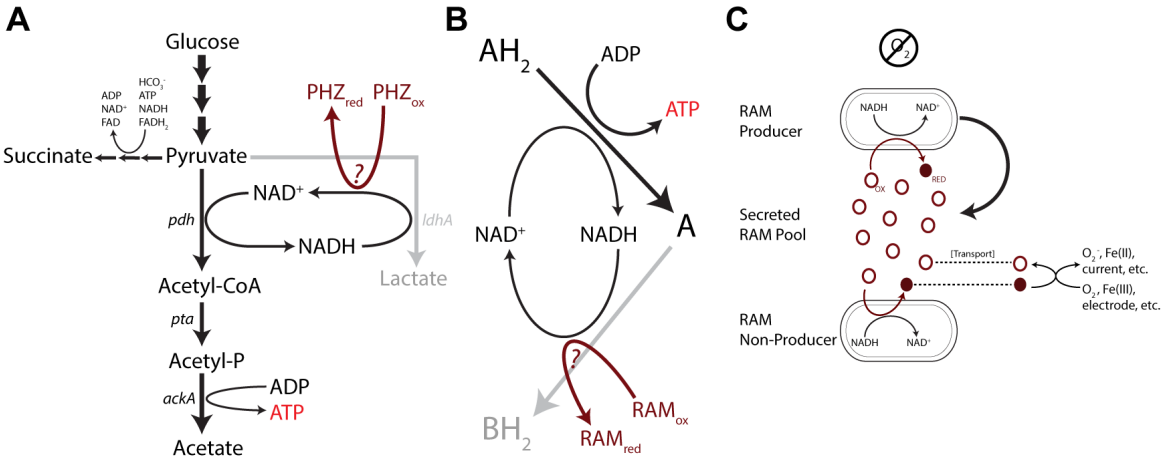

Figure 2. Illustration of how RAMs can facilitate oxidative metabolism. (A) Working model of phenazine-based anaerobic survival catabolism in *Pseudomonas aeruginosa* (Glasser et al., 2014 (23)). (B) A general way RAMs (e.g. phenazines) may serve as an oxidant to permit substrate-level phosphorylation in diverse aerobes. (C) In a microbial community, RAMs have the potential to benefit both producers and non-producers by serving as shared oxidants. PHZ, phenazine; RAM, redox-active metabolite; Ox, oxidized; Red, reduced.

References

1. Manson MD, Tedesco P, Berg HC, Harold FM, Van der Drift C. 1977. A protonmotive force drives bacterial flagella. Proc Natl Acad Sci U S A 74:3060–3064.

2. Shioi J-I, Matsuura S, Imae Y. 1980. Quantitative measurements of proton motive force and motility in *Bacillus subtilis*. J Bacteriol 144:7.

3. Harold F. 1977. Ion currents and physiological functions in microorganisms. Annu Rev Microbiol 31:181–203.

4. Bergkessel M, Basta DW, Newman DK. 2016. The physiology of growth arrest: uniting molecular and environmental microbiology. Nat Rev Microbiol 14:549–562.

5. Stewart PS, Franklin MJ. 2008. Physiological heterogeneity in biofilms. Nat Rev Microbiol 6:199–210.

6. Babin BM, Atangcho L, van Eldijk MB, Sweredoski MJ, Moradian A, Hess S, Tolker-Nielsen T, Newman DK, Tirrell DA. 2017. Selective proteomic analysis of antibiotic-tolerant cellular subpopulations in *Pseudomonas aeruginosa* biofilms. mBio 8.

7. Teal TK, Lies DP, Wold BJ, Newman DK. 2006. Spatiometabolic stratification of *Shewanella oneidensis* biofilms. Appl Environ Microbiol 72:7324–7330.

8. Silver WL, Lugo AE, Keller M. 1999. Soil oxygen availability and biogeochemistry along rainfall and topographic gradients in upland wet tropical forest soils. Biogeochemistry 44:301–328.

9. Worlitzsch D, Tarran R, Ulrich M, Schwab U, Cekici A, Meyer KC, Birrer P, Bellon G, Berger J, Weiss T, Botzenhart K, Yankaskas JR, Randell S, Boucher RC, Döring G. 2002. Effects of reduced mucus oxygen concentration in airway *Pseudomonas* infections of cystic fibrosis patients. J Clin Invest 109:317–325.

10. Cowley ES, Kopf SH, LaRiviere A, Ziebis W, Newman DK. 2015. Pediatric cystic fibrosis sputum can be chemically dynamic, anoxic, and extremely reduced due to hydrogen sulfide formation. mBio 6:e00767-15.

11. Eschbach M, Schreiber K, Trunk K, Buer J, Jahn D, Schobert M. 2004. Long-term anaerobic survival of the opportunistic pathogen *Pseudomonas aeruginosa* via pyruvate fermentation. J Bacteriol 186:4596–4604.

12. Nakano MM, Dailly YP, Zuber P, Clark DP. 1997. Characterization of anaerobic fermentative growth of *Bacillus subtilis*: identification of fermentation end products and genes required for growth. J Bacteriol 179:6749–6755.

13. Eschbach M, Möbitz H, Rompf A, Jahn D. 2003. Members of the genus *Arthrobacter* grow anaerobically using nitrate ammonification and fermentative processes: anaerobic adaptation of aerobic bacteria abundant in soil. FEMS Microbiol Lett 223:227–230.

14. Pelliccione N, Jaffin B, Sobel ME, Krulwich TA. 1979. Induction of the phosphoenolpyruvate: hexose phosphotransferase system associated with relative anaerobiosis in an obligate aerobe. Eur J Biochem 95:69–75.

15. Setubal JC, dos Santos P, Goldman BS, Ertesvag H, Espin G, Rubio LM, Valla S, Almeida NF, Balasubramanian D, Cromes L, Curatti L, Du Z, Godsy E, Goodner B, Hellner-Burris K, Hernandez JA, Houmiel K, Imperial J, Kennedy C, Larson TJ, Latreille P, Ligon LS, Lu J, Maerk M, Miller NM, Norton S, O'Carroll IP, Paulsen I, Raulfs EC, Roemer R, Rosser J, Segura D, Slater S, Stricklin SL, Studholme DJ, Sun J, Viana CJ, Wallin E, Wang B, Wheeler C, Zhu H, Dean DR, Dixon R, Wood D. 2009. Genome sequence of *Azotobacter vinelandii*, an obligate aerobe specialized to support diverse anaerobic metabolic processes. J Bacteriol 191:4534–4545.

16. van Keulen G, Alderson J, White J, Sawers RG. 2007. The obligate aerobic actinomycete *Streptomyces coelicolor* A3(2) survives extended periods of anaerobic stress. Environ Microbiol 9:3143–3149.

17. Berney M, Greening C, Conrad R, Jacobs WR, Cook GM. 2014. An obligately aerobic soil bacterium activates fermentative hydrogen production to survive reductive stress during hypoxia. Proc Natl Acad Sci U S A 111:11479–11484.

18. Watanabe S, Zimmermann M, Goodwin MB, Sauer U, Barry CE, Boshoff HI. 2011. Fumarate reductase activity maintains an energized membrane in anaerobic *Mycobacterium tuberculosis*. PLoS Pathog 7:e1002287.

19. Carlson CA, Ingraham JL. 1983. Comparison of denitrification by *Pseudomonas stutzeri*, *Pseudomonas aeruginosa*, and *Paracoccus denitrificans*. Appl Environ Microbiol 45:1247–1253.

20. Bazylinski DA, Soohoo CK, Hollocher TC. 1986. Growth of *Pseudomonas aeruginosa* on nitrous oxide. Appl Environ Microbiol 51:1239–1246.

21. Yoon SS, Hennigan RF, Hilliard GM, Ochsner UA, Parvatiyar K, Kamani MC, Allen HL, DeKievit TR, Gardner PR, Schwab U, Rowe JJ, Iglewski BH, McDermott TR, Mason RP, Wozniak DJ, Hancock REW, Parsek MR, Noah TL, Boucher RC, Hassett DJ. 2002. *Pseudomonas aeruginosa* anaerobic respiration in biofilms: Relationships to cystic fibrosis pathogenesis. Dev Cell 11.

22. Wauven CV, Pijrard A, Kley-Raymann M, Haas D. 1984. *Pseudomonas aeruginosa* mutants affected in anaerobic growth on arginine: evidence for a four-gene cluster encoding the arginine deiminase pathway. J Bacteriol 160:7.

23. Glasser NR, Kern SE, Newman DK. 2014. Phenazine redox cycling enhances anaerobic survival in *Pseudomonas aeruginosa* by facilitating generation of ATP and a proton-motive force: Phenazines facilitate energy generation. Mol Microbiol 92:399–412.

24. Basta DW, Bergkessel M, Newman DK. 2017. Identification of fitness determinants during energy-limited growth arrest in *Pseudomonas aeruginosa*. mBio 8.

25. Yin L, Ma H, Nakayasu ES, Payne SH, Morris DR, Harwood CS. 2019. Bacterial longevity requires protein synthesis and a stringent response. mBio 10.

26. Lever MA, Rogers KL, Lloyd KG, Overmann J, Schink B, Thauer RK, Hoehler TM, Jørgensen BB. 2015. Life under extreme energy limitation: a synthesis of laboratory- and field-based investigations. FEMS Microbiol Rev 39:688–728.

27. Amy PS, Morita RY. 1983. Starvation-survival patterns of sixteen freshly isolated open- ocean bacteria. Appl Environ Microbiol 45:7.

28. Fida TT, Moreno-Forero SK, Heipieper HJ, Springael D. 2013. Physiology and transcriptome of the polycyclic aromatic hydrocarbon-degrading *Sphingomonas* sp. LH128 after long-term starvation. Access Microbiol 159:1807–1817.

29. Amy PS, Morita RY. 1983. Protein patterns of growing and starved cells of a marine *Vibrio* sp. Appl Environ Microbiol 45:1748–1752.

30. Reeve CA, Amy PS, Matin A. 1984. Role of protein synthesis in the survival of carbon-starved *Escherichia coli* K-12. J Bacteriol 160.

31. Basta DW, Angeles-Albores D, Spero MA, Ciemniecki JA, Newman DK. 2020. Heat-shock proteases promote survival of *Pseudomonas aeruginosa* during growth arrest. Proc Natl Acad Sci U S A 201912082.

32. Morita RY. 1988. Bioavailability of energy and its relationship to growth and starvation in nature. Can J Microbiol 34:436–441.

33. Hoehler TM, Jørgensen BB. 2013. Microbial life under extreme energy limitation. Nat Rev Microbiol 11:83–94.

34. van den Berg LJL, Shotbolt L, Ashmore MR. 2012. Dissolved organic carbon (DOC) concentrations in UK soils and the influence of soil, vegetation type and seasonality. Sci Total Environ 427–428:269–276.

35. Morita RY. 1984. Substrate capture by marine heterotrophic bacteria in the marine environment., p. 83–100. *In* Heterotrophic activity in the sea. Plenum Publishing.

36. Lockwood JL, Filonow AB. 1981. Responses of fungi to nutrient-limiting conditions and to inhibitory substances in natural habitats., p. 1–62. *In* Advances in Microbial Ecology. Plenum Press.

37. Tijhuis L, Van Loosdrecht MCM, Heijnen JJ. 1993. A thermodynamically based correlation for maintenance Gibbs energy requirements in aerobic and anaerobic chemotrophic growth. Biotechnol Bioeng 42:509–519.

38. Kempes CP, van Bodegom PM, Wolpert D, Libby E, Amend J, Hoehler T. 2017. Drivers of bacterial maintenance and minimal energy requirements. Front Microbiol 8.

39. Bradley JA, Amend JP, LaRowe DE. 2018. Bioenergetic controls on microbial ecophysiology in marine sediments. Front Microbiol 9.

40. van Bodegom P. 2007. Microbial maintenance: A critical review on its quantification. Microb Ecol 53:513–523.

41. Milo R, Phillips R. 2016. Cell Biology by the numbers. Garland Science.

42. Imlay JA. 2019. Where in the world do bacteria experience oxidative stress?: Oxidative stress in natural environments. Environ Microbiol 21:521–530.

43. Maloney PC, Wilson TH. Ion-coupled transport and transporters, p. 1130–1148. *In Escherichia coli* and *Salmonella*: Cellular and molecular biology, 2nd ed. ASM Press.

44. Arjes HA, Vo L, Dunn CM, Willis L, DeRosa CA, Fraser CL, Kearns DB, Huang KC. 2019. Biosurfactant production maintains viability in anoxic conditions by depolarizing the membrane in *Bacillus subtilis*. bioRxivorg.

45. Anantharam V, Maloney P. 1989. Oxalate:Formate exchange, the basis for energy coupling in *Oxalobacter*. J Biol Chem 264:7244–7250.

46. Mendoza-Hoffmann F, Zarco-Zavala M, Ortega R, García-Trejo JJ. 2018. Control of rotation of the F_1F_O-ATP synthase nanomotor by an inhibitory α-helix from unfolded ε or intrinsically disordered ζ and IF1 proteins. J Bioenerg Biomembr 50:403–424.

47. Hunt KA, Flynn JM, Naranjo B, Shikhare ID, Gralnick JA. 2010. Substrate-level phosphorylation is the primary source of energy conservation during anaerobic respiration of *Shewanella oneidensis* strain MR-1. J Bacteriol 192:3345–3351.

48. Rao SPS, Alonso S, Rand L, Dick T, Pethe K. 2008. The protonmotive force is required for maintaining ATP homeostasis and viability of hypoxic, nonreplicating *Mycobacterium tuberculosis*. Proc Natl Acad Sci U S A 105:11945–11950.

49. Richardson DJ, King GF, Kelly DJ, McEwan AG, Ferguson SJ, Jackson JB. 1988. The role of auxiliary oxidants in maintaining redox balance during phototrophic growth of *Rhodobacter capsulatus* on propionate or butyrate. Arch Microbiol 150:131–137.

50. McKinlay JB, Harwood CS. 2010. Carbon dioxide fixation as a central redox cofactor recycling mechanism in bacteria. Proc Natl Acad Sci U S A 107:11669–11675.

51. San K-Y, Bennett GN, Berríos-Rivera SJ, Vadali RV, Yang Y-T, Horton E, Rudolph FB, Sariyar B, Blackwood K. 2002. Metabolic engineering through cofactor manipulation and its effects on metabolic flux redistribution in *Escherichia coli*. Metab Eng 4:182–192.

52. Wimpenny JWT, Firth A. 1972. Levels of nicotinamide adenine dinucleotide and reduced nicotinamide adenine dinucleotide in facultative bacteria and the effect of oxygen. J Bacteriol 111.

53. de Graef MR, Alexeeva S, Snoep JL, de Mattos MJT. 1999. The steady-state internal redox state (NADH/NAD) reflects the external redox state and is correlated with catabolic adaptation in *Escherichia coli*. J Bacteriol 181:2351–2357.

54. Green J, Paget MS. 2004. Bacterial redox sensors. Nat Rev Microbiol 2:954–966.

55. Imlay J. 2013. The molecular mechanisms and physiological consequences of oxidative stress: Lessons from a model bacterium. Nat Rev Microbiol 11:443–454.

56. Basan M, Hui S, Okano H, Zhang Z, Shen Y, Williamson JR, Hwa T. 2015. Overflow metabolism in *Escherichia coli* results from efficient proteome allocation. Nature 528:99–104.

57. Klappenbach JA, Dunbar JM, Schmidt TM. 2000. rRNA operon copy number reflects ecological strategies of bacteria. Appl Environ Microbiol 66:1328–1333.

58. Roller BRK, Stoddard SF, Schmidt TM. 2016. Exploiting rRNA operon copy number to investigate bacterial reproductive strategies. Nat Microbiol 1:16160.

59. Pfeiffer T, Schuster S, Bonhoeffer S. 2001. Cooperation and competition in the evolution of ATP-producing pathways. Science 292:504–507.

60. Korshunov S, Imlay JA. 2010. Two sources of endogenous hydrogen peroxide in *Escherichia coli*. Mol Microbiol 75:1389–1401.

61. Neuhard J, Kellin RA. Biosynthesis and Conversions of Pyrimidines, p. 580–599. *In Escherichia coli* and *Salmonella*: Cellular and molecular biology, 2nd ed. ASM Press.

62. Sellars MJ, Hall SJ, Kelly DJ. 2002. Growth of *Campylobacter jejuni* supported by respiration of fumarate, nitrate, nitrite, trimethylamine-N-oxide, or dimethyl sulfoxide requires oxygen. J Bacteriol 184:4187–4196.

63. Arai H. 2011. Regulation and function of versatile aerobic and anaerobic respiratory metabolism in *Pseudomonas aeruginosa*. Front Microbiol 2.

64. Borrero-de Acuña JM, Timmis KN, Jahn M, Jahn D. 2017. Protein complex formation during denitrification by *Pseudomonas aeruginosa*. Microb Biotechnol 10:1523–1534.

65. Glasser NR, Saunders SH, Newman DK. 2017. The colorful world of extracellular electron shuttles. Annu Rev Microbiol 71:731–751.

66. Friedheim EAH. 1934. The effect of pyocyanine on the respiration of some normal tissues and tumours. Biochem J 28:173–179.

67. Price-Whelan A, Dietrich LEP, Newman DK. 2006. Rethinking “secondary” metabolism: physiological roles for phenazine antibiotics. Nat Chem Biol 2:71–78.

68. Hassan HM, Fridovich I. 1979. Intracellular production of superoxide radical and of hydrogen peroxide by redox active compounds. Arch Biochem Biophys 196:385–395.

69. Hassan HM, Fridovich I. 1980. Mechanism of the antibiotic action of pyocyanine. J Bacteriol 141.

70. Meirelles LA, Newman DK. 2018. Both toxic and beneficial effects of pyocyanin contribute to the lifecycle of *Pseudomonas aeruginosa*: Pyocyanin’s effects on *P. aeruginosa* under different conditions. Mol Microbiol 110:995–1010.

71. Hernandez ME, Newman DK. 2001. Extracellular electron transfer. Cell Mol Life Sci 58:1562–1571.

72. Wang Y, Kern SE, Newman DK. 2010. Endogenous phenazine antibiotics promote anaerobic survival of *Pseudomonas aeruginosa* via extracellular electron transfer. J Bacteriol 192:365–369.

73. Price-Whelan A, Dietrich LEP, Newman DK. 2007. Pyocyanin alters redox homeostasis and carbon flux through central metabolic pathways in *Pseudomonas aeruginosa* PA14. J Bacteriol 189:6372–6381.

74. Dietrich LEP, Okegbe C, Price-Whelan A, Sakhtah H, Hunter RC, Newman DK. 2013. Bacterial community morphogenesis is intimately linked to the intracellular redox state. J Bacteriol 195:1371–1380.

75. Kempes CP, Okegbe C, Mears-Clarke Z, Follows MJ, Dietrich LEP. 2014. Morphological optimization for access to dual oxidants in biofilms. Proc Natl Acad Sci U S A 111:208–213.

76. Dietrich LEP, Teal TK, Price-Whelan A, Newman DK. 2008. Redox-active antibiotics control gene expression and community behavior in divergent bacteria. Science 321:1203–1206.

77. Okegbe C, Fields BL, Cole SJ, Beierschmitt C, Morgan CJ, Price-Whelan A, Stewart RC, Lee VT, Dietrich LEP. 2017. Electron-shuttling antibiotics structure bacterial communities by modulating cellular levels of c-di-GMP. Proc Natl Acad Sci U S A 201700264.

78. Saunders S, Tse ECM, Yates MD, Otero FJ, Trammell SA, Stemp EDA, Barton JK, Tender LM, Newman DK. 2019. Extracellular DNA promotes efficient extracellular electron transfer by pyocyanin in *Pseudomonas aeruginosa* biofilms. bioRxivorg.

79. Jo J, Cortez KL, Cornell WC, Price-Whelan A, Dietrich LE. An orphan cbb3-type cytochrome oxidase subunit supports *Pseudomonas aeruginosa* biofilm growth and virulence. Elife.

80. Glasser NR, Wang BX, Hoy JA, Newman DK. 2017. The pyruvate and α-ketoglutarate dehydrogenase complexes of *Pseudomonas aeruginosa* catalyze pyocyanin and phenazine-1-carboxylic acid reduction via the subunit dihydrolipoamide dehydrogenase. J Biol Chem 292:5593–5607.

81. Turner JM, Messenger AJ. 1986. Occurrence, biochemistry and physiology of phenazine pigment production. Adv Microb Physiol 27:211–275.

82. Fischer M, Falke D, Pawlik T, Sawers RG. 2014. Oxygen-dependent control of respiratory nitrate reduction in mycelium of *Streptomyces coelicolor* A3(2). J Bacteriol 196:4152–4162.

83. Fischer M, Alderson J, van Keulen G, White J, Sawers RG. 2010. The obligate aerobe *Streptomyces coelicolor* A3(2) synthesizes three active respiratory nitrate reductases. Access Microbiol 156:3166–3179.

84. Fischer M, Falke D, Sawers RG. 2013. A respiratory nitrate reductase active exclusively in resting spores of the obligate aerobe *Streptomyces coelicolor* A3(2): Spore-specific nitrate reductase in *Streptomyces*. Mol Microbiol 89:1259–1273.

85. Sawers RG, Fischer M, Falke D. 2019. Anaerobic nitrate respiration in the aerobe *Streptomyces coelicolor* A3(2): helping maintain a proton gradient during dormancy. Environ Microbiol Rep 11:645–650.

86. Sohaskey CD. 2008. Nitrate enhances the survival of *Mycobacterium tuberculosis* during inhibition of respiration. J Bacteriol 190:2981–2986.

87. Hodgson DA. 2000. Primary metabolism and its control in *Streptomyces*. Adv Microb Physiol 42:47–238.

88. Wolfe AJ. 2005. The acetate switch. Microbiol Mol Biol Rev 69:12–50.

89. Hockenhull DJD, Fantes KH, Herbert M, Whitehead B. 1954. Glucose utilization by *Streptomyces griseus*. J Gen Microbiol 10:353–370.

90. Brian P, Riggle PJ, Santos RA, Champness WC. 1996. Global negative regulation of *Streptomyces coelicolor* antibiotic synthesis mediated by an *absA*-encoded putative signal transduction system. J Bacteriol 178:3221–3231.

91. Hobbs G, Frazer CM, Gardner DCJ, Flett F, Oliver SG. 1990. Pigmented antibiotic production by *Streptomyces coelicolor* A3(2): kinetics and the influence of nutrients. J Gen Microbiol 136:2291–2296.

92. Coisne S, Béchet M, Blondeau R. 1999. Actinorhodin production by *Streptomyces coelicolor* A3(2) in iron-restricted media: iron and actinorhodin from *S. Coelicolor*. Lett Appl Microbiol 28:199–202.

93. Hernandez ME, Kappler A, Newman DK. 2004. Phenazines and other redox-active antibiotics promote microbial mineral reduction. Appl Environ Microbiol 70:921–928.

94. Wang Y, Newman DK. 2008. Redox reactions of phenazine antibiotics with ferric (hydr)oxides and molecular oxygen. Environ Sci Technol 42:2380–2386.

95. Korth H. 1971. Effect of iron and oxygen on the formation of pigments in some *Pseudomonas* spp. Arch Mikrobiol 77.

96. Frank LH, Demoss RD. 1959. On the biosynthesis of pyocyanine. J Bacteriol 77:776–782.

97. Singh AK, Shin J-H, Lee K-L, Imlay JA, Roe J-H. 2013. Comparative study of SoxR activation by redox-active compounds: SoxR activation by redox-active compounds. Mol Microbiol 90:983–996.

98. Dietrich LEP, Price-Whelan A, Petersen A, Whiteley M, Newman DK. 2006. The phenazine pyocyanin is a terminal signaling factor in the quorum sensing network of *Pseudomonas aeruginosa*. Mol Microbiol 61:1308–1321.

99. Gu M, Imlay JA. 2011. The SoxRS response of <I>Escherichia coli</i> is directly activated by redox-cycling drugs rather than by superoxide: Redox-cycling drugs directly activate SoxR. Mol Microbiol 79:1136–1150.

100. Mak S, Nodwell JR. 2017. Actinorhodin is a redox-active antibiotic with a complex mode of action against Gram-positive cells: Molecular action of actinorhodin. Mol Microbiol 106:597–613.

101. Brutinel ED, Gralnick JA. 2012. Shuttling happens: soluble flavin mediators of extracellular electron transfer in *Shewanella*. Appl Microbiol Biotechnol 93:41–48.

102. Light SH, Su L, Rivera-Lugo R, Cornejo JA, Louie A, Iavarone AT, Ajo-Franklin CM, Portnoy DA. 2018. A flavin-based extracellular electron transfer mechanism in diverse Gram-positive bacteria. Nature 562:140–144.

103. Freguia S, Masuda M, Tsujimura S, Kano K. 2009. *Lactococcus lactis* catalyzes electricity generation at microbial fuel cell anodes via excretion of a soluble quinone. Bioelectrochemistry 76:14–18.

104. Keck A, Rau J, Reemtsma T, Mattes R, Stolz A, Klein J. 2002. Identification of quinoide redox mediators that are formed during the degradation of naphthalene-2-sulfonate by *Sphingomonas xenophaga* BN6. Appl Environ Microbiol 68:4341–4349.

105. Mevers E, Su L, Pishchany G, Baruch M, Cornejo J, Hobert E, Dimise E, Ajo-Franklin CM, Clardy J. 2019. An elusive electron shuttle from a facultative anaerobe. Elife 8:e48054.

106. Deng L, Li F, Zhou S, Huang D, Ni J. 2010. A study of electron-shuttle mechanism in *Klebsiella pneumoniae* based-microbial fuel cells. Chin Sci Bull 55:99–104.

107. Hadjithomas M, Chen I-MA, Chu K, Ratner A, Palaniappan K, Szeto E, Huang J, Reddy TBK, Cimermančič P, Fischbach MA, Ivanova NN, Markowitz VM, Kyrpides NC, Pati A. 2015. IMG-ABC: A knowledge base to fuel discovery of biosynthetic gene clusters and novel secondary metabolites. mBio 6:e00932-15.

108. Imlay JA. 2015. Diagnosing oxidative stress in bacteria: Not as easy as you might think. Curr Opin Microbiol 24:124–131.

109. Ingram JM, Blackwood AC. 1970. Microbial production of phenazines. Adv Appl Microbiol 13:267–282.

110. Massey V, Singer TP. 1957. Studies on succinic dehydrogenase: VI. The reactivity of beef heart succinic dehydrogenase with electron carriers. J Biol Chem 229:755–762.

111. Harrington TD, Tran VN, Mohamed A, Renslow R, Biria S, Orfe L, Call DR, Beyenal H. 2015. The mechanism of neutral red-mediated microbial electrosynthesis in *Escherichia coli*: Menaquinone reduction. Bioresour Technol 192:689–695.

112. Sakhtah H, Koyama L, Zhang Y, Morales DK, Fields BL, Price-Whelan A, Hogan DA, Shepard K, Dietrich LEP. 2016. The *Pseudomonas aeruginosa* efflux pump MexGHI-OpmD transports a natural phenazine that controls gene expression and biofilm development. Proc Natl Acad Sci U S A 113:E3538–E3547.

113. Sheplock R, Recinos DA, Mackow N, Dietrich LEP, Chander M. 2013. Species-specific residues calibrate SoxR sensitivity to redox-active molecules: Differential redox sensing by SoxR homologues. Mol Microbiol 87:368–381.

114. Sebastián M, Estrany M, Ruiz-González C, Forn I, Sala MM, Gasol JM, Marrasé C. 2019. High growth potential of long-term starved deep ocean opportunistic heterotrophic bacteria. Front Microbiol 10:760.

115. Schippers A, Neretin LN, Kallmeyer J, Ferdelman TG, Cragg BA, John Parkes R, Jørgensen BB. 2005. Prokaryotic cells of the deep sub-seafloor biosphere identified as living bacteria. Nature 433:861–864.

C h a p t e r 3

NADH DEHYDROGENASES ARE THE PREDOMINANT PHENAZINE REDUCTASES IN THE ELECTRON TRANSPORT CHAIN OF PSEUDOMONAS AERUGINOSA

Abstract

Phenazines are redox-active secondary metabolites produced by diverse bacteria including the opportunistic pathogen *Pseudomonas aeruginosa*. Extracellular electron transfer via phenazines enhances anaerobic survival by serving as an electron sink for glucose catabolism. However, the specific phenazine reductase(s) used to support this catabolism are unknown. Because electron transport chain components have been previously implicated in phenazine reduction, we sought to determine which of them possess phenazine reductase activity. We show that phenazine-1-carboxamide (PCN) and pyocyanin (PYO) are reduced at the highest rate by cells and are localized to the cell envelope while reduced. Using a coupled genetic and biochemical approach, we show that phenazine reductase activity in membrane fractions is attributable to the three NADH dehydrogenases present in *P. aeruginosa* and that their order of phenazine reductase activity is Nqr > Nuo > Ndh. In mutants possessing only one functional NADH dehydrogenase, whole cell reduction rates of PCN, but not PYO, recapitulate the pattern of biochemical results, implying that PYO reduction is predominantly occurring in the cytosol. Lastly, we show ubiquinone rapidly and non-enzymatically oxidizes reduced phenazines, demonstrating that phenazines have the capability to serve in a redox loop between the NADH and ubiquinone pools, a finding that carries bioenergetic implications.

Introduction

Phenazines are a class of colorful, redox-active secondary metabolites produced by diverse bacteria, including streptomycetes and pseudomonads (1,2). Commonly characterized as antibiotics due to their toxicity to numerous species (3,4), phenazines nevertheless can also confer a variety of beneficial physiological functions to their producers, including supporting energy conservation, nutrient acquisition, and protection against antibiotics (5–7). Although phenazine reduction underpins all these functions, we lack a mechanistic understanding of how and where it occurs in the cell. A key missing piece has been knowledge of whether a predominant, energy-conserving phenazine reductase exists. Motivating our interest in this problem is the fact that when cells are oxidant-limited, phenazine extracellular electron transfer (EET) acts as an electron sink for glucose catabolism, thereby enabling substrate-level phosphorylation and enhancing long-term anaerobic survival (8). In the absence of EET, *P. aeruginosa* cannot survive anaerobically via glucose fermentation (9). It has been proposed that EET may contribute to the survival of the anoxic core of biofilms via redox cycling electrons to peripheral oxygen (10,11) using a combination of diffusion and electron-hopping mechanisms (12) and play a role in biofilm antibiotic tolerance by promoting a slow metabolic state (13,14). The absence of knowing where phenazine reduction is predominantly catalyzed has hindered our ability to specifically disrupt this metabolism and test this hypothesis.

Prior biochemical work (15) discovered that the pyruvate dehydrogenase and alpha-ketoglutarate dehydrogenase complexes are potent phenazine reductases. Accordingly, a hypothesis was presented that phenazines could substitute for NAD^+ in pyruvate dehydrogenase, and through EET, promote redox balance and sustained flux toward acetyl-

CoA and downstream ATP generation via acetate kinase. While this cytosolic mechanism may contribute to phenazine reduction in the whole cell context, the potential for promiscuous reactions of phenazines with various flavoproteins in the cytosol poses a challenge (16) and would require careful management. Indeed, recent work has shown the phenazine tolerance of *Pseudomonas aeruginosa* is largely supported in both oxic and anoxic conditions by the expression of RND efflux pumps, which presumably work to keep cellular concentrations of these compounds low (7,17). Accordingly, we wondered whether reduction at another subcellular location might enable beneficial reduction and subsequent export in a manner that would minimize phenazine reduction in the cytosol.

Intriguingly, previous genetic work found phenazine reduction deficits in *P. aeruginosa* electron transport chain (ETC) mutants, notably mutants of the bc_1 complex (18) and the high-affinity cbb_3-type cytochrome *c* oxidases (19). These data suggest that phenazine reduction may occur in part at the inner membrane through some component of the ETC. Given the relatively low midpoint potential of phenazines (20), it seemed possible that these mutants' phenazine reduction defect might be due to adaptations in the expression of upstream ETC components, a response to the loss of downstream components that has been previously observed (21). Consistent with this prediction, it has long been known that NADH dehydrogenases can react with redox-active secondary metabolites (22,23) and other redox-active compounds (*e.g.* menadione and phenazine methosulfate) have been used as experimental electron acceptors to assay ETC dehydrogenase activity for decades (24).

The ETC in *P. aeruginosa* (Figure 1A) consists of multiple dehydrogenases that feed electrons from the cytosol to a common ubiquinone pool. Ubiquinol can be oxidized by two terminal oxidases that reduce oxygen: the cyanide insensitive oxidase (CIO) and the bo_3-type

oxidase (CYO). Ubiquinol can also be oxidized by a bc_1 complex that reduces a periplasmic cytochrome *c* pool. While the *P. aeruginosa* genome contains multiple cytochrome *c* genes, there is limited knowledge of their individual physiological functions (25). The cytochrome *c* pool can be oxidized by one of three terminal oxidases, the aa_3 (COX), cbb_3-1 (CCO-1) and cbb_3-2 (CCO-2) complexes. Prior studies have found that under most laboratory conditions, including in biofilms, the predominantly expressed terminal oxidases are CCO-1 and CCO-2 (26,27).

Here we sought to characterize the interactions of phenazines with the stationary-phase ETC of *P. aeruginosa* strain PA14 using a coupled genetic and biochemical approach. *P. aeruginosa* synthesizes multiple phenazines, including phenazine-1-carboxylic acid (PCA), phenazine-1-carboxamide (PCN), 5-methyl-phenazine-1-carboxylic acid (5Me-PCA), pyocyanin (PYO), and 1-hydroxy phenazine (1-OH-PCA) (Figure 1B; (28). We focused on the reduction of PYO, PCN, and PCA because they are commonly and consistently secreted into the medium of both planktonic cultures and biofilms (29). Our goal was to work towards an integrative model of how and where phenazines are reduced within the cell.

Results

Phenazine derivatives are reduced at different rates by P. aeruginosa

We first asked whether ETC mutations known to cause phenazine reduction deficits affected the reduction of all phenazine derivatives. To control the phenazine concentrations present in the assay, we used a phenazine-null mutant lacking both copies of its core phenazine biosynthesis operon, Δ*phz1/2*. We compared phenazine reduction by this strain to

that achieved by mutants in the bc_1 complex (Δ*phz1/2* Δ*fbcC*) and cbb_3-type terminal oxidase complexes (Δ*phz1/2* Δ*cco1/2*) that were previously found to have PYO and non-specified phenazine reduction deficits, respectively (18,19). Both Δ*phz1/2* Δ*fbcC* and Δ*phz1/2* Δ*cco1/2* displayed growth phenotypes that were complemented by insertion of the respective gene and operons in *trans* at the *att*Tn7 site (Figure S1).

Measuring the phenazine reduction rate by non-growing cells can be achieved by monitoring changes in absorbance at wavelengths indicative of the redox state of the phenazine. We observed that the three phenazine derivatives were reduced at different rates by whole cells (Figure 2A). In all strains, PYO was reduced most quickly, and PCN was reduced faster than PCA despite having a lower midpoint potential (Figure 1B). We confirmed that the Δ*phz1/2* Δ*fbcC* and Δ*phz1/2* Δ*cco1/2* strains displayed PYO reduction phenotypes under our assay conditions (Figure 2A). However, we found that these strains did not have deficits in their PCN or PCA reduction rate, which had not been tested before.

Reduced phenazine derivatives differentially localize to the cell envelope

A factor potentially contributing to differential phenazine cellular reduction rate is the phenazines' sub-cellular localization. While phenazines' localization in biofilms has been reported (30), to our knowledge there have been no measurements of phenazine localization within single cells. Given our hypothesis that some phenazines react with electron transport chain components in the inner membrane, we sought to directly visualize phenazine localization *in vivo*. Conveniently, most phenazines are fluorescent when reduced (31), and can therefore be visualized via fluorescence microscopy after reduction occurs. However, given their rapid reactivity with oxygen, this fluorescence is dependent on maintaining strict

anoxic conditions during imaging. To achieve this, we used a small, closed stage chamber with a gas line hookup to constantly flush the microscope stage with N_2 gas. We used a strain that cannot synthesize siderophores, Δ*phz1/2* Δ*pvdA* Δ*pchE*, because siderophore fluorescence overlaps spectrally with phenazines (31). When cells were mounted on agar pads and imaged, we observed a fluorescence increase above background only when phenazines had been added to the pad and the stage was anoxic (Figure S2). Returning a sample with notable fluorescence to oxic conditions also eliminated the fluorescence (Figure S2).

Using this experimental system, we found that both reduced PYO and reduced PCN localized to the cell envelope, forming rings of fluorescence in every cell (Figure 2B). Interestingly, reduced PCN fluorescence displayed noticeably more single-cell heterogeneity than reduced PYO. Average profiles of fluorescence across the short axis of the cell body display a clear bimodal shape for reduced PYO and PCN (Figure 2C). In contrast, reduced PCA fluorescence exhibited a lower signal localized diffusely over the cell body (Figure 2B). The average profile for PCA is unimodally centered over the cell body with a minor but significant intracellular increase in fluorescence relative to autofluorescence measured on a buffer-only agar pad, suggesting little, if any, was retained (Figure 2C). Indeed, PCA is likely excluded from the membrane and only slowly enters the cell because of the charge on its carboxylate moiety at circumneutral pH ($pK_a \sim 4.2$, (32).

Although our microscope achieves near the upper limit of resolution via conventional fluorescence microscopy, it is too low to distinguish an outer membrane, periplasmic, and/or inner membrane localization for reduced PYO and PCN. We also note that this patterning only revealed the localization of the phenazine after it had been reduced, which is not

necessarily the site of reduction. These results nevertheless encouraged a deeper exploration into the interactions of phenazines with the ETC.

PYO reduction catalyzed by membrane fractions occurs at the NADH dehydrogenases

Given the Δ*phz1/2* Δ*cco1/2* and Δ*phz1/2* Δ*fbcC* ETC mutants displayed a PYO reduction phenotype (Figure 2A) and some reduced phenazine derivatives localize to the cell envelope (Figure 2B), we hypothesized that phenazines were at least in part reduced by some component(s) of the ETC. To determine which component(s) contributed to phenazine reduction, we biochemically characterized the redox reactions of PYO with membrane fractions collected from stationary phase *P. aeruginosa* grown in LB. PYO was chosen as the representative phenazine because it was reduced at the highest rate by whole cells and was affected by ETC mutations (Figure 2A), suggesting any differences between test conditions would be clearest to distinguish in a biochemical assay using this phenazine. The structure of the *P. aeruginosa* ETC allows for a deductive approach to finding phenazine reduction sites by first testing dehydrogenases using different cytosolic electron donors, followed by testing downstream reduction sites using electron branch point donors (Figure 1A, blue electron donors). Of the known cytosolic electron donors (*i.e.*, NADH, succinate, lactate, malate, and glycerol-3-phosphate), only NADH caused significant PYO reductase activity (Figure 3A). To ensure the membrane fractions had activity in each of the dehydrogenases being tested, we also assayed them for reduction of a synthetic analogue of their natural electron acceptor, ubiquinone-1 (Ub-1). The membrane fractions showed significant ubiquinone reductase activity for all electron donors tested except glycerol-3-phosphate, indicating the cognate dehydrogenases were present and active in the fractions

(Figure 3B). Given the absence of glycerol-3-phosphate:Ub-1 oxidoreductase activity, we cannot comment on the phenazine reductase activity of the glycerol-3-phosphate dehydrogenase (GPDH).

Although these results implicated the NADH dehydrogenases in phenazine reduction, they did not rule out the possibility that electrons were being passed to a downstream reduction site. We tested this scenario by assaying each of the electron branch points in the ETC, namely NADH, ubiquinol, and reduced cytochrome *c*. However, we observed again that only NADH caused significant PYO reduction (Figure 3C). Because the bc_1 and CCO complexes had been implicated in PYO reduction (Figure 2A), we ensured they were present and active in our membrane fractions by assaying the membrane fractions for their respective activities. The fractions showed significant cytochrome *c* reductase and oxidase activity, and those activities were dependent on the expected genes knocked out in this study (Figure 3D). Altogether, these results show that when grown on LB, the stationary-phase ETC in *P. aeruginosa* reduces PYO solely through one or some combination of the NADH dehydrogenases.

The Nqr complex has the largest phenazine reductase contribution

We next asked what the relative contribution to PYO reduction was for each of the NADH dehydrogenases. *P. aeruginosa* contains three NADH dehydrogenases in its genome: the Nuo complex, the Ndh enzyme, and the Nqr complex first identified in *Vibrio* species (33). We made knockouts of these enzymes' activity by clean deleting the genes encoding their NADH-oxidizing domains, *i.e. nuoF*, *nqrF*, and the whole gene in the case of *ndh*. The Δ*phz1/2* Δ*nuoF* mutant displayed a growth phenotype that was complemented by insertion

of the *nuoF* gene in *trans* at the *att*Tn7 site (Figure S1). The Δ*phz1/2* Δ*nqrF* and Δ*phz1/2* Δ*ndh* mutants had no growth defect (Figure S1). Similar growth phenotypes were seen in LB (Figure S3) and are consistent with one prior study of NADH dehydrogenases in *P. aeruginosa* strain PAO1 (34), while contrasting findings in another study in PAO1 that showed none of the NADH dehydrogenase mutations resulted in a growth defect (35). We assayed the mutants' membrane fractions for NADH:PYO oxidoreductase activity (hereafter abbreviated PYO reductase activity). We also assayed the PYO reductase activity of membrane fractions collected from the clean deletion mutants in the bc_1 (Δ*phz1/2* Δf*bcC*) and CCO (Δ*phz1/2* Δ*cco1/2*) complexes to assess if these strains' previously observed PYO reduction phenotypes in whole cells could be explained by changes in their membranes' PYO reductase activity.

Interestingly, there was no decrease in the PYO reductase activity of the membrane fractions of the bc_1 and CCO mutants (Figure 4A). Deletion of the *ndh* gene resulted in no activity change, while deletion of the *nuoF* and *nqrF* genes each significantly decreased the activity of the membrane fractions (Figure 4A). However, when also assayed for NADH:Ub-1 oxidoreductase activity, the membrane fractions from Δ*phz1/2* Δn*uoF* and Δ*phz1/2* Δ*nqrF* showed a decrease in activity (Figure 4B), so it was possible that the decrease in PYO reductase activity was only due to changes in overall NADH dehydrogenase activity in the membrane fractions. Attempting to clarify our interpretation, we made NADH dehydrogenase double mutants and assayed their activities as well. Multiple attempts to construct an NADH dehydrogenase triple mutant were unsuccessful.

While all the membrane fractions from the double mutants showed decreased NADH:Ub-1 oxidoreductase activity, the activity was equal between them (Figure 4C),

allowing for an even comparison of the relative phenazine reductase activity of each NADH dehydrogenase. In these membrane fractions, we observed a pattern of PYO reductase activity consistent with that of the single mutants, where the membrane fraction containing Nqr only had the highest activity, followed by Nuo only, and lastly Ndh only, which displayed minimal activity above the no membrane protein control (Figure 4D). We also assayed these membrane fractions for their PCN and PCA reductase activity. PCN and PCA were reduced at rates about 20 times slower than PYO, qualitatively but not quantitatively consistent with differences in whole cells (Figure 4D, Figure 2A). Both showed the same pattern of reduction largely dependent on the Nqr complex. From these results, the order of phenazine reductase activity of the NADH dehydrogenases in *P. aeruginosa* appears to be Nqr > Nuo > Ndh, though this model requires validation with purified proteins.

PCN is predominantly reduced at the inner membrane, while PYO is predominantly reduced in the cytosol

Given the consistent patterns of phenazine reductase activity observed in our biochemical experiments, we asked whether the same patterns of reduction in our NADH dehydrogenase double mutants would be reflected in whole cells. This was tested using the same assay as in Figure 2A. We found that PCN reduction patterns by the NADH dehydrogenase double mutant strains matched the results observed biochemically, while PYO patterns did not (Figure 5). The mutants displayed minor deficits in PYO reduction relative to the overall reduction rate (Figure 5), which together with our biochemical results implied that the majority of PYO reduction *in vivo* occurs in the cytosol. No significant differences were observed in PCA reduction between the mutants (Figure 5).

Given the membrane fractions of the Ndh-only strain displayed negligible overall phenazine reduction rates (Figure 4D), we inferred that the phenazine reduction rates by whole cells of the Ndh-only mutant represent an estimate of the cytosolic contribution to the overall reduction rate observed. Assuming the contributions of the cytosol and membrane are additive, the results suggest that among the NADH dehydrogenases, Nuo predominantly contributes to PYO reduction, while Nqr predominantly contributes to PCN reduction *in vivo* (Figure 5). Variation in the measured reduction rates of PCA prevented any clear conclusion being drawn for it using this analysis.

Phenazines constitute a redox loop between the NADH and ubiquinone pools

We next wanted to test if phenazines competed with Ub-1 for a common reduction site in the NADH dehydrogenases. We found that pre-addition of equimolar Ub-1 to the PYO reductase assay completely abolished PYO reductase activity (Figure 6A). However, an alternative experiment where Ub-1 was added after PYO was fully reduced by membrane fractions revealed that PYO was rapidly oxidized by Ub-1 (Figure 6A) at rates that were too fast to measure with our system. Accordingly, we tested if this reaction depended on the presence of membrane fractions by reducing PYO with limiting dithionite and then adding Ub-1. We found that membrane fractions were not necessary to recapitulate the rapid reaction, and that it also occurred with PCN and PCA (Figure 6B). Given the rapid oxidation of phenazine by Ub-1, we cannot comment on the competition between these substrates for a common binding site in the NADH dehydrogenases. However, together with our previous results implicating NADH as the predominant reductant for phenazine reduction via the ETC (Figure 3A, 3C), these data revealed that phenazines can form a redox loop between the

NADH and ubiquinone pools, flux through which is limited by the reduction rate of phenazines. The clear reduction of phenazines observed in our prior anoxic assays (Figure 3, 4) implies that under those assay conditions, any endogenous ubiquinone present in the membrane fractions was rapidly reduced once the reaction was initiated.

Discussion

Spurred by an interest in the redox mechanisms underlying phenazines' enhancement of anaerobic survival, we undertook this study to characterize phenazine interactions with the ETC. Phenazine reductase activity of membrane fractions isolated from ETC mutants revealed that the NADH dehydrogenase complex Nqr has the highest phenazine reductase activity in the membrane regardless of the derivative, with lower activity from the Nuo complex and minimal activity from Ndh (Figure 4D). Interestingly, we found that in whole cells, our biochemical results were recapitulated with PCN reduction, but not PYO, implying that PYO is predominantly reduced in the cytosol (Figure 5). The smaller fraction of PYO reduction occurring at the inner membrane is predominantly carried out by the Nuo complex (Figure 5, 7A). This contrasts with PCN, which is predominantly reduced at the inner membrane by the Nqr complex (Figure 5, 7A). We also show that PYO and PCN localize to the cell envelope once reduced (Figure 2B,C), and that phenazines are rapidly and non-enzymatically oxidized by ubiquinone, which would permit the formation of a redox loop between the NADH and ubiquinone pools (Figure 6, 7B).

Our results clarify previous work that showed mutants in the bc_1 complex and cbb_3-type cytochrome *c* oxidase complexes displayed phenazine reduction deficits. In particular, it was found that mutants in the bc_1 complex grown planktonically displayed a PYO

reduction deficit (18), and that mutants in the CCO complexes showed biofilm spatial redox profiles consistent with a phenazine-null mutant (19). In contrast to the implication that these complexes may act directly as reductases, our results show that changes in the whole cell reduction rates of these mutants are not due to any changes in the phenazine reductase activity of the ETC (Figure 4A). These phenotypes instead likely arise due to indirect effects of perturbing these critical components of metabolism. Indeed, *P. aeruginosa*'s growth rate is highly dependent on its ETC composition (25); Figure S1, S3), and under most conditions it relies on flux through the bc_1 complex and the cbb_3-type oxidases (26,27). We speculate that removal of these complexes may cause changes to the steady-state cytosolic flavoprotein concentration to balance metabolic fluxes between the cytosol and the membrane, limiting the number of reaction sites available in the cytosol for PYO reduction. This interpretation is consistent with the fact that whole cell reduction rates of PCN, the derivative that our data suggests is predominantly reduced at the inner membrane, are not significantly affected by mutation of the bc_1 complex and the cbb_3-type oxidases (Figure 2A).

Though our results suggest PYO is predominantly reduced in the cytosol, a significant fraction appears to also be reduced by membrane NADH dehydrogenases. Paradoxically, in membrane fraction assays employing mutants where only a single NADH dehydrogenase was active, Nqr had the highest PYO reductase activity but in whole cells Nuo appears to make the largest contribution to PYO reduction (Figure 4D, 5). This incongruence is intriguing given the accord between these experiments observed for PCN using the same strains (Figure 4D, 5). It seems likely that these differences may arise from the different chemical properties of the phenazine derivatives that impact their ability to cross membranes, either by diffusion or active transport. Transport presents an important hurdle to

phenazine reduction that could be limiting in whole cells but that is eliminated *in vitro*, and thus a better understanding of phenazine trafficking within the cell is needed—including both enzymatic and non-enzymatic components. Indeed, that PYO localizes to the envelope after reduction (Figure 2B,C) despite being predominantly reduced in the cytosol (Figure 4D, 5) exemplifies that phenazines' redox state likely affects their subcellular localization. It also seems probable that the rate of PCA reduction is limited by this trafficking in the cell, given it is charged at circumneutral pH and none of the NADH dehydrogenase mutations we tested had any significant effect on whole-cell PCA reduction despite their effect on PCA reduction *in vitro* (Figure 5, Figure 4D).

Importantly, phenazines, along with many redox-active secondary metabolites, have higher redox potentials than the NADH pool (-320 mV) but lower ones than the quinone pool (+100 mV), meaning they are expected to be reduced before quinones in the ETC. Though lactate and malate both have low enough midpoint potentials to reduce phenazines, the lack of PYO reductase activity in membrane fractions using these donors (Figure 3A) suggests there is some specificity to phenazine reduction. Clarifying the nature of this specificity is a priority for future research that may additionally shed light on where phenazines are reduced within the NADH dehydrogenase complexes. NADH dehydrogenases contain at least two active sites, one for NADH oxidation and the other for ubiquinone reduction. Elucidation of whether phenazines are reduced at the ubiquinone reduction site and if phenazine reduction supports proton pumping via these complexes has important bioenergetic implications (Figure 7B, boxed). The Nqr complex in *P. aeruginosa*, which displayed the highest phenazine reductase activity (Figure 4D), was recently shown to translocate protons (36). Proton translocation via respiration of a self-produced terminal electron acceptor would be

advantageous to cells otherwise limited for oxidants, and we hypothesize could be a major contributor to overall energy conservation during phenazine-dependent anaerobic survival.

At a larger scale in the context of mature biofilms, NADH dehydrogenase expression profiles are largely unknown. One prior study in PAO1 using Δ*nuoG*, Δ*nqrF*, and Δ*ndh* strains found that while the Δ*ndh* strain exhibited a Crystal Violet retention deficit, each of the NADH dehydrogenase mutants grew into mature biofilms indistinguishable from wild-type in surface-area and thickness (35), indicating that interchangeability or compensation between the dehydrogenases is possible without affecting biofilm growth yield. However, our results suggest interchangeability does not apply to phenazine reduction given that NADH dehydrogenase mutants had significantly different whole cell reduction rates (Figure 5). Given prior work has implicated PCN as being retained in the interior of the biofilm while PYO occupies the periphery (12,30), investigating how the specificity of phenazine reduction elucidated here corresponds to spatial expression of the dehydrogenases in biofilms is an interesting avenue for future research. Moreover, that PCN reduction is predominantly achieved by the Nqr complex (Figure 5) makes PCN an attractive candidate for being the primary terminal electron acceptor in the biofilm core. We hypothesize that if EET-dependent metabolism occurs in the core, PCN would stimulate the highest net energy conservation compared to other derivatives because its reduction largely circumvents promiscuous phenazine reactions with other flavoproteins in the cytosol, allowing for more specific oxidation of the NADH pool and therefore an increased rate of substrate-level phosphorylation.

While in the absence of oxygen, phenazine reduction may provide a bioenergetic benefit, in the presence of oxygen, reduction at the membrane may carry costs—particularly the loss of

reducing equivalents from the downstream ETC and the production of reactive oxygen species (ROS; (3,37). In addition to scavenging ROS via superoxide dismutases and catalase (38), the ability to limit phenazines' reaction with oxygen might help. Our findings suggest that the rapid oxidation of reduced phenazines by ubiquinone has the potential to serve in this capacity. We present a working model of phenazine reduction under different conditions in Figure 7B. When terminal electron acceptors like oxygen or N-oxides become depleted, the availability of ubiquinone becomes limited and the phenazine pool accumulates electrons, serving as an electron shuttle to distant oxidants until oxygen or N-oxides return. Under oxic conditions, the cell stands to dissipate reducing equivalents if phenazines shuttle electrons directly to oxygen. Intriguingly, our results reveal nearly instantaneous phenazine oxidation by quinone *in vitro* (Figure 6B), while the half-life of reduced phenazine in the presence of oxygen is on the order of minutes under hypoxic conditions (2% oxygen)(20). Assuming that electron transfer from phenazine to ubiquinone is similarly fast in cells, we hypothesize that under some oxygen concentrations ubiquinone may outcompete oxygen for electrons from phenazines *in vivo*. It is tempting to speculate that the rapid localization of reduced phenazine to the cell envelope (Figure 2B,C) may aid in this. By outcompeting oxygen, not only would ROS generation be mitigated, but a fraction of electron flux through energy-conserving steps of the ETC could remain intact in the presence of phenazine (Figure 7B). This proposed mechanism would appear most salient to PCN, as the *in vitro* reduction rate of PCN is slower than the NADH oxidation rate driven by Δ*phz1/2* membrane fractions when aerobically respiring (0.14 ± 0.03 μmol min^{-1} mg^{-1}, data not shown), whereas PYO reduction is about four times faster than the aerobic respiration rate and would therefore likely overwhelm the ubiquinol oxidation rate of the ETC. Careful hypoxic studies that allow

direct measurements of ETC flux upon addition of reduced phenazine are necessary to test this hypothesis and are a priority for future research.

Methods

Bacterial strains and culture conditions

Strains used in this study are listed in Table S1. Experiments were conducted with *P. aeruginosa* UCBPP-PA14 strains streaked from 15% glycerol freezer stocks onto LB-agar and incubated overnight at 37˚C or over two-three days at room temperature. In liquid culture, phenazine biosynthesis occurs during the onset of stationary phase (39) and contributes to the survival of non-growing cell populations, so we chose to assay cells in stationary phase as the relevant physiological state. Since *P. aeruginosa* PA14 reaches the onset of stationary phase within approximately 6 h in lysogeny broth (LB, Difco) at 37˚C, 250 RPM, a standard culture incubation time of 20 h was chosen to ensure the culture population was no longer growing. LB was chosen as the experimental medium to maximize growth yield for membrane collection. For growth experiments confirming proper complementation, growth curves were conducted in 96-well plates in a minimal medium consisting of MOPS (100 mM, pH 7.2, adjusted with NaOH), NH_4Cl (50 mM), KH_2PO_4 (3.7 mM), and $MgSO_4$ (1 mM). The medium was supplemented at the beginning of experiments with $FeSO_4$ (3.6 μM, solubilized fresh) and D-glucose (20 mM). Overnight LB cultures with an OD_{500nm} between 5 and 6 (depending on the growth yield of the strain) were used to inoculate fresh minimal medium on the plate. Growth was measured at 500 nm optical density using a BioTek Epoch 2 plate reader held at 37˚C with continuous shaking set to slow at a 4 mm orbit.

Mutant strain construction and complementation

All plasmids used in this work are listed in Table S1. Primers were synthesized by Integrated DNA Technologies and are listed in Table S2. For all molecular cloning, plasmids were constructed using Gibson assembly. Plasmids were chemically transformed into *E. coli* strain S17 and then conjugated into *P. aeruginosa* PA14. Mutants were constructed using standard homologous recombination using 1 kb regions flanking the gene(s) of interest in the pMQ30 plasmid (40). Genetic complement strains were constructed by reintroducing the deleted gene or operon in *trans* at the *att*Tn7 site downstream of *glmS* in the *P. aeruginosa* genome using the pJM220 plasmid (41,42). For each complementation, the gene or operon was designed to have its expression driven by a rhamnose-inducible promoter, and accordingly all complementation experiments were conducted using cultures grown in media supplemented with L-rhamnose (0.005% w/v, 305 μM).

Synthesis of PYO

PYO was synthesized from phenazine methosulfate (Fischer) using a protocol described previously (43) with slight modifications. Changes included eliminating purification of PYO via thin-layer chromatography plates and utilizing dichloromethane in the place of chloroform. PYO was analyzed for purity via high-performance liquid chromatography analysis and was found to be >95% pure. Lyophilized PYO was stored at 4 °C until use. Other phenazines were purchased commercially as solid stocks: phenazine-1-carboxylic acid, Princeton Biomolecular; phenazine-1-carboxamide, Chemscene.

Whole cell phenazine reduction assay

Phenazine reduction by cells was monitored in a clear 96-well plate on a BioTek Synergy HTX plate reader housed in an anaerobic chamber (Coy). Media and plastics were allowed to equilibrate to the anoxic headspace for at least three days in the chamber prior to the experiment. Stationary phase cultures were washed in un-supplemented minimal medium (*i.e.*, without glucose or iron added) twice, resuspended to an OD_{500nm} of 8.0, and then brought into the anaerobic chamber. We found separately that such suspensions of strains with intact respiration (Δ*phz1/2*) and impaired respiration (Δ*phz1/2* Δ*cco1/2*) depleted oxygen from their medium in 30-45 min, as indicated by the addition of resazurin (10 μM). The cell suspensions' OD did not change during this time. Therefore, the cell suspensions were left to rest in the chamber for 1 h (without resazurin) before being diluted into N_2-sparged, un-supplemented minimal medium (pH 7.0) with 100 μM of the appropriate phenazine to a final OD_{500nm} of approximately 0.4 and final volume of 200 μL. The minimal medium was stored in the anaerobic chamber between experiments and protected from light because MOPS buffer is light-sensitive and can become discolored over time. Absorbance was simultaneously monitored at 440 nm and 690 nm every 2 min for 3 h at 30˚C, with continuous shaking set to slow at a 4 mm orbit. Slopes were acquired from the steepest linear regions of the reduction curves, fit using a least-squares regression. The slope of controls lacking phenazine were subtracted from the reduction rates as background and never exceeded 10% of the measured reduction rate. Beer's law was used to convert absorbance measurements to concentrations for this and all other kinetic absorbance experiments. An average pathlength of 0.525 cm was used, the average measured across the plate. The following phenazine extinction coefficients were used (measured for this study, data not

shown): reduced phenazine carboxylic acid (PCA), ε_{440nm} = 2381 M^{-1} cm^{-1}; reduced phenazine carboxamide (PCN), ε_{440nm} = 5053 M^{-1} cm^{-1}; oxidized pyocyanin (PYO), ε_{690nm} = 4351 M^{-1} cm^{-1}.

Anoxic microscopy of reduced phenazines

Reduced phenazines were imaged using a Nikon Eclipse Ti-2 inverted microscope outfitted with a custom OKOLab closed stage insert with a gas line hookup that allowed for constant N_2 flushing of the sample during the experiment. Gas flow was controlled through the OKOLab bold line system, and temperature was maintained at 25˚C using a secondary OKOLab temperature control vestibule housing the entire stage of the microscope. Stationary phase Δ*phz1/2* Δ*pvdA* Δ*pchE* cultures were spotted under agarose (1% w/v), MOPS (50 mM, pH 7.0), and appropriate phenazine (100 μM) pads. Pads were incubated in the N_2-flushing stage insert for 5 min before imaging began. Timelapses were acquired for 1 min with an ORCA-Flash4.0 V3 camera (Hamamatsu) with images taken every second in phase contrast and fluorescence at 395ex/528em through a 100x objective. Excitation light was supplied through a SpectraX LED light engine for a 200 ms exposure, and emission light was passed through a standard GFP filter cube (Semrock) with the excitation filter removed. Final images from the timelapse are shown. Due to large differences in fluorescence brightness between phenazine derivatives, fluorescence LUTs were adjusted independently for each phenazine to maximize ease of visualization.

To quantify the on-cell fluorescence for each phenazine, approximately 2.2 micrometer lines with a 7-pixel width were manually drawn along the short-axis of 15 random cells in the phase contrast images. The corresponding fluorescence values along

those lines were averaged across cells, and the minimum value of the average profile was subtracted to compare the fluorescence above background across conditions.

Membrane fractionation

One liter of LB in a 2.8 L baffled flask was inoculated with an overnight LB culture of the strain of interest (OD_{500nm} 3.5 to 6, depending on the growth yield of the strain) to a starting OD_{500nm} of approximately 0.03. The culture was incubated at 37˚C and shaken at 150 RPM for 20 h. The cultures were centrifuged at 8000*xg* to pellet cells. Spheroplasts were formed by resuspending the cell pellet in cold hypertonic solution (0.5M sucrose, 20 mM Tris-HCl, pH 8), adding lysozyme to a final concentration of 150 µg/mL, incubating for 5 min on ice, and then diluting the suspension with cold water to a final concentration of 0.25 M sucrose. $MgCl_2$ was added to a final concentration of 20 mM to stabilize the spheroplasts. The suspension was centrifuged at 6800*xg* to pellet the intact spheroplasts, which were then resuspended in isotonic solution (0.25 M sucrose, 10 mM Tris-HCl, pH 8). One tablet of Sigmafast™ protease inhibitor cocktail (EDTA-free) was solubilized in a milliliter of isotonic solution and added to the suspension, along with DNase (Sigma), RNase (Sigma), and $MgCl_2$ to final concentrations of 15 µg mL^{-1}, 15 µg mL^{-1}, and 1 mM, respectively. The suspension was lysed by running the sample through an Avestin Emusiflex-c3 homogenizer for 1 min at approximately 17,500 psi with recirculation. The Emulsiflex homogenizer produces a heterogeneous mix of inverted and non-inverted vesicles such that reactions occurring on both faces of the inner membrane can be assayed. Lysate was centrifuged at 8000*xg* and the supernatant collected to remove intact cells. The lysate was then centrifuged at 38,000*xg* for 1 h on a Beckman Optima ultracentrifuge to pellet the membrane fraction.

Membrane fractions were resuspended in MOPS (50 mM, pH 7.2), KCl (150 mM), N-dodecyl-β-D-maltoside (DDM, 0.05% w/v) and flash-frozen as ~30 µL drops in liquid nitrogen. Frozen droplets were stored at -80˚C and thawed as needed. Protein concentration was determined using the Bradford method. Thawed membrane fractions were kept at room temperature during experiments: it was observed that keeping them on ice accelerated precipitation of protein. There was no measurable change in activity of the fractions over the timespan of an experiment.

Membrane fraction biochemical assays

Membrane fractions were assayed for various enzyme activity using a Thermo Scientific Evolution 260 Bio UV-Vis Spectrophotometer housed in an anaerobic chamber (Coy), except for experiments measuring the reduction of ubiquinone-1 at 280 nm (detailed below). Plastics used for experiments were allowed to equilibrate to the anoxic headspace for at least three days. Reactions were conducted in semi-micro polystyrene cuvettes (Greiner) with 500 µL reaction volumes. The reaction buffer consisted of N_2-sparged MOPS (50 mM, pH 7.2) and KCl (150 mM) that was stored in the anaerobic chamber and protected from light. At the start of the experiment, the buffer was supplemented with DDM (0.05% w/v) and an oxygen-scrubbing enzyme system which included glucose oxidase (375 nM, Sigma), catalase (750 nM, Sigma), and D-glucose (10 mM). Initial investigations lacking this oxygen scrubbing system were characterized by significant fluctuations between technical replicates and day-to-day experiments using the same reagents. Replicability was sharply improved with its inclusion. Membrane fractions were added to a final protein concentration of 0.25 mg mL^{-1} for all reactions. Reactions were conducted at room

temperature and in all cases were initiated with the addition of the electron donor. In the case of no electron donor controls, reactions were initiated with the addition of membrane protein.

For phenazine reduction experiments, stock phenazine solutions were stored at 4˚C and aliquots were brought into the anaerobic chamber. All electron donor solutions were made fresh, solubilized anoxically in un-supplemented reaction buffer (*i.e.*, without DDM or the oxygen-scrubbing enzyme system). This included NADH disodium salt (Sigma), sodium succinate dibasic hexahydrate (Sigma), sodium DL-lactate (Sigma), L-malic acid (MP Bio), and sn-glycerol-3-phosphate lithium salt (Sigma). The reaction was monitored for 1 min for PYO reduction, 4 min for PCN, and 10 min for PCA. Absorbance was measured at the wavelengths listed above to monitor reduction of each phenazine derivative, and the extinction coefficients listed above were again used.

For cytochrome bc_1 activity assays, decylubiquinol was prepared by reducing decylubiquinone (Sigma) with sodium dithionite according to a previously published protocol (44). The decylubiquinol solutions in DMSO were stored in aliquots at -80˚C. At the start of each experiment an aliquot was thawed and brought into the anaerobic chamber. Solutions of oxidized bovine cytochrome *c* (Sigma) were prepared fresh for each experiment, solubilized anaerobically in un-supplemented reaction buffer. Cytochrome *c* reduction was monitored at 550 nm with an extinction coefficient of ε_{550nm} = 18.5 mM^{-1} cm^{-1} (45). Final DMSO concentration in each reaction was 0.5% (v/v).

For cytochrome *c* oxidase activity assays, reduced cytochrome *c* was prepared fresh for each experiment as described previously (45) with the modification of adding anoxically solubilized dithionite in equimolar concentration to reduce a solution of oxidized cytochrome *c*. The absorbance ratio of 550 nm versus 565 nm of a 20 μM solution was confirmed to be

above 10 before use. Air-equilibrated reaction buffer was made fresh for each experiment at the bench (supplemented only with DDM) and brought into the anaerobic chamber. Cytochrome *c* oxidation was monitored at 550 nm with the same extinction coefficient as above.

For NADH oxidation experiments, ubiquinone-1 (Sigma) was solubilized in DMSO and aliquots stored at -80˚C were thawed and brought into the anaerobic chamber. NADH was solubilized fresh and anoxically as above. NADH oxidation was monitored at 340 nm with an extinction coefficient of $\varepsilon_{340nm} = 6.22\ mM^{-1}\ cm^{-1}$ (Sigma). Final DMSO concentration in each reaction was 0.5% (v/v).

Ubiquinone-1 reduction experiments were assayed on a BioTek HTX plate reader in an anaerobic chamber using a quartz 96-well plate. Reactant concentrations were the same as in phenazine reduction experiments with various ETC electron donors, except with ubiquinone-1 as the acceptor and in 200 µL reaction volumes. Reduction was monitored at 280 nm with an extinction coefficient of $\varepsilon_{280nm} = 6.03\ mM^{-1}\ cm^{-1}$ (measured for this study, difference between oxidized and reduced extinction coefficients, data not shown).

Phenazine oxidation by ubiquinone-1 experiments were conducted using the same reaction buffer as above. Dithionite was solubilized anoxically in un-supplemented reaction buffer and added in equimolar concentration to the phenazine for each reaction.

Data analysis and plotting

Data processing and analysis were done in Python 3.7. Image processing and analysis were done in ImageJ 1.52. Plotting and 95% confidence interval calculations were done in GraphP**ad Prism 9.**

Figures

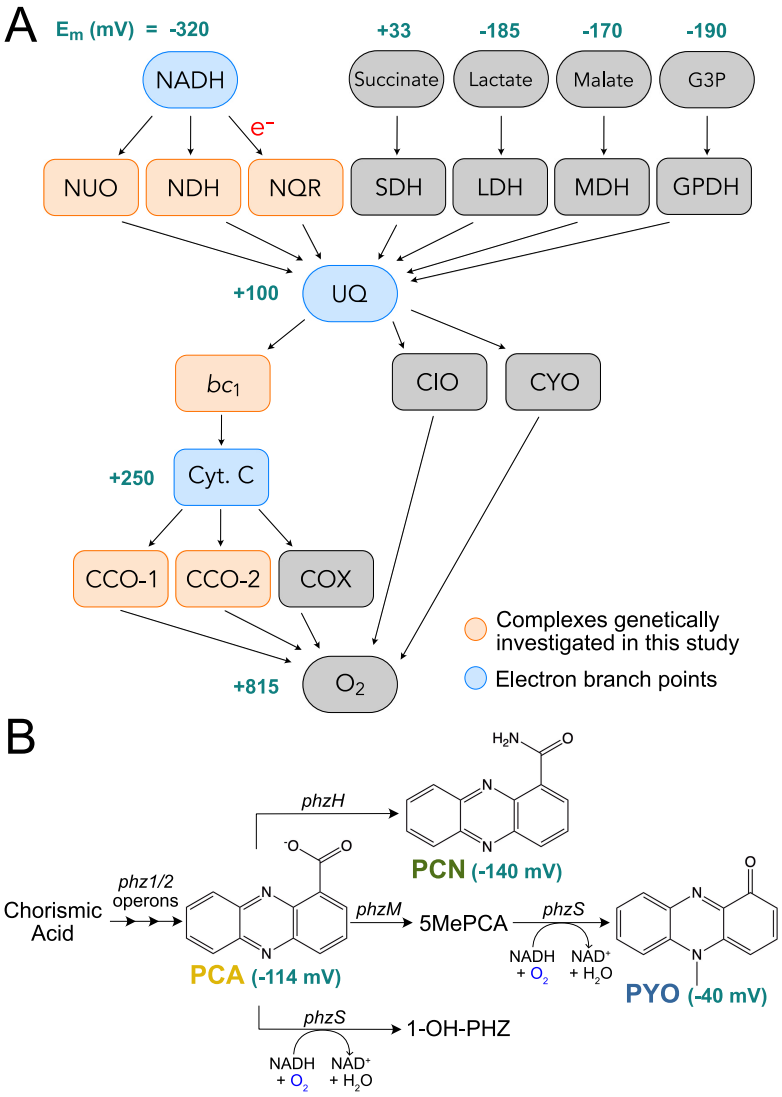

Figure 1: Schematic of *P. aeruginosa* phenazine biosynthesis and electron transport chain. (A) Possible electron paths from cytosolic electron donors to oxygen are shown as arrows. Donors' standard midpoint potentials vs. SHE at pH 7.0 are shown in teal (48). G3P, glycerol-3-phosphate. (B) Phenazine-1-carboxylic acid is synthesized via the gene products of either of two core synthesis operons, and modifications via the gene products shown produce other phenazine derivatives. Structures of the derivatives studied in this work are displayed along with their standard midpoint potentials vs. SHE at pH 7.0 in teal (20). PCA, phenazine-1-carboxylic acid; PCN, phenazine-1-carboxamide; 5MePCA, 5-methyl-phenazine-1-carboxylic acid; PYO, pyocyanin; 1-OH-PHZ, 1-hydroxy-phenazine.

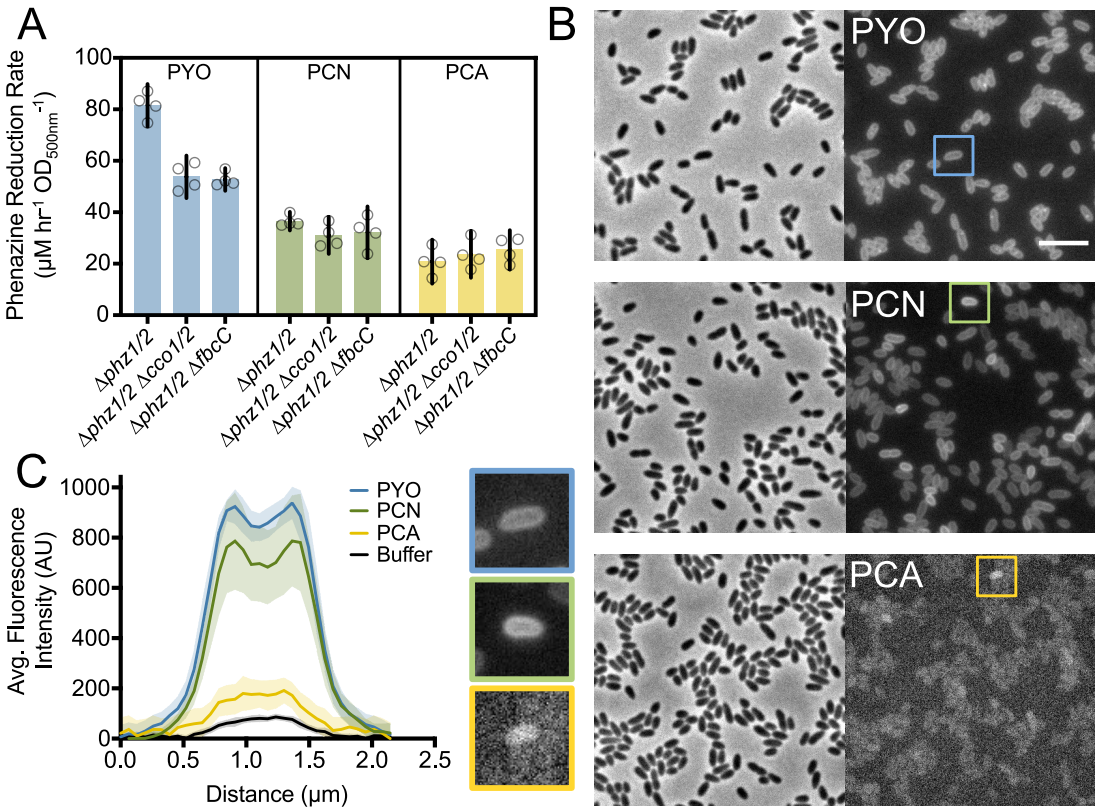

Figure 2: Whole-cell phenazine reduction rates and sub-cellular localization of reduced phenazine derivatives. (A) Anaerobic phenazine reduction rates by Δ*phz1/2* cells in a MOPS minimal medium (pH 7.0) lacking a carbon source. Each data point represents an independent biological replicate and error bars represent the 95% confidence interval of the mean. (B) Phenazines were reduced by Δ*phz1/2* Δ*pvdA* Δ*pchE* (phenazine and siderophore null) cells and directly imaged using a fluorescence microscope. Cells were incubated under MOPS (pH 7.0) agar pads and constantly flushed in a sealed stage chamber with N_2 gas. Left images, phase contrast; right images, corresponding fluorescence at 395 nm ex / 528 nm em. Right edge is 25 μm, scale bar is 5 μm. Images are representative of two independent experiments with six total fields captured per condition. (C) Background-subtracted average fluorescence profiles drawn along the short axis of 15 random cells per condition. Shaded regions represent the 95% confidence intervals. Representative fluorescence images of single cells are shown for each phenazine derivative. Right edge is 4.1 μm.

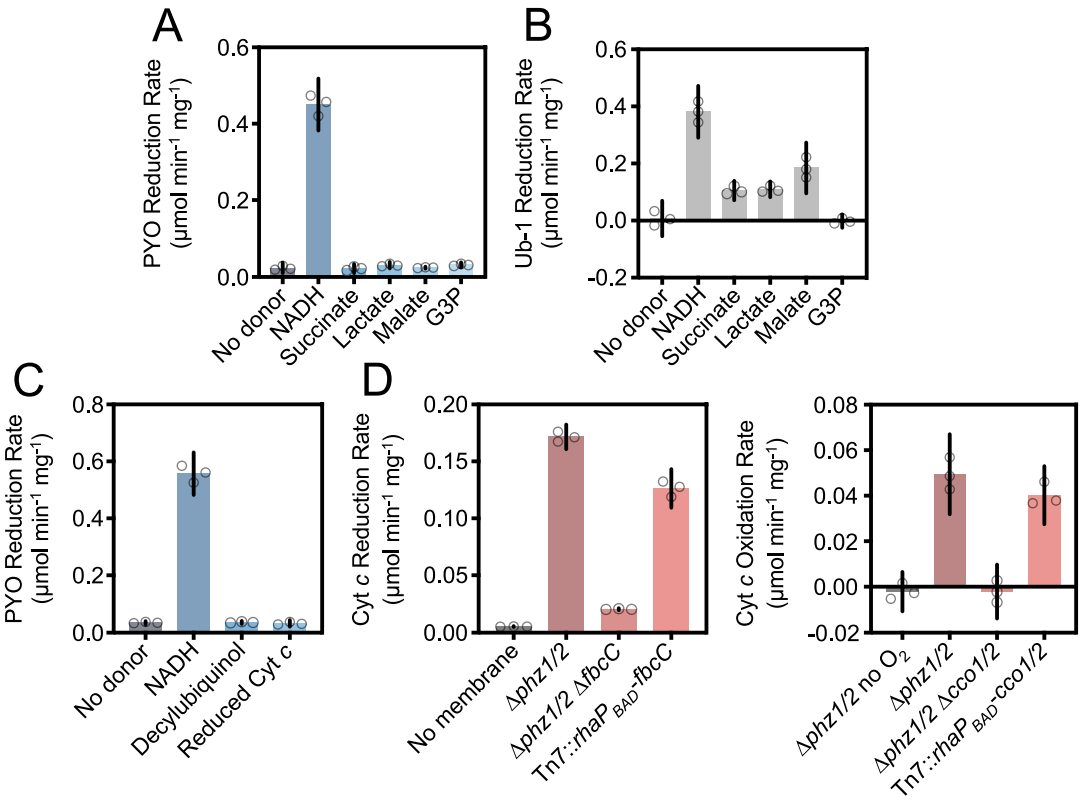

Figure 3: Pyocyanin reductase activity of Δ*phz1/2* membrane fractions using various electron donors. (A) Anaerobic PYO reduction rates using various ETC electron donors. Reaction contained 150 µM PYO and NADH, 1.5 mM of other electron donors, and 0.25 mg mL^{-1} membrane protein. Reaction buffer contained an oxygen scavenging enzyme system (see Experimental Procedures). (B) Ubiquinone-1 reduction rates using the same electron donors and reaction buffer as in A. Reactions contained 150 µM Ub-1. (C) PYO reduction rates using electron branch point donors, measured as in A. Reactions contained 150 µM decylubiquinol and 75 µM reduced cytochrome *c*. (D) Cytochrome *c* reduction and oxidation rates and their activities' dependence on the *fbcC* gene and *cco1/2* operons, respectively. Complementations (indicated by Tn7::X) were performed in the respective mutant backgrounds. In the cytochrome *c* oxidation experiment only, all reactions were assayed using air-equilibrated buffer except for the first, where 'no O_2' indicates inclusion of the oxygen scavenging system. In all plots, data points represent technical replicates, error bars represent the 95% confidence interval of the mean, and data shown are representative of two experiments using independent membrane preparations.

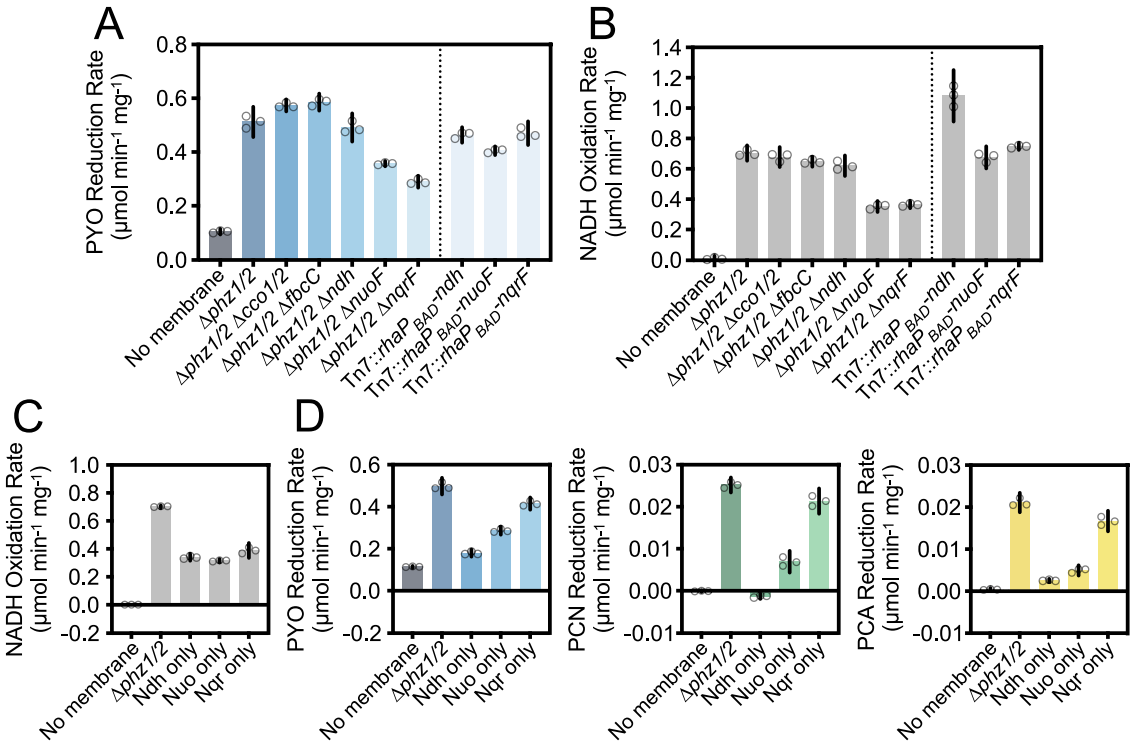

Figure 4: Anaerobic NADH:phenazine and NADH:Ub-1 oxidoreductase activity of NADH dehydrogenase mutant membrane fractions. (A) PYO reductase activity of ETC mutant membrane fractions using the same reaction conditions as in Figure 3A. Complementations (indicated by Tn7::X) were performed in the respective mutant backgrounds. (B) NADH:Ub-1 oxidoreductase activity of the same membrane fractions as in (A). The reactions contained 150 µM NADH and Ub-1. (C) NADH:Ub-1 oxidoreductase activity of NADH dehydrogenase double mutant membrane fractions. Ndh only, Δ*phz1/2* Δ*nuoF* Δ*nqrF*; Nuo only, Δ*phz1/2* Δ*nqrF* Δ*ndh*; Nqr only, Δ*phz1/2* Δ*ndh* Δ*nuoF*. (D) NADH:phenazine oxidoreductase activity of the same membrane fractions as in (C). Reactions contained 150 µM NADH and the indicated phenazine. In all plots, data points represent technical replicates, error bars represent the 95% confidence interval of the mean, and data shown are representative of two experiments using independent sets of membrane preparations.

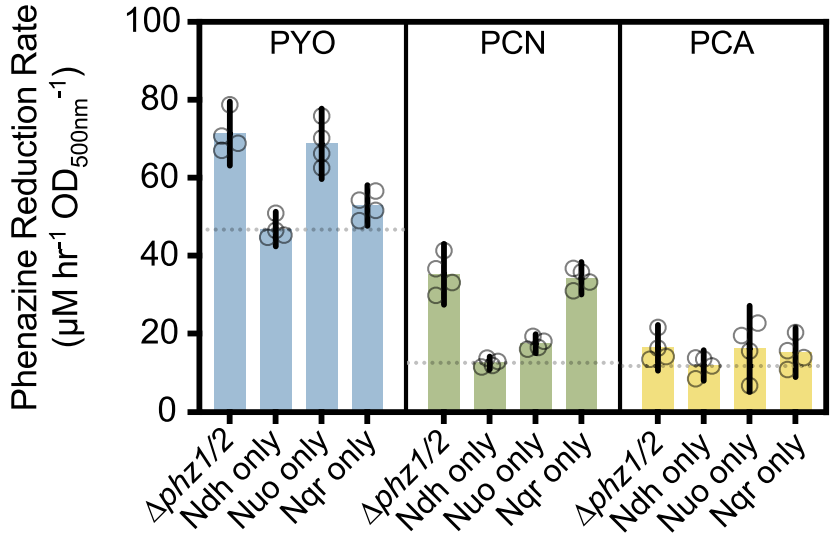

Figure 5: Whole cell phenazine reduction rates of NADH dehydrogenase double mutants. Anaerobic phenazine reduction rates using the same experimental conditions as in figure 1B. Dotted lines equal to the mean reduction rates of the Ndh only mutant, an estimate of the cytosolic reductase contribution to reduction. Each data point represents an independent biological replicate and error bars represent the 95% confidence interval of the mean.

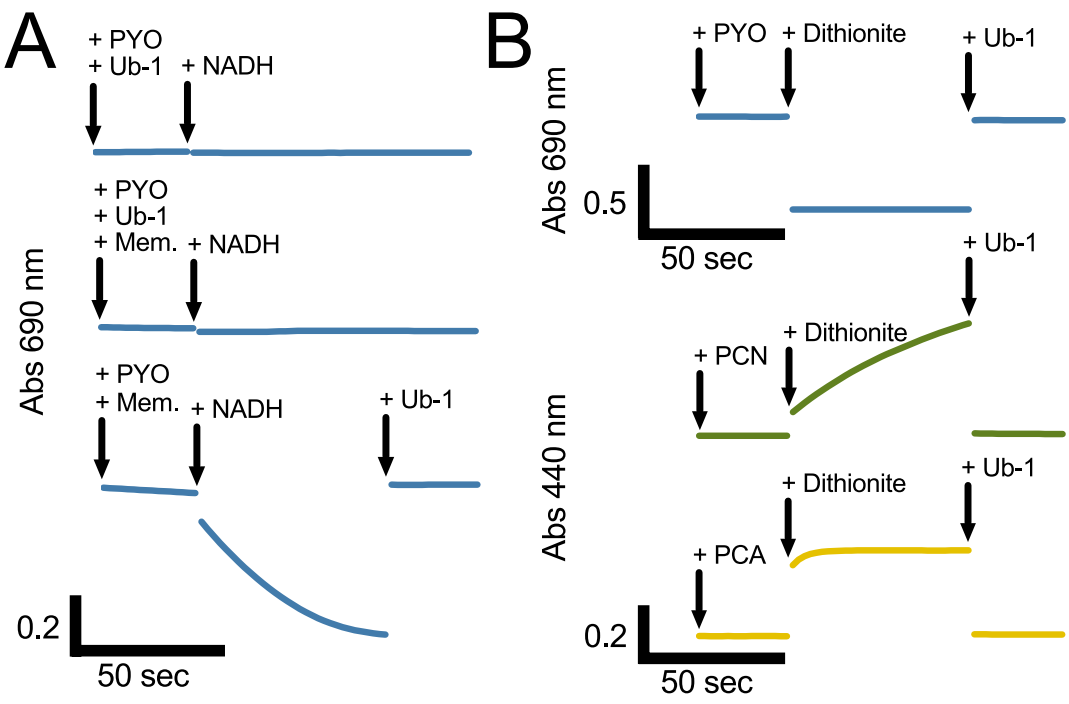

Figure 6: Phenazine oxidation by ubiquinone *in vitro*. (A) PYO reduction by Δ*phz1/2* membrane fractions and re-oxidation by Ub-1. Reactions contained 150 µM PYO and Ub-1, 75 µM NADH. All other conditions were the same as described in Figure 3A. (B) Phenazine reduction by dithionite and re-oxidation by Ub-1. Oxidized PYO absorbs at 690 nm such that reduction results in a decrease of absorbance, while reduced PCN and PCA absorb at 440 nm such that reduction results in an increase in absorbance. Reactions contained 150 µM phenazine and Ub-1 in the same reaction buffer as in Figure 3A. Plots are representative of two independent experiments, with axes shown in lower left.

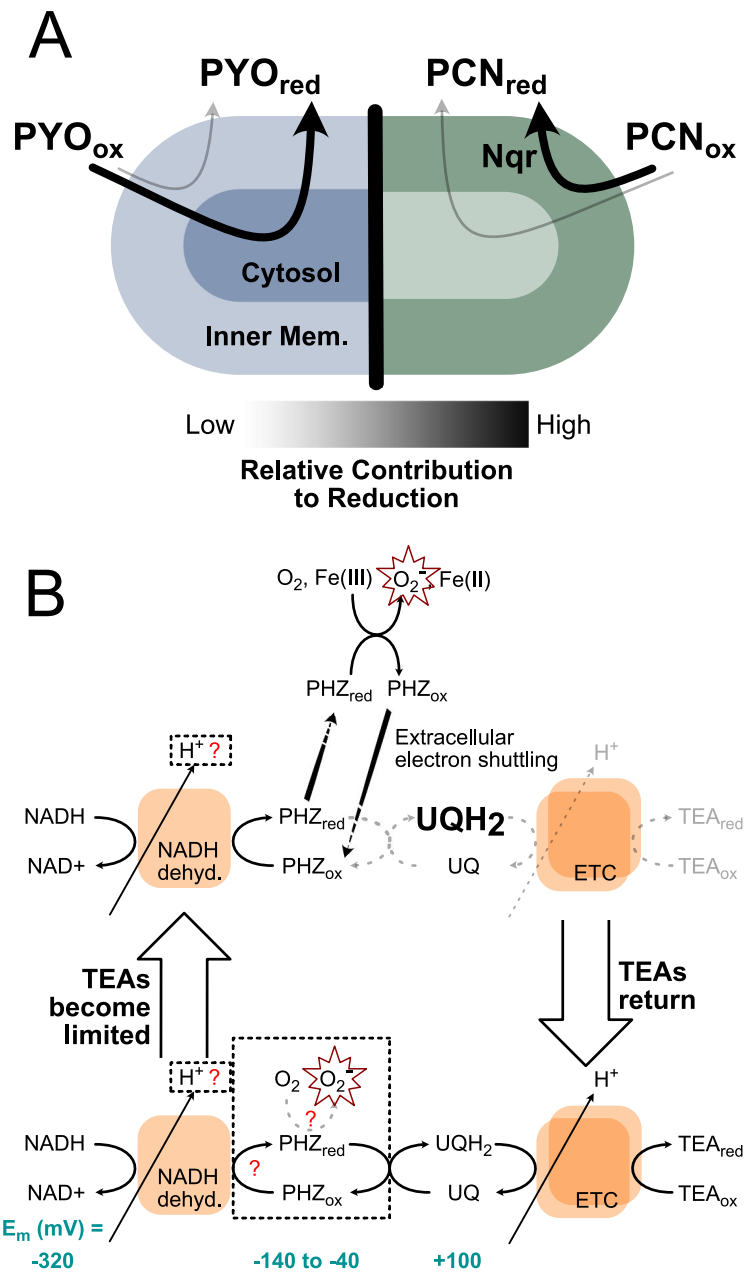

Figure 7: Working model for sub-cellular distribution of PYO / PCN and their redox reactions with the ETC in *P. aeruginosa*. (A) PYO is predominantly reduced in the cytosol, with a smaller contribution at the inner membrane from the Nuo complex. In contrast, PCN is predominantly reduced at the inner membrane by the Nqr complex. Our results do not clearly support PCA reduction being predominantly localized to one sub-cellular location. (B) When standard terminal electron acceptors (*e.g.* oxygen, N-oxides) are absent, a fraction of phenazine reduction occurs at the NADH dehydrogenases (to a degree depending on the phenazine derivative) and can shuttle electrons to distal oxidants. It is unknown if this reduction is coupled to the export of protons. When terminal electron acceptors return, it is possible phenazines form a redox loop between the NADH and ubiquinone pools as an intermediate within the ETC. It is unknown to what extent phenazines outcompete ubiquinone for electrons from NADH dehydrogenases, or to what extent ubiquinone outcompetes oxygen for electrons from reduced phenazines. The respective standard midpoint potentials vs. SHE at pH 7.0 of each redox intermediate are listed below in teal. PHZ, phenazine derivative; UQH_2, ubiquinol; UQ, ubiquinone.

Supplementary Table 1: Strains and plasmids used in this study.

Strain	Description	Reference
P. aeruginosa		
PA14 WT	DKN263, wild-type UCBPP-PA14 *Pseudomonas aeruginosa*, parent strain	Laboratory collection
PA14 Δ*phz1/2*	DKN330, phenazine-null via deletions of the phenazine biosynthesis operons *phzA1-G1* (PA14_09480 - PA14_09410) and *phzA2-G2* (PA14_39970 – PA14_39880)	Dietrich *et al*., 2006
PA14 Δ*phz1/2* Δ*pvdA* Δ*pchE*	DKN620, phenazine-null with deletions in pyoverdine (PA14_33810) and pyochelin (PA14_09270) siderophore biosynthesis genes	Wang *et al.*, 2011
PA14 Δ*phz1/2* Δ*cco1/2*	DKN2707, phenazine-null with a deletion spanning from *ccoN1* (PA14_44340) to *ccoP2* (PA14_44400)	This study
PA14 Δ*phz1/2* Δ*cco1/2, att*Tn7::*rhaP*$_{BAD}$-*cco1/2*	DKN2708, rhamnose-inducible genetic complement to PA14 Δ*phz1/2* Δ*cco1/2*	This study
PA14 Δ*phz1/2* Δ*fbcC*	DKN809, phenazine-null with a deletion in cytochrome c_1 (PA14_57540)	Price-Whelan, 2009
PA14 Δ*phz1/2* Δ*fbcC, att*Tn7::*rhaP*$_{BAD}$-*fbcC*	DKN2709, rhamnose-inducible genetic complement to PA14 Δ*phz1/2* Δ*fbcC*	This study
PA14 Δ*phz1/2* Δ*ndh*	DKN2710, phenazine-null with a deletion in *ndh* (PA14_58870)	This study
PA14 Δ*phz1/2* Δ*ndh, att*Tn7::*rhaP*$_{BAD}$-*ndh*	DKN2711, rhamnose-inducible genetic complement to PA14 Δ*phz1/2* Δ*ndh*	This study
PA14 Δ*phz1/2* Δ*nuoF*	DKN2712, phenazine-null with a deletion in *nuoF* (PA14_29970)	This study
PA14 Δ*phz1/2* Δ*nuoF, att*Tn7::*rhaP*$_{BAD}$-*nuoF*	DKN2713, rhamnose-inducible genetic complement to PA14 Δ*phz1/2* Δ*nuoF*	This study
PA14 Δ*phz1/2* Δ*nqrF*	DKN2714, phenazine-null with a deletion in *nqrF* (PA14_25350)	This study

PA14 Δ*phz1/2* Δ*nqrF*, *att*Tn7::*rhaP*$_{BAD}$-*nqrF*	DKN2715, genetic complement to PA14 Δ*phz1/2* Δ*nqrF*	This study
PA14 Δ*phz1/2* Δ*ndh* Δ*nuoF*	DKN2716, phenazine-null with two deletion mutations according to descriptions above	This study
PA14 Δ*phz1/2* Δ*nuoF* Δ*nqrF*	DKN2717, phenazine-null with two deletion mutations according to descriptions above	This study
PA14 Δ*phz1/2* Δ*nqrF* Δ*ndh*	DKN2718, phenazine-null with two deletion mutations according to descriptions above	This study
E. coli		
S17	DKN1096, host for cloning	Simon *et al.*, 1983
SM10/pTNS1	DKN1298, helper strain for triparental mating	Choi and Schweizer, 2006
Plasmids		
pJC11	2 kb fragment containing Δ*cco1/2* cloned into pMQ30	This study
pJC13	2 kb fragment containing Δ*nuoF* cloned into pMQ30	This study
pJC15	2 kb fragment containing Δ*nqrF* cloned into pMQ30	This study
pJC17	2 kb fragment containing Δ*ndh* cloned into pMQ30	This study
pJC21	*ccoN1-ccoP2* span cloned into pJM220	This study
pJC22	*fbcC* gene cloned into pJM220	This study
pJC23	*ndh* gene cloned into pJM220	This study
pJC25	*nuoF* gene cloned into pJM220	This study
pJC30	*nqrF* gene cloned into pJM220	This study

Supplementary Table 2: Primers used in this study.

Construct (source vector - cut sites)	**Primer Sequence (5'-3')**
pJC11 - Δ*cco1/2* (pMQ30 – SacI / HindIII)	
Up Fwd	ACGACGGCCAGTGCCAAGCTCGAACCGCCGAGAAAGCCGG
Up Rev	GTCGTGGGGGAGGGGAGCGCGCTATGGGCTTCCATCCACGG
Dn Fwd	CGTGGATGGAAGCCCATAGCGCGCTCCCCTCCCCCACGAC
Dn Rev	CATGATTACGAATTCGAGCTTCGAGGGACTTCTTGCGCGG
pJC13 - Δ*nuoF* (pMQ30 – SacI / HindIII)	
Up Fwd	ACGACGGCCAGTGCCAAGCTCGACTTCGACCTGCGCAAGG
Up Rev	GGCCGTCCGGCTGCAAAGCATCATACGTAGGCCTCCAGCA
Dn Fwd	TGCTGGAGGCCTACGTATGATGCTTTGCAG
Dn Rev	CATGATTACGAATTCGAGCTCTTCTGCTTGCTCAGCACCAGC
pJC15 - Δ*nqrF* (pMQ30 – SacI / XbaI)	
Up Fwd	TGCCTGCAGGTCGACTCTAGAGCAAGCAGCTCTCGGTGTT
Up Rev	GGACGGAAAGGCTCAGCCACGGGGCCTCTCCTTACAACTG
Dn Fwd	CAGTTGTAAGGAGAGGCCCCGTGGCTGAGCCTTTCCGTCC
Dn Rev	CATGATTACGAATTCGAGCTGTTGCTCGTAGCGTGG
pJC17 - Δ*ndh* (pMQ30 – BamHI / HindIII)	
Up Fwd	ACGACGGCCAGTGCCAAGCTCGAGCTGCAGGCACGGCT
Up Rev	GGCAAACGGGGCGCAATGGCGTGGATATCTCATAGTGGGAATTCCGTGAGG
Dn Fwd	TCCCACTATGAGATATCCACGCCATTGCGCCCCGTTTGC
Dn Rev	GAGCTCGGTACCCGGGGATCTCTTCATCTCGATCGATTGGCGGAGC
pJC21 - P_{rhaBAD}-*cco1/2* (pJM220 – KpnI / HindIII)	

RBS + Fwd	CAGGAATTCCTCGAGAAGCTTAAGGAGGAACAG CTATGAGCACCACTAACCCAGAGTCCG
Rev	GCAAGGCCTTCGCGAGGTACTTATTCGGCGCTCT TCTCGCCG
pJC22 - P_{rhaBAD}-*fbcC* (pJM220 – KpnI / HindIII)	
RBS + Fwd	CAGGAATTCCTCGAGAAGCTTAAGGAGGAACAG CTATGAAAAAGCAATTCGCTGCACTGA
Rev	GCAAGGCCTTCGCGAGGTACTTAGTGCACGTCCT TCCAGTACTCGC
pJC23 - P_{rhaBAD}-*ndh* (pJM220 – KpnI / HindIII)	
RBS + Fwd	CAGGAATTCCTCGAGAAGCTTAAGGAGGAACAG CTATGTCCCATCGCATCGTGATCGTC
Rev	GCAAGGCCTTCGCGAGGTACTCAGTGCAGCTTGA GGCGTGG
pJC25 - P_{rhaBAD}-*nuoF* (pJM220 – KpnI / HindIII)	
RBS + Fwd	CAGGAATTCCTCGAGAAGCTTAAGGAGGAACAG CTATGACCCTTACCTCCATTGGTCCGG
Rev	GCAAGGCCTTCGCGAGGTACTCAGGCGCCGACC GTTGC
pJC30 - P_{rhaBAD}-*nqrF* (pJM220 – KpnI / HindIII)	
RBS + Fwd	CAGGAATTCCTCGAGAAGCTTAAGGAGGAACAG CTGTGATCGGATTCGAGATTTTCCTGG
Rev	GCAAGGCCTTCGCGAGGTACTCAGCCACCGAAA TCGTCCA

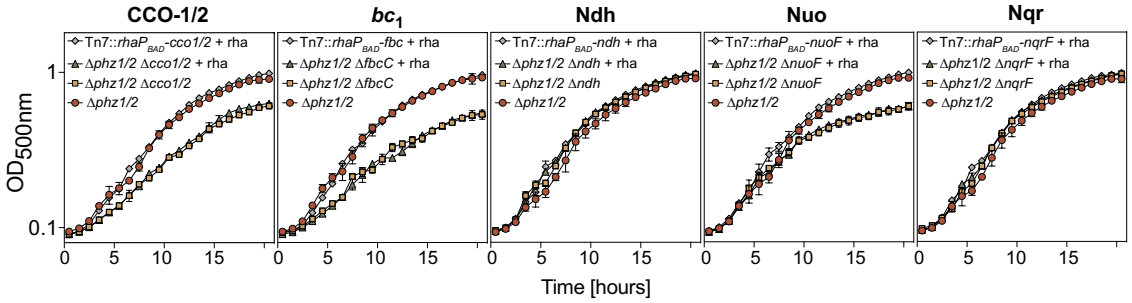

Supplementary Figure 1: Growth and complementation of ETC mutants used in this study. Cells were sub-cultured 1:200 from overnight LB cultures into a 20 mM glucose minimal medium with or without 0.005% (w/v) rhamnose in a 96-well plate. Growth curves were obtained in technical triplicate and averaged to obtain the curves shown. Error bars represent the standard deviation of the technical replicates. Complementations (indicated by Tn7::X) were performed in the respective mutant backgrounds. Plots are representative of three independent experiments.

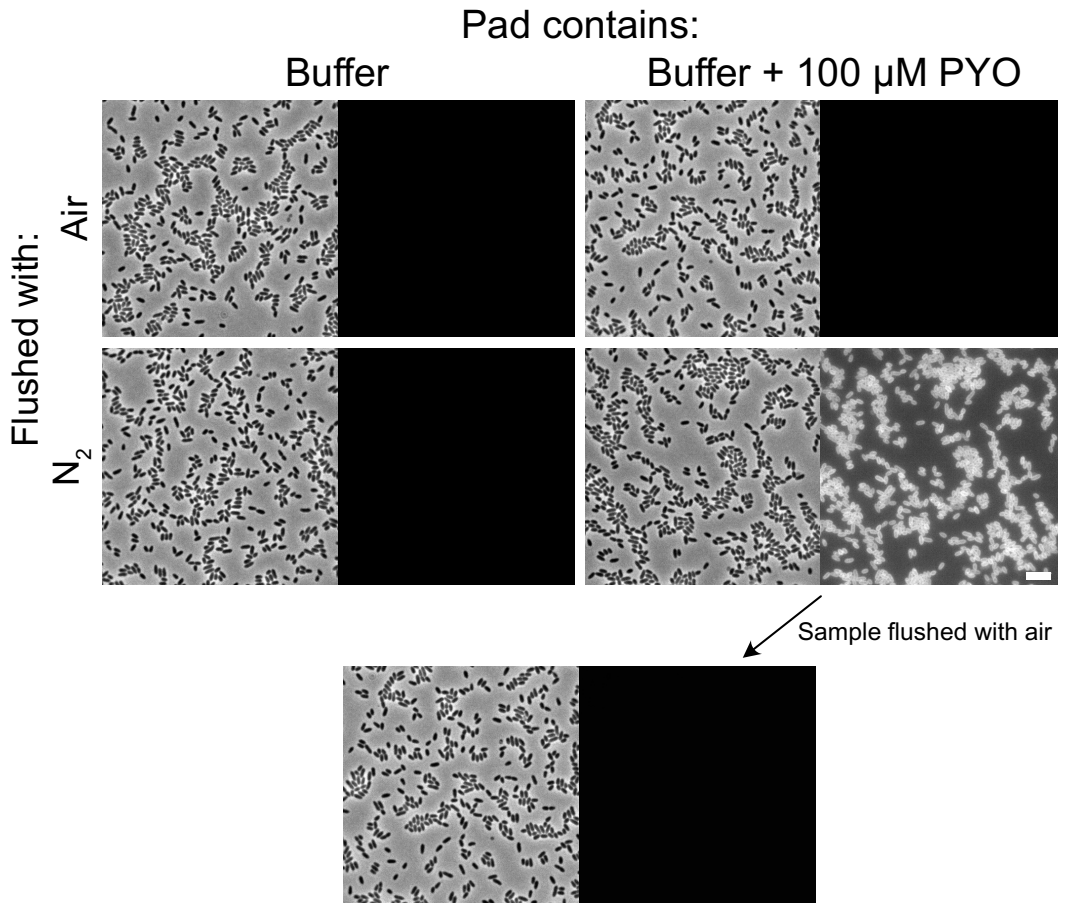

Supplementary Figure 2: On-cell PYO fluorescence dependence on anoxic conditions. PYO was reduced by Δ*phz1/2* Δ*pvdA* Δ*pchE* cells and directly imaged using a fluorescence microscope. Cells were incubated under 50 mM MOPS (pH 7.0) agarose pads with or without 100 µM PYO added and constantly flushed in a sealed stage chamber with the gas indicated. An anoxic, fluorescent sample flushed with air after imaging no longer displays any significant fluorescence. Left images, phase contrast; right images, corresponding fluorescence at 395 nm ex / 528 nm em. Scale bar is 5 µm, right edge is 48.6 µm. Images are representative of two independent experiments with six total fields captured per condition.

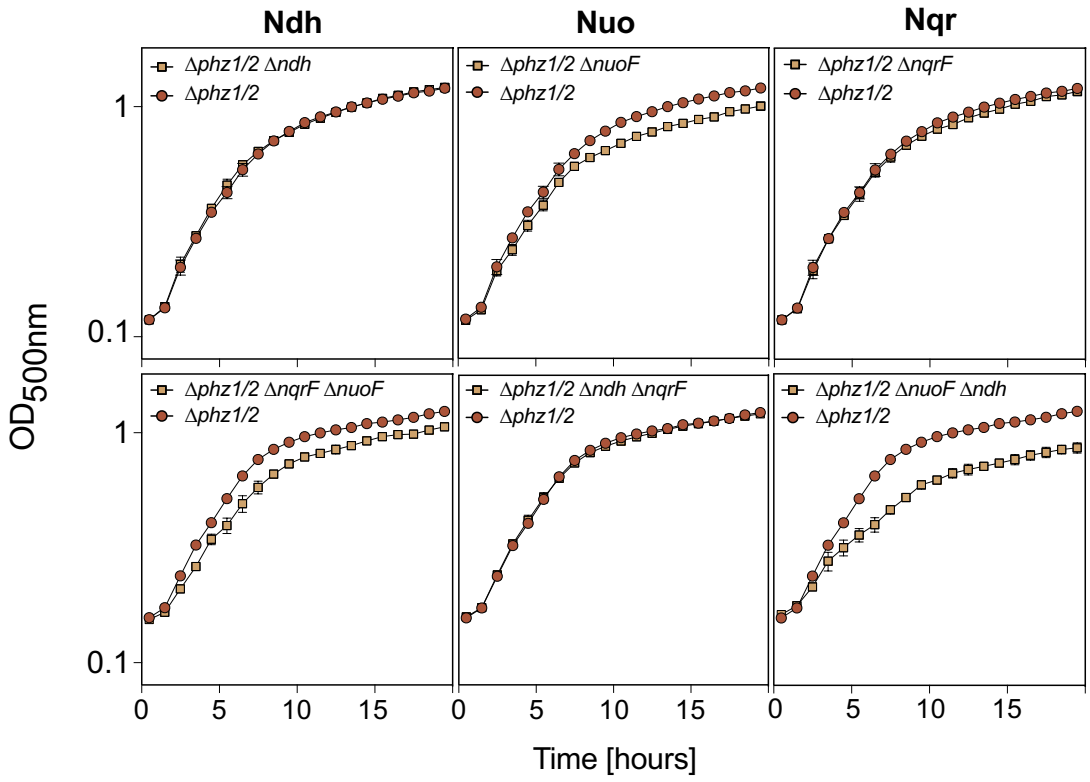

Supplementary Figure 3: Growth of NADH dehydrogenase mutants in LB. Cells were sub-cultured 1:200 from an overnight LB culture into fresh LB in a 96-well plate. Growth curves were obtained in technical triplicate and averaged to obtain the curves shown. Error bars represent the standard deviation of the technical replicates. Plots are representative of three independent experiments.

References

1. Turner JM, Messenger AJ. Occurrence, biochemistry and physiology of phenazine pigment production. Adv Microb Physiol. 1986;27:211–75.

2. Glasser NR, Saunders SH, Newman DK. The colorful world of extracellular electron shuttles. Annu Rev Microbiol. 2017 Sep 8;71:731–51.

3. Hassan HM, Fridovich I. Mechanism of the antibiotic action of pyocyanine. J Bacteriol. 1980;141.

4. Baron SS, Terranova G, Rowe JJ. Molecular mechanism of the antimicrobial action of pyocyanin. Curr Microbiol. 1989 Apr;18(4):223–30.

5. Wang Y, Kern SE, Newman DK. Endogenous phenazine antibiotics promote anaerobic survival of *Pseudomonas aeruginosa* via extracellular electron transfer. J Bacteriol. 2010 Jan;192(1):365–9.

6. McRose DL, Newman DK. Redox-active antibiotics enhance phosphorus bioavailability. Science. 2021 Mar 5;371(6533):1033–7.

7. Meirelles LA, Perry EK, Bergkessel M, Newman DK. Bacterial defenses against a natural antibiotic promote collateral resilience to clinical antibiotics. PLoS Biol. 2021 Mar 10;19(3):e3001093.

8. Glasser NR, Kern SE, Newman DK. Phenazine redox cycling enhances anaerobic survival in *Pseudomonas aeruginosa* by facilitating generation of ATP and a proton-motive force. Mol Microbiol. 2014 Apr;92(2):399–412.

9. Eschbach M, Schreiber K, Trunk K, Buer J, Jahn D, Schobert M. Long-term anaerobic survival of the opportunistic pathogen *Pseudomonas aeruginosa* via pyruvate fermentation. J Bacteriol. 2004 Jul;186(14):4596–604.

10. Arai H. Regulation and Function of Versatile Aerobic and Anaerobic Respiratory Metabolism in *Pseudomonas aeruginosa*. Front Microbiol. 2011 May 5;2:103.

11. Dietrich LEP, Okegbe C, Price-Whelan A, Sakhtah H, Hunter RC, Newman DK. Bacterial community morphogenesis is intimately linked to the intracellular redox state. J Bacteriol. 2013 Apr;195(7):1371–80.

12. Saunders SH, Tse ECM, Yates MD, Otero FJ, Trammell SA, Stemp EDA, et al. Extracellular DNA promotes efficient extracellular electron transfer by pyocyanin in *Pseudomonas aeruginosa* biofilms. Cell. 2020 Aug 20;182(4):919-932.e19.

13. Schiessl KT, Hu F, Jo J, Nazia SZ, Wang B, Price-Whelan A, et al. Phenazine production promotes antibiotic tolerance and metabolic heterogeneity in *Pseudomonas aeruginosa* biofilms. Nat Commun. 2019 Feb 15;10(1):762.

14. VanDrisse CM, Lipsh-Sokolik R, Khersonsky O, Fleishman SJ, Newman DK. Computationally designed pyocyanin demethylase acts synergistically with tobramycin to kill recalcitrant *Pseudomonas aeruginosa* biofilms. Proc Natl Acad Sci USA. 2021 Mar 23;118(12).

15. Glasser NR, Wang BX, Hoy JA, Newman DK. The Pyruvate and α-Ketoglutarate Dehydrogenase Complexes of *Pseudomonas aeruginosa* Catalyze Pyocyanin and Phenazine-1-carboxylic Acid Reduction via the Subunit Dihydrolipoamide Dehydrogenase. J Biol Chem. 2017 Mar 31;292(13):5593–607.

16. Imlay JA. The molecular mechanisms and physiological consequences of oxidative stress: lessons from a model bacterium. Nat Rev Microbiol. 2013 Jul;11(7):443–54.

17. Sakhtah H, Koyama L, Zhang Y, Morales DK, Fields BL, Price-Whelan A, et al. The *Pseudomonas aeruginosa* efflux pump MexGHI-OpmD transports a natural phenazine that controls gene expression and biofilm development. Proc Natl Acad Sci USA. 2016 Jun 21;113(25):E3538-47.

18. Price-Whelan AM. Physiology and Mechanisms of Pyocyanin Reduction in *Pseudomonas aeruginosa*. [Internet] [Doctoral dissertation]. California Institute of Technology; 2009 [cited 2022 Oct 17]. Available from: https://resolver.caltech.edu/CaltechETD:etd-02182009-100346

19. Jo J, Cortez KL, Cornell WC, Price-Whelan A, Dietrich LE. An orphan cbb_3-type cytochrome oxidase subunit supports *Pseudomonas aeruginosa* biofilm growth and virulence. eLife. 2017 Nov 21;6:e30205.

20. Wang Y, Newman DK. Redox reactions of phenazine antibiotics with ferric (hydr)oxides and molecular oxygen. Environ Sci Technol. 2008 Apr 1;42(7):2380–6.

21. Calhoun MW, Oden KL, Gennis RB, de Mattos MJ, Neijssel OM. Energetic efficiency of *Escherichia coli*: effects of mutations in components of the aerobic respiratory chain. J Bacteriol. 1993 May;175(10):3020–5.

22. Imlay J, Fridovich I. Exogenous Quinones Directly Inhibit the Respiratory NADH Dehydrogenase in *Escherichia coli*. Arch Biochem Biophys. 1992 Mar 12;296(1):337–46.

23. Krishna KV, Mohan SV. Purification and Characterization of NDH-2 Protein and Elucidating Its Role in Extracellular Electron Transport and Bioelectrogenic Activity. Front Microbiol. 2019 May 7;10:880.

24. Massey V, Singer TP. Studies on succinic dehydrogenase: VI. The reactivity of beef heart succinic dehydrogenase with electron carriers. J Biol Chem. 1957;229:755–62.

25. Arai H, Kawakami T, Osamura T, Hirai T, Sakai Y, Ishii M. Enzymatic characterization and in vivo function of five terminal oxidases in *Pseudomonas aeruginosa*. J Bacteriol. 2014 Dec;196(24):4206–15.

26. Kawakami T, Kuroki M, Ishii M, Igarashi Y, Arai H. Differential expression of multiple terminal oxidases for aerobic respiration in *Pseudomonas aeruginosa*. Environ Microbiol. 2010 Jun;12(6):1399–412.

27. Alvarez-Ortega C, Harwood CS. Responses of *Pseudomonas aeruginosa* to low oxygen indicate that growth in the cystic fibrosis lung is by aerobic respiration. Mol Microbiol. 2007 Jul;65(1):153–65.

28. Mavrodi DV, Bonsall RF, Delaney SM, Soule MJ, Phillips G, Thomashow LS. Functional analysis of genes for biosynthesis of pyocyanin and phenazine-1-carboxamide from *Pseudomonas aeruginosa* PAO1. J Bacteriol. 2001 Nov;183(21):6454–65.

29. Jo J, Price-Whelan A, Cornell WC, Dietrich LEP. Interdependency of Respiratory Metabolism and Phenazine-Associated Physiology in *Pseudomonas aeruginosa* PA14. J Bacteriol. 2020 Jan 29;202(4).

30. Bellin DL, Sakhtah H, Zhang Y, Price-Whelan A, Dietrich LEP, Shepard KL. Electrochemical camera chip for simultaneous imaging of multiple metabolites in biofilms. Nat Commun. 2016 Jan 27;7:10535.

31. Sullivan NL, Tzeranis DS, Wang Y, So PTC, Newman D. Quantifying the dynamics of bacterial secondary metabolites by spectral multiphoton microscopy. ACS Chem Biol. 2011 Sep 16;6(9):893–9.

32. Brisbane PG, Janik LJ, Tate ME, Warren RFO. Revised Structure for the Phenazine Antibiotic from *Pseudomonas fluorescens* 2-79 (NRRL B-15132). Antimicrob Agents Chemother. 1987;31(12):1967–71.

33. Tokuda H, Unemoto T. Na^+ is translocated at NADH:quinone oxidoreductase segment in the respiratory chain of *Vibrio alginolyticus*. J Biol Chem. 1984 Jun 25;259(12):7785–90.

34. Torres A, Kasturiarachi N, DuPont M, Cooper VS, Bomberger J, Zemke A. NADH Dehydrogenases in Pseudomonas aeruginosa Growth and Virulence. Front Microbiol. 2019 Feb 5;10:75.

35. Hreha TN, Foreman S, Duran-Pinedo A, Morris AR, Diaz-Rodriguez P, Jones JA, et al. The three NADH dehydrogenases of Pseudomonas aeruginosa: Their roles in energy metabolism and links to virulence. PLoS ONE. 2021 Feb 3;16(2):e0244142.

36. Raba DA, Rosas-Lemus M, Menzer WM, Li C, Fang X, Liang P, et al. Characterization of the *Pseudomonas aeruginosa* NQR complex, a bacterial proton pump with roles in autopoisoning resistance. J Biol Chem. 2018 Oct 5;293(40):15664–77.

37. Hassan HM, Fridovich I. Intracellular production of superoxide radical and of hydrogen peroxide by redox active compounds. Arch Biochem Biophys. 1979 Sep;196(2):385–95.

38. Hassett DJ, Charniga L, Bean K, Ohman DE, Cohen MS. Response of *Pseudomonas aeruginosa* to pyocyanin: mechanisms of resistance, antioxidant defenses, and demonstration of a manganese-cofactored superoxide dismutase. Infect Immun. 1992 Feb;60(2):328–36.

39. Price-Whelan A, Dietrich LEP, Newman DK. Pyocyanin alters redox homeostasis and carbon flux through central metabolic pathways in *Pseudomonas aeruginosa* PA14. J Bacteriol. 2007 Sep;189(17):6372–81.

40. Shanks RMQ, Caiazza NC, Hinsa SM, Toutain CM, O'Toole GA. *Saccharomyces cerevisiae*-based molecular tool kit for manipulation of genes from gram-negative bacteria. Appl Environ Microbiol. 2006 Jul;72(7):5027–36.

41. Choi K-H, Schweizer HP. mini-Tn7 insertion in bacteria with single *att*Tn7 sites: example *Pseudomonas aeruginosa*. Nat Protoc. 2006;1(1):153–61.

42. Jeske M, Altenbuchner J. The *Escherichia coli* rhamnose promoter $rhaP_{BAD}$ is in *Pseudomonas putida* KT2440 independent of Crp–cAMP activation. Appl Microbiol Biotechnol. 2010 Feb;85(6):1923–33.

43. Cheluvappa R. Standardized chemical synthesis of *Pseudomonas aeruginosa* pyocyanin. MethodsX. 2014 Jul 8;1:67–73.

44. Rustin P. Mitochondrial Respiratory Chain. In: Blau N, Duran M, Gibson KM, editors. Laboratory Guide to the Methods in Biochemical Genetics. Springer; 2008.

45. Spinazzi M, Casarin A, Pertegato V, Salviati L, Angelini C. Assessment of mitochondrial respiratory chain enzymatic activities on tissues and cultured cells. Nat Protoc. 2012 May 31;7(6):1235–46.

46. Simon R, Priefer U, Pühler A. A Broad Host Range Mobilization System for *in vivo* Genetic Engineering: Transposon Mutagenesis in Gram Negative Bacteria. Nat Biotechnol. 1983;

47. Wang Y, Wilks JC, Danhorn T, Ramos I, Croal L, Newman DK. Phenazine-1-carboxylic acid promotes bacterial biofilm development via ferrous iron acquisition. J Bacteriol. 2011 Jul;193(14):3606–17.

48. White D, Drummond J (James T, Fuqua Clay. The physiology and biochemistry of prokaryotes. 4th ed. New York: Oxford University Press; 2011.

C h a p t e r 4

THE SHORT-CIRCUITING EFFECT OF PHENAZINES ON AEROBIC CHEMIOSMOSIS

Abstract

Phenazines are a class of redox-active metabolites produced by many bacteria including the opportunistic pathogen *Pseudomonas aeruginosa*. Phenazines are known to interact with the respiratory electron transport chain, a key site of energy conservation in the cell, specifically via NADH dehydrogenases. In this study, the aerobic bioenergetic consequences of phenazine reduction are explored. Using a classic oxygen pulse assay, increasing concentrations of phenazine are shown to repress the total number of protons translocated per oxygen atom reduced during aerobic respiration (the H^+/O ratio). The strength of each derivatives' repression of the H^+/O ratio correlated with their known rates of reduction by cells. In respirometry experiments, each of the phenazine derivatives was able to restore azide-inhibited oxygen consumption to degrees also correlating with their reduction rates. Both H^+/O suppression and recovery of oxygen consumption in *P. aeruginosa* were most pronounced when using toxoflavin, a redox-active metabolite made by a different genus of bacteria, *Burkholderia*. Together, these results suggest a redox short-circuiting mechanism where phenazines divert reducing equivalents away from the electron transport chain and directly to oxygen instead. This proposed model is described and its bioenergetic implication are discussed.

Introduction

Pseudomonas aeruginosa is perhaps best known for its production of colorful phenazine metabolites, especially the cerulean blue pyocyanin (1). One of the earliest studies of pyocyanin was carried out by Ernst Friedheim, a colleague of Michaelis and Menten, where he characterized its enhancing effects on the respiration rate of tumor cells (2). Friedheim accordingly called pyocyanin an "accessory respiratory pigment" hypothesizing that it directly increased the biochemical pace of respiration in the cell. While he had no way to know this at the time, the hypothesis he posited was like the effects of a protonophore—that is, a chemical that decouples electron movement through the electron transport chain (ETC) from the generation of a proton motive force (PMF). This PMF drives ATP synthesis via a membrane-bound ATP synthase and constitutes the major site of aerobic energy conservation in the cell (3). Classically, treatment with a protonophore dissipates a cell's PMF. Without any thermodynamic backpressure from that PMF, the enzymes of the electron transport chain that translocate protons then increase their reaction rate, ultimately reducing oxygen faster, which is observed as an increase in the respiration rate. Was the increased respiration rate observed by Friedheim and others because pyocyanin is a protonophore? Perhaps, but these results could also be explained by the fact that pyocyanin is capable of redox-cycling (4). Like all the phenazines made by *P. aeruginosa* it can be reduced by many metabolic flavoproteins in the cell (5,6) and oxidized non-enzymatically by oxygen to form superoxide (4). It can then be reduced again by another intracellular reductant, forming a cycle. The net result of this is the gradual dissipation of reducing equivalents in the cell. Could this non-enzymatic reduction of oxygen alone explain the increased "respiration" rate observed in these past studies?

Underlying this niche biochemical mystery is a broader desire to better understand the consequences phenazines have upon aerobic respiration, as this could possibly serve as a mechanistic link connecting phenazines to their promotion of antibiotic tolerance in biofilms (7,8) and in planktonic culture (9). The goal of this study was therefore to make preliminary inquiries into the bioenergetic consequences of phenazine reduction in aerobic conditions. In the previous chapter, I demonstrated that all phenazines can interact with the *P. aeruginosa* electron transport chain via the NADH dehydrogenases Nuo and Nqr. But regardless of where phenazines are reduced in the cell, if oxygen is present, I reasoned phenazines would reduce some fraction of it before it could act as a terminal electron acceptor for the ETC (Figure 1). This activity could be observed as an apparent decrease of the chemiosmotic efficiency, or H^+/O ratio, of the respiratory chain when oxygen was limited. I also show that phenazines can re-initiate cells' oxygen consumption after it has been blocked by treatment with azide, a strong inhibitor of terminal oxidases. I present a theory to explain these results: unlike a protonophore which decouples electron flux through the ETC from proton transport, phenazines decouple upstream metabolic reducing power from flux through the ETC. I propose calling this kind of uncoupling short-circuiting. The results of my experiments carry bioenergetic implications and likely explain classic observations made by others such as Friedheim.

Results

Phenazines reduce the H^+/O ratio during aerobic respiration

I first sought to measure the number of protons translocated across the cytoplasmic membrane during respiration using a classic oxygen pulse assay (10,11). In this assay a

high-density, anaerobic suspension of cells is constantly stirred in an anaerobic chamber and pulsed with small quantities of air-equilibrated water. The oxygen carried in the water is rapidly respired, and the concomitant proton translocation is measured as a ΔpH via a sensitive pH electrode held in the suspension.

Using this setup, I measured a H^+/O ratio of 5 in *P. aeruginosa* PA14 Δ*phz1/2* cells (a mutant that cannot make phenazines) that had been grown in LB (Figure 1A,B), similar to the value of 4 previously measured in the PAO1 strain (12). To test the effects of phenazines, small amounts of anoxic phenazine solution were added and allowed to equilibrate for 1.5 minutes before oxygen pulses began. During these pulses, proton translocation was repressed in a concentration dependent manner (Figure 1B). The degree of repression was derivative-dependent, with pyocyanin (PYO) repressing the most, then phenazine-1-carboxamide (PCN), then phenazine-1-carboxylic acid (PCA) (Figure 1C).

I also assessed the effect of another redox-active metabolite, toxoflavin (TOX). TOX is made by various *Burkholderia* species (13), and while its beneficial physiological functions are unexplored, it has many properties in common with phenazines. Namely, it can undergo a redox-cycle with oxygen as terminal electron acceptor (13), and it can activate the SoxR iron-sulfer cluster transcription factor that specifically detects redox-active metabolites and modulates gene expression in response (14). However, *P. aeruginosa* does not make TOX, so I reasoned it may have fewer defenses against TOX, leading to it causing a stronger effect. Indeed, TOX's repressive effect on the H^+/O ratio in *P. aeruginosa* was significantly stronger than that of the phenazines; I was unable to detect any ΔpH in response to an oxygen pulse at the highest concentration tested (Figure 1C). Overall, I conclude that

phenazines and at least some other redox-active metabolites (RAMs) reduce the H^+/O ratio during aerobic respiration.

Phenazines relieve azide-inhibited oxygen consumption

I next investigated the mechanism underlying phenazines' depression of the H^+/O ratio. I hypothesized two models of their predominant action: in the first model, phenazines predominantly act as a protonophore, shuttling and equilibrating protons across the cytoplasmic membrane, thereby dissipating any measurable ΔpH in response to oxygen. Experiments with FCCP, a known protonophore, have been shown to have this effect during oxygen pulse experiments (15). In the second model, phenazines are predominantly acting as what I call a short-circuiting molecule, or a molecule that takes electrons from reducing equivalents in the cell and diverts them directly to oxygen, bypassing some or all components of the ETC (Figure 2A). In this way only a fraction of the total electron flux becomes chemiosmotically coupled, resulting in reduced H^+/O ratios.

While these models are not mutually exclusive, the presence of the latter mechanism can be tested via a respirometry experiment. As explained in the introduction, the consequence of protonophores upon respiration is that they increase the respiration rate, but this effect is dependent on functional terminal oxidases. The protonophore does not interact with oxygen directly. Short-circuiting molecules, in contrast, do not require the activity of terminal oxidases to reduce oxygen. The ETC can be abrogated, and in the presence of these molecules measurable oxygen consumption should continue (Figure 2B).

To test this idea, I conducted respirometry experiments with cells that had been grown overnight in LB. The cells were placed in a concentrated, stirred, aerobic suspension with

an oxygen electrode covered by a thin teflon membrane (i.e. a Clark electrode). Once added, the cells consumed the aqueous oxygen faster than oxygen from the surrounding air could re-solubilize into the stirred suspension (Figure 2C). This respiration could be near-immediately stopped with the addition of 20 mM sodium azide (Figure 2C). After addition of azide, the rate of solubilization of fresh oxygen from the surrounding air overtook the respiration rate and the oxygen level slowly increased (Figure 2C). After the addition of azide, phenazine was added, and after a short lag, net oxygen consumption resumed to a degree that correlated with each derivatives' repression of the H^+/O ratio (Figure 2C). TOX was also tested, and strikingly, its addition to azide-treated cultures immediately recovered oxygen consumption at the same rate as uninhibited respiration (Figure 2C). I conclude that phenazines and at least some other RAMs can short-circuit normal electron flow through the ETC.

Discussion

Phenazines and other redox-active metabolites are often regarded as antibiotics that generate reactive oxygen species in cells and thereby kill or inhibit cells' growth (16). In this work, I show that another consequence they carry under aerobic conditions is the repression of the bioenergetic efficiency of the ETC (Figure 1C). I suggest a short-circuiting theory that can explain this phenomenon and show that these molecules can shuttle electrons from intracellular reductants to oxygen independent of normal ETC flux (Figure 2C). Regardless of the exact reduction site, the consequence is that electrons circumvent all or part of the ETC, resulting in a decreased apparent H^+/O ratio (Figure 1C).

Previous classical studies interested in understanding the effects of pyocyanin have repeatedly shown the addition of it to cultures of eukaryotic cells increases the respiration rate (2,17). These observations have spurred speculation that phenazines may act as protonophores that have the same effect upon respiration. The work here does not rule out the possibility that phenazines may have the capability to act as protonophores. However, a requirement of protonophores is that they have a pK_a near to the experimental conditions (18). Given none of the pK_a's of phenazines are circumneutral (19), the condition under which all experiments here were conducted, it seems unlikely that this putative mechanism plays a significant role. For comparison, even acetate is a surprisingly good protonophore, but only in low-pH environments near its pK_a of 4.76 (20). Indeed, the observations made here are so far explainable with the short-circuiting mechanism alone, but further *in vitro* work such as incubation of charged membrane vesicles with phenazine (21) are needed to definitively rule out the protonophore possibility.

This bioenergetic consequence of phenazines in aerobic conditions raises the question: how does PA tolerate or manage these effects on its energy conservation efficiency? One way that has previously been established is the upregulation of efflux pumps that are necessary for limiting intracellular ROS production in the presence of oxygen (9), but these enzymes also require a PMF to function. Another layer of protection may be that specific enzyme modifications have evolved: I demonstrated in the last chapter that even though some flavoprotein complexes in the ETC should be thermodynamically capable of reducing phenazines, reduction was not detectable, suggesting there may be enzyme modifications that limit and control phenazine reduction sites. I speculate that this is why TOX had such dramatic affects in lowering the H^+/O ratio (Figure 1C) and

recovering rapid oxygen consumption after azide inhibition (Figure 2C)—unlike phenazines, the cell has not evolved enzyme protections against TOX. Investigating if modifications such as this exist and if they can be identified via an amino acid motif is a priority for future research that will aid in ruling out—and in—the full set of relevant phenazine reductases in the cell. Metabolomics studies that identify how metabolic fluxes shift between identified phenazine reduction sites will provide a holistic understanding of how phenazines are metabolically tolerated.

However, any protections that do exist are clearly not complete, as repression of energy conservation was measurable. Therefore, it is a possibility that one biological function of phenazines is to purposefully lower the bioenergetic state of the cell in a regulated way. This counter-intuitive possibility makes sense when one considers that phenazines are only produced when the population of cells reaches a quorum-sensing density; at this point, the cells' maximum fitness may be achieved not by maximizing their energy yield but instead by maximizing their survival potential. Purposefully attenuating their bioenergetic state, and consequently their overall metabolic state, could protect them against oxygen depletion (22) and antibiotics (7,8) while the phenazines simultaneously protect them from competitors and predators through ROS production. If this is the correct perspective, the key question may instead be how cells manage consumption of the relative slow trickle of energy (i.e. ATP) phenazines impose such that their effects result in net survival.

Methods

H^+-translocation assay

Cultures of Δ*phz1/2* cells were inoculated from LB-agar plates and grown for 20 hours in LB at 37˚C, 250 RPM on a slant. Cells were centrifuged at 6800*xg* for 5 min and washed twice in 0.5 mM HEPES (pH 7.0, adjusted KOH), 125 mM KCl. Cell pellets were brought into an anaerobic chamber (Coy) and resuspended in a N_2-sparged suspension buffer consisting of 0.5 mM HEPES (pH 7.0, adjusted KOH), 75 mM KCl, and 100 mM KSCN. Suspensions were adjusted with this buffer to 4 mL total volume with an OD_{500nm} of approximately 4.0 and placed in a small glass vial (Fisher Cat. No. 03-339-26C) with a magnetic stirbar (Fisher Cat. No. 14-513-93). The suspension was allowed to rest for 30 min. A sensitive pH electrode (Thermo Orion 8103BNUWP) was calibrated at the beginning of each experimental day. The suspension was placed on a styrofoam holder over a magnetic stir plate. With the pH electrode submerged and the solution stirring, the pH was allowed to equilibrate for 4 min. If necessary, the pH was adjusted with 10 mM KOH such that the initial pH was between 6.9 and 7.1. A 2 min baseline was then recorded using the Thermo Orion STAR COM software, followed by three sequential additions of 10 µL of air-equilibrated water (250 µM O_2). In samples with RAM added to measure inhibition, the RAM was added after the 2 min baseline and 10 µL of water was added every 1.5 min after. At the end of this series of respiratory pulses, 10, 20, and 30 µL of anoxic 1 mM HCl were added in sequence to generate a standard curve to convert ΔpH to protons extruded. The largest ΔpH caused by the three oxygen pulses was recorded for averaging. All experiments were conducted at room temperature (~25˚C).

Respiration measurements

Cultures of Δ*phz1/2* cells were inoculated from LB-agar plates and grown for 20 hours in LB at 37˚C, 250 RPM. 10 mL of culture was centrifuged at 6800*xg* for 5 min and the cell pellet was resuspended in 1 mL of PBS with 500 μM Na-EDTA added. This suspension was incubated at room temperature for at least 15 minutes. A small glass vial (Fisher Cat. No. 03-339-26C) with a magnetic stirbar (Fisher Cat. No. 14-513-93) was placed on a styrofoam holder over a magnetic stir plate and filled with 4 mL PBS. The tip of a Clark-type oxygen electrode (Microelectrodes, Inc.) was suspended about one centimeter below the water-air interface. A baseline was collected for 30 sec – 1 min, after which the 1 mL suspension of cells was added to bring the suspension to a 5 mL volume. 20 mM Na-Azide was added to halt oxygen consumption and 200 μM of phenazine or toxoflavin to resume it. Data were recorded in mV and normalized to set the baseline to 250 μM oxygen and 0 mV to 0 μM oxygen.

Figures

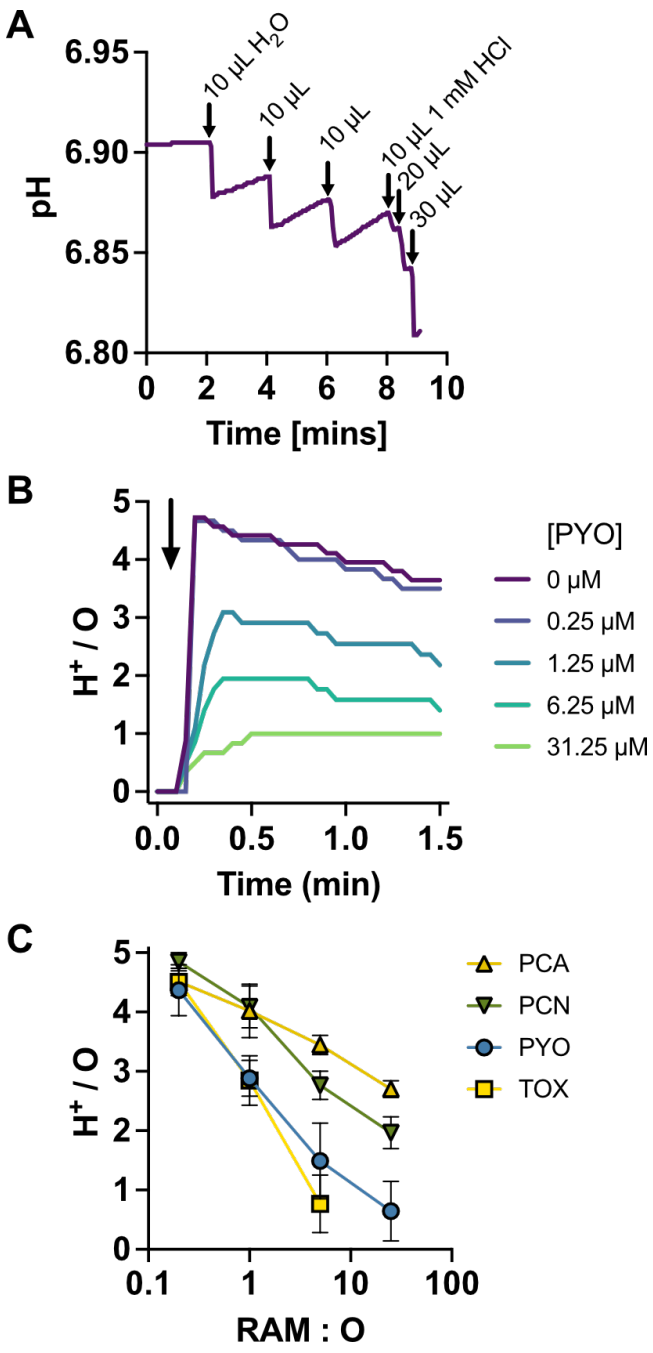

Figure 1: H^+/O ratio measurements in response to increasing RAM concentrations. (A) Respiratory proton translocation measured from whole cells in response to pulses of oxygen added as air-equilibrated water. Anoxic HCl added to calculate a proton standard curve. See Methods for conditions. (B) Proton translocation inhibition in response to increasing concentrations of PYO. Cells were incubated with the added PYO for 1.5 min before oxygen pulses began. (C) Proton translocation inhibition of various RAMs. RAM : O is the molar ratio of the RAM added to the O atoms added in a single oxygen pulse. Each data point is an average of two biological replicates and error bars represent the standard deviation. H^+ translocation at the highest concentration of toxoflavin was not detectable.

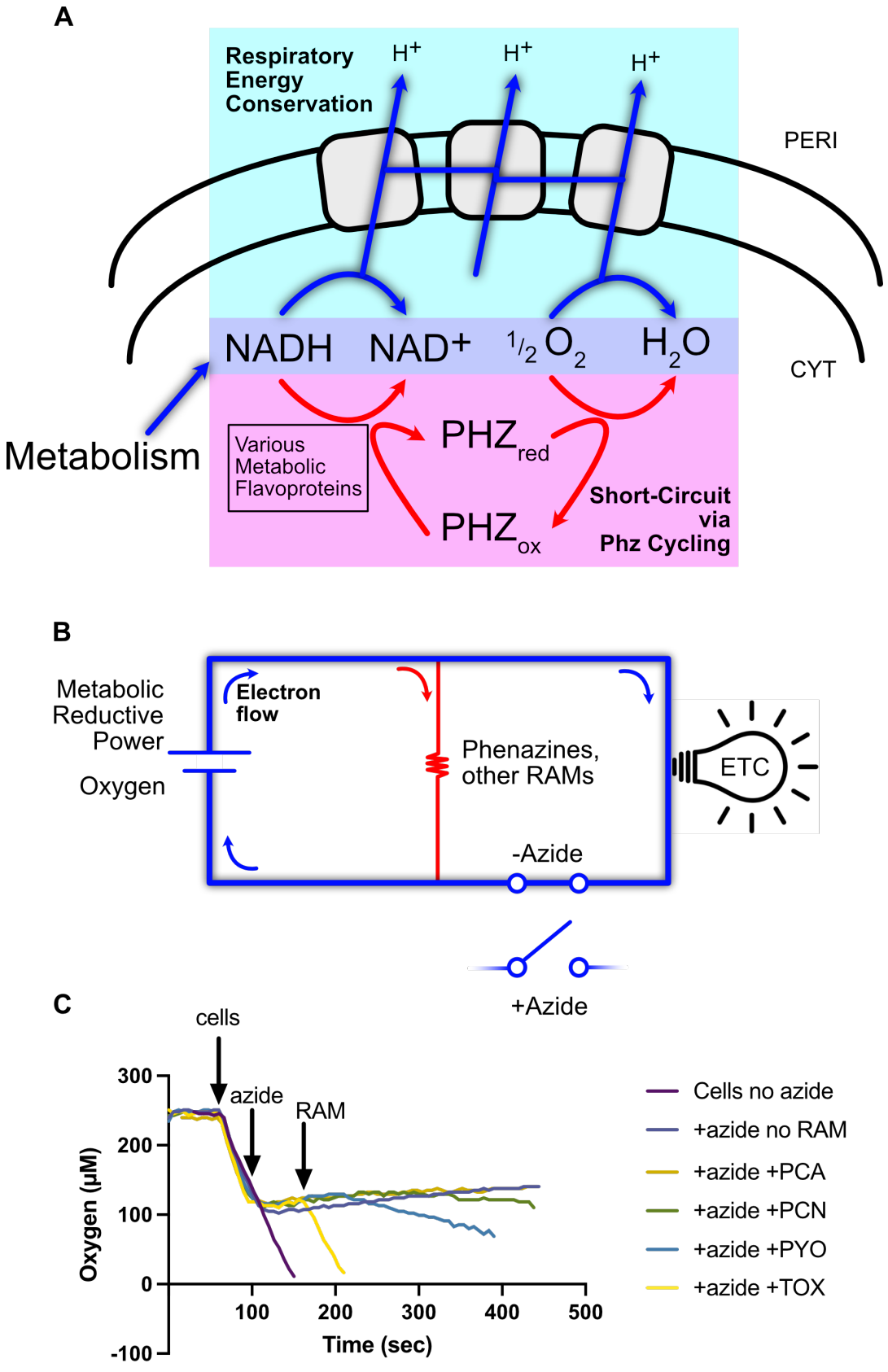
A
Respiratory Energy Conservation
H+
H+
H+
PERI
CYT
NADH
NAD+
1/2 O2
H2O
Metabolism
Various Metabolic Flavoproteins
PHZred
PHZox
Short-Circuit via Phz Cycling
B
Metabolic Reductive Power
Oxygen
Electron flow
Phenazines, other RAMs
ETC
-Azide
+Azide
C
cells
azide
RAM
Oxygen (µM)
300
200
100
0
-100
100
200
300
400
500
Time (sec)
Cells no azide
+azide no RAM
+azide +PCA
+azide +PCN
+azide +PYO
+azide +TOX

Figure 2. Cellular oxygen consumption in response to azide and RAM treatment. (A) Working model for short-circuiting reaction relative to normal metabolic electron flow. By metabolic reducing power being diverted away from the ETC, net respiratory energy conservation is lost. (B) Circuit diagram analogy of short-circuiting model. The amount of electron flux through the red wire is proportional to the concentration of the RAM. Azide blocks electron flow through the ETC but not through the RAM pool. (C) Respiration measurements of cell suspensions. Respiration is inhibited by azide addition but oxygen consumption can resume upon the addition of RAM.

References

1. Glasser NR, Saunders SH, Newman DK. The colorful world of extracellular electron shuttles. Annu Rev Microbiol. 2017 Sep 8;71:731–51.

2. Friedheim EA. The effect of pyocyanine on the respiration of some normal tissues and tumours. Biochem J. 1934;28(1):173–9.

3. Kaila VRI, Wikström M. Architecture of bacterial respiratory chains. Nat Rev Microbiol. 2021 May;19(5):319–30.

4. Hassan HM, Fridovich I. Mechanism of the antibiotic action of pyocyanine. J Bacteriol. 1980;141.

5. Imlay JA. The molecular mechanisms and physiological consequences of oxidative stress: lessons from a model bacterium. Nat Rev Microbiol. 2013 Jul;11(7):443–54.

6. Glasser NR, Wang BX, Hoy JA, Newman DK. The Pyruvate and α-Ketoglutarate Dehydrogenase Complexes of *Pseudomonas aeruginosa* Catalyze Pyocyanin and Phenazine-1-carboxylic Acid Reduction via the Subunit Dihydrolipoamide Dehydrogenase. J Biol Chem. 2017 Mar 31;292(13):5593–607.

7. Schiessl KT, Hu F, Jo J, Nazia SZ, Wang B, Price-Whelan A, et al. Phenazine production promotes antibiotic tolerance and metabolic heterogeneity in *Pseudomonas aeruginosa* biofilms. Nat Commun. 2019 Feb 15;10(1):762.

8. VanDrisse CM, Lipsh-Sokolik R, Khersonsky O, Fleishman SJ, Newman DK. Computationally designed pyocyanin demethylase acts synergistically with tobramycin to kill recalcitrant *Pseudomonas aeruginosa* biofilms. Proc Natl Acad Sci USA. 2021 Mar 23;118(12).

9. Meirelles LA, Perry EK, Bergkessel M, Newman DK. Bacterial defenses against a natural antibiotic promote collateral resilience to clinical antibiotics. PLoS Biol. 2021 Mar 10;19(3):e3001093.

10. Mitchell P, Moyle J. Respiration-driven proton translocation in rat liver mitochondria. Biochem J. 1967 Dec;105(3):1147–62.

11. Mitchell P, Moyle J, Mitchell R. Measurement of H+/O in Mitochondria and Submitochondrial Vesicles. Meth Enzymol. 1979;55.

12. Arai H, Kawakami T, Osamura T, Hirai T, Sakai Y, Ishii M. Enzymatic characterization and in vivo function of five terminal oxidases in *Pseudomonas aeruginosa*. J Bacteriol. 2014 Dec;196(24):4206–15.

13. Lee J, Park J, Kim S, Park I, Seo Y-S. Differential regulation of toxoflavin production and its role in the enhanced virulence of *Burkholderia gladioli*. Mol Plant Pathol. 2016 Jan;17(1):65–76.

14. Meirelles LA, Newman DK. Phenazines and toxoflavin act as interspecies modulators of resilience to diverse antibiotics. Mol Microbiol. 2022 Jun;117(6):1384–404.

15. Scholes P, Mitchel P. Respiration-Driven Proton Translocation in Micrococcus. Bioenergetics. 1970;1:309–23.

16. Hassett DJ, Charniga L, Bean K, Ohman DE, Cohen MS. Response of *Pseudomonas aeruginosa* to pyocyanin: mechanisms of resistance, antioxidant defenses, and demonstration of a manganese-cofactored superoxide dismutase. Infect Immun. 1992 Feb;60(2):328–36.

17. Young L. The Effect of Pyocyanine on the Metabolism of Cerebral Cortex. J Biol Chem. 1937;120(2):659–75.

18. Kotova EA, Antonenko YN. Fifty years of research on protonophores: mitochondrial uncoupling as a basis for therapeutic action. Acta Naturae. 2022;14(1):4–13.

19. Price-Whelan A, Dietrich LEP, Newman DK. Rethinking "secondary" metabolism: physiological roles for phenazine antibiotics. Nat Chem Biol. 2006 Feb;2(2):71–8.

20. Wolfe AJ. The acetate switch. Microbiol Mol Biol Rev. 2005 Mar;69(1):12–50.

21. Dolder N, Müller P, von Ballmoos C. Experimental platform for the functional investigation of membrane proteins in giant unilamellar vesicles. Soft Matter. 2022 Aug 10;18(31):5877–93.

22. Wang Y, Kern SE, Newman DK. Endogenous phenazine antibiotics promote anaerobic survival of *Pseudomonas aeruginosa* via extracellular electron transfer. J Bacteriol. 2010 Jan;192(1):365–9.

C h a p t e r 5

ANAEROBIC PHENAZINE CYCLING POWERS PSEUDOMONAS AERUGINOSA *MAINTENANCE AT EXTREMELY LOW METABOLIC RATES*

Abstract

Mechanistic studies of life's lower metabolic limits have been limited due to a lack of tractable experimental systems. Here we show that redox-cycling of phenazines by *Pseudomonas aeruginosa* supports anaerobic survival with a mass-specific metabolic rate of 8.7×10^{-4} W $(g\ C)^{-1}$ at 25˚C, 10 times slower than the average mass-specific basal metabolic rate recently estimated across the biosphere, 100 times slower than previous estimates of bacterial maintenance energy requirements, and 1,000 times slower than *P. aeruginosa*'s metabolic rate during aerobic growth. Under these conditions, single cells maintain viability but do not grow. Leveraging a high-throughput electrochemical culturing device to test multiple conditions and mutant strains, we find that the amount of phenazine reduced limits survival and cells conserve energy via a hybrid form of fermentation and respiration. The cell-specific metabolic rate across phenazine concentrations is constant, indicating the cells are operating near their maintenance energy limit. These results open the door to investigations of metabolic attenuation, a physiological state that underpins microbial survival in nature and disease.

Introduction

The physiology of bacteria in non- or slowly-growing states is poorly understood relative to its ubiquity in natural, clinical, and engineered systems(1,2). A fundamental question underlying the study of this state is how much energy is needed to maintain cell viability in the absence of growth(3). Previous laboratory attempts to quantify this value inferred maintenance metabolic rates by extrapolating the energy needed to support zero growth from values measured during slow growth in continuous culture(4). Yet these estimates are consistently two to four orders of magnitude higher than metabolic rates measured in stable natural environments where sources of energy or nutrients are limiting(5). How can we bridge the gap between the two to study the cellular strategies underpinning maintenance metabolism?

While environmental measurements inspire an interest in this attenuated energetic state, it is important to note that metabolic rates estimated from environmental samples, by necessity, also rest on inferences rather than direct measurements. First, it is assumed that all the cells counted in the sample are metabolically active. Second, the fraction of cells using the measured nutrient is often estimated using educated guesses. Third, it is unclear which percentage of cells are in a normal vs. viable-but-non-culturable (VBNC) with a diminished metabolism(6). Overestimates of any of these parameters can inflate the relevant cell count, leading to underestimates of the cell-specific metabolic rate. Accordingly, the development of laboratory systems in which to study metabolic rates at or near zero growth coupled to measurements of single-cell metabolic activity is needed (7). While progress is being made towards this end(8–10), to our knowledge, no high-throughput experimental systems have been established that permit direct measurements of metabolic power output.

We hypothesized that anaerobic extracellular electron transfer (EET) could be leveraged to measure the metabolic flux powering maintenance (*i.e*. the minimum energy needed to support cellular integrity and preserve a culturable state in the absence of growth). *Pseudomonas aeruginosa*, an opportunistic pathogen and model biofilm-forming organism, produces phenazines, a widespread class of colorful, redox-active metabolites(11). Phenazines promote biofilm development and attenuated metabolism (sometimes referred to as "dormancy") in biofilm regions where oxygen is unavailable, rendering cells physiologically tolerant to conventional drugs(12,13). Previously, using low-throughput electrochemical reactors, we showed that phenazines act as extracellular electron shuttles that facilitate an anaerobic survival metabolism(14). Importantly, this metabolism does not promote any measurable bulk population growth. While *P. aeruginosa* cannot survive anaerobically via glucose fermentation(15), when provided with phenazines and a re-oxidizing potential, intracellular redox-balance is achieved, permitting glucose catabolism and substrate-level phosphorylation (SLP) via the AckA-Pta pathway(16) (Figure 1B). In this way, ATP is generated via a hybrid form of energy conservation where reduction of the extracellular electron shuttle facilitates SLP and organic acid excretion(16), similar to energy conservation strategies inferred for other bacteria in the presence of humic substances or flavins(17–20). Given this fermentative energy conservation pathway requires redox-balancing using an exogenous oxidant, we refer to it as a facilitated fermentation (Figure 1A).

In this study, we investigated the limit of phenazine EET survival metabolism using a recently developed high-throughput electrochemical system that enables nearly 100 measurements of current generated by planktonic cultures to be measured concurrently(21).

By leveraging this system to survey a wide range of conditions and directly measure power output, we asked: What is the metabolic rate of phenazine EET-mediated survival and how does it compare to the basal metabolic rates measured for other organisms across the tree of life? At the single-cell level, are cells surviving without growth or is the population surviving via a balance of growth and death? Which enzymes contribute to the metabolism? And does phenazine EET power cell survival at or above the maintenance power requirement? Broadly, our results introduce a tractable experimental platform that permits quantitative investigations into maintenance metabolism in mechanistic detail. More specifically, they shed light on the minimal metabolic requirements and catabolic pathways that contribute to powering *P. aeruginosa* cells under anoxic conditions relevant to the antibiotic tolerant core of biofilms.

Results

To study phenazine-dependent survival metabolism at the lowest thermodynamic limit, we performed our studies using phenazine-1-carboxamide (PCN), the phenazine species with the lowest standard midpoint potential (-140 mV E°', (22)) of those produced in significant quantities by *P. aeruginosa* (23,24). Due to its low potential, PCN reduction should permit survival metabolism with the smallest possible energy conserved per phenazine molecule reduced. In biofilms, PCN is the phenazine produced and retained at the highest levels (24), making it of additional interest to our understanding of cell survival. In all experiments, a Δ*phz1/2* mutant was used that cannot synthesize phenazines, and PCN was exogenously provided at physiologically-relevant concentrations. Data analysis details and

the rationale for using electrons sec^{-1} units, as opposed to Watts, when reporting metabolic rates are provided in the Supplemental Information.

PCN EET promotes anaerobic survival at extremely low metabolic rates

We first conducted weeklong PCN anaerobic survival assays as previously reported (14) to compare survival phenotypes on PCN to those made for other phenazines and make metabolic rate measurements. Cells were incubated anaerobically in large, well-mixed, custom glass electrochemical reactors connected to potentiostats poised to re-oxidize the PCN reduced by the cells (Figure 1C). Samples were removed periodically from the reactors to measure colony forming units (CFUs). After one week of incubation at 33˚C, cultures provided with PCN and a re-oxidizing potential (+PCN/pot) lost less than an order of magnitude of their initial viability while anaerobic cultures incubated in the same medium - PCN/pot lost viability by three orders of magnitude (Figure 1D). At the end of the incubation, we measured the cumulative acetate produced by the cells, finding it to be 122±34 μmoles (n=2), approximately balanced with the total PCN reduced, 107±4 μmoles (n=2) and an order of magnitude higher in the +PCN/pot than the -PCN/pot cultures (Figure 1E), in agreement with our working model (Figure 1B). To assess the percentage of cells that were metabolically active in these different conditions, we stained culture samples on day 5 with the fluorescent viability dye propidium iodide (PI is taken up when cells are metabolically compromised), finding that the majority (88%, n=794 cells) of -PCN/pot cells fluoresced brightly whereas very few (2.4%, n=830 cells) +PCN/pot cells were fluorescent (Figure 1F). Notably, the population sustained by PCN cycling appeared to be homogeneous with respect to PI staining. Contrary to expectations for cell size when challenged by extreme energy

limitation (7,25) the cells imaged from the +PCN/pot condition were not especially small; we measured their dry weight on day five to be 2.0±0.1 x 10^{-13} g $cell^{-1}$, comparable to measurements of various species in the early stationary phase of growth (26). Overall, these results are consistent with PCN EET powering a facilitated fermentation that enables anaerobic survival, similar to what we have observed for other phenazines.

Recently, Hoehler et al. (27) collated a large dataset of metabolic rates measured across all life on Earth to estimate the average mass-specific metabolic rate of the biosphere. We wondered how the metabolic rate of PCN survival would compare to both bacterial measurements and other organismal measurements in their published dataset. We summarize our findings here, with a more detailed accounting of our analysis of our samples and the Hoehler et al. dataset found in the Supplemental Information. Consistently, the current produced by the +PCN/pot cultures during their survival is characterized by an initial spike, followed by a decrease in current to a steady state held between days one and seven (Figure 2A). Given the spike occurs before the onset of death in the -PCN/pot condition, this likely reflects adjustment of the cells to a new condition and thus we interpret the lower, stable current as the survival metabolism. Averaging this current and the associated CFUs across days one to five, we estimated the bulk cell-specific metabolic rate of the surviving cells to be 1.6 x 10^3 electrons sec^{-1} $cell^{-1}$ at 25˚C. Assuming a $\Delta G'^{\circ}$ = -65.6 kJ $(mol\ PCN)^{-1}$ (see Supplemental Information), this is equal to a mass-specific power of 8.7 x 10^{-4} W $(g\ C)^{-1}$. This value is about one order of magnitude below the average basal metabolic rate across all organisms reported by Hoehler et al., 1.2 x 10^{-2} W $(g\ C)^{-1}$. The PCN EET mass-specific metabolic rate falls within the lower 2% of measurements across all organismal groups, and among those groups, only the gelatinous invertebrates are noticeably lower (27).

We then sought to further contextualize this metabolic rate across the hundreds of bacterial measurements in the dataset. To avoid the accumulation of potential errors stemming from assumptions about how much energy is conserved per electron transferred, we analyzed the cell-specific metabolic rates in units of electrons sec^{-1} $cell^{-1}$. Notably, across disparate catabolic pathways the ratio of ATP generated per electron transferred varies by less than an order of magnitude: for example, the PCN survival metabolism using glucose has an energy conservation ratio of 0.5 ATP $electron^{-1}$ while aerobic catabolism of glucose is 1.3 ATP $electron^{-1}$ (Supplemental Information). Given these values represent disparate metabolisms yet do not deviate far from unity, we conclude that within this dataset that is dominated by measurements of glucose metabolism and aerobic respiration rates, units of electrons have an approximate equivalency to ATP units of energy, and therefore transformed the values originally reported in the primary publications collected by Hoehler et al. to units of electrons sec^{-1} $cell^{-1}$.

Within the categories of bacterial measurements, those reporting on endogenous metabolism, or the oxidation of endogenous carbon sources, contained the lowest and most heterogeneous values; the PCN EET cell-specific metabolic rate was in the lower 15% of them (Figure 1G). The maximum cell-specific metabolic rate of *P. aeruginosa* growing aerobically on glucose has been measured to be approximately 10^6 electrons sec^{-1} $cell^{-1}$ (28,29), three orders of magnitude higher than PCN EET, revealing that this organism has a remarkably plastic metabolic pace. We also found that the cell-specific metabolic rate of PCN EET, while supporting the maintenance of the population (Figure 1D), was nonetheless 2-3 orders of magnitude lower than maintenance metabolic rates inferred from continuous culture studies. This finding supports those of prior studies showing the metabolic rates of

microbes in oligotrophic natural environments are significantly lower than the maintenance requirements predicted from continuous culture (5). We conclude that PCN facilitated fermentation occurs at an extremely low cell-specific metabolic rate.

PCN facilitated fermentation powers a non-growth maintenance state

Because PCN metabolism is positioned at the lower end of measured metabolic rates documented for any life form, we wondered whether the weeklong population survival phenotype promoted by PCN EET reflected a non-growing survival state or a dynamic balance of growth and death, akin to the growth advantage in stationary phase phenomenon observed in *E. coli* under nutrient limitation(30). To distinguish between these possibilities, we performed a pulse-chase experiment using the fluorescent cell wall stain 7-hydroxycoumarincarbonylamino-D-alanine (HADA), a stain that has been previously used in *P. aeruginosa* to monitor cell growth(31). During bacterial growth, HADA is covalently incorporated into the cell wall, and after unincorporated HADA is washed away, new growth can be visualized as a loss of fluorescence in the non-pole regions of the cell(32) (Figure 2A). As a positive control, we checked to see whether we could observe HADA dilution during anaerobic growth on nitrate(33). As expected, HADA fluorescence was lost in a topological manner consistent with non-pole incorporation of new, non-fluorescent cell wall material (Figure S1) and was mostly diminished save for a few dimly fluorescent poles by day four (Figure 3B). HADA distribution over the cell body was unchanged after four days in the absence of nitrate (Figure 3B, S1). The presence of HADA in the cell wall did not affect the growth rate of the culture (Figure 2C).

Having validated HADA for *P. aeruginosa* in our media, we applied it to observe cells in our electrochemical reactors. HADA-stained cells in the +PCN/pot condition retained HADA throughout the entirety of their cell wall over the course of seven days (Figure 3D, S1). Notably, some cells that had not finished dividing during the inoculum transfer from oxic to anoxic conditions had HADA-labeled septa that remained intact even after the seven days of anaerobic incubation (Figure 3D, inset). The presence of HADA did not affect the survival or viability loss of the +PCN/pot and -PCN/pot cultures, respectively (Figure 3E). Lastly, the poles of at least 400 cells from each day and condition were counted to estimate the number of divisions across the population. These values for each day were close to zero (Figure 2F). Our results indicate that cells are statically surviving without growth during anaerobic PCN EET, and therefore this metabolism powers cellular maintenance.

While imaging cells from the -PCN/pot condition, we noticed in phase contrast that a significant number of cells displayed dark foci in their cytoplasm (Figure 3D), reminiscent of protein aggregates associated with ATP depletion and the viable but non-culturable (VBNC) state(34). To test if this state explained the loss of cell viability in the -PCN/pot condition, throughout the experimental time course, we incubated a sample of -PCN/pot cells in aerobic resuscitation conditions for two days before plating (see methods). At day seven of the anaerobic incubation, the CFU counts from the resuscitated cells were about two orders of magnitude higher than the counts from cells that were immediately plated (Figure S2B). The remaining order of magnitude discrepancy between the +PCN/pot and -PCN/pot conditions, representing most of the population, was not recovered (Figure S2A). Consistent with this finding, cell pellets of the cultures on day seven showed a clear size disparity between the +PCN/pot and -PCN/pot condition, indicating significant amounts of cell lysis

had occurred in this sample during anaerobic incubation (Figure S2C). We also confirmed that cells in the -PCN/pot condition were ATP-depleted relative to the +PCN/pot condition (Figure S2D), consistent with the presence of cells in the VBNC state(34). We conclude that the majority of CFU loss in the -PCN/pot condition is caused by death, with a minor subpopulation entering a VBNC state.

Cells are energy-limited and surviving near their maintenance requirement

While the preceding large reactor experiments enabled us to determine the pace of PCN EET metabolism relative to life's average basal metabolic rate and determine it relies on a facilitated fermentation for energy conservation, important mechanistic questions remained that required significantly greater experimental throughput. First, we sought to define the facilitated fermentation metabolic pathway more precisely by comparing mutant strains lacking enzymes of bioenergetic importance that we had reason to think might contribute to PCN-based survival (16,35). Second, we sought to determine whether the amount of PCN cycling was limiting survival. Previous studies have shown that the amount of current generated via EET is proportional to the concentration of electron shuttle provided (Torres et al. 2010). Accordingly, we leveraged a custom 96-well plate potentiostat system that permits high-throughput EET survival experiments(21) (Figure 4A) to measure the metabolic current of hundreds of cultures (including various mutant strains) over a range of PCN concentrations with multiple tiers of replication to increase our experimental statistical power (Figure 4B).

After five days of anaerobic incubation in this high-throughput system across PCN concentrations spanning three orders of magnitude, we found that survival of the Δ*phz1/2*

strain was dose-dependent up to at least 75 μM, with increasing concentrations having only marginal effects on survival (Figure 4C). Phenazine reduction can occur promiscuously via multiple metabolic flavoproteins (36,37), but we have shown recently that PCN is predominantly reduced by two NADH dehydrogenases in the cell membrane, Nuo and Nqr ((35), Figure 1B). While the current produced by a Δ*phz1/2* Δ*nuoF* Δ*nqrF* mutant was initially lower, after a day it approximately equaled that of the Δ*phz1/2* cells, suggesting other PCN reductases compensate after this time (Figure 4D). However, full survival across PCN concentrations nonetheless depended upon functional NADH dehydrogenases (Figure 4C), consistent with our working model (Figure 1B). Complementation of either NADH dehydrogenase restored survival at most concentrations of PCN, indicating they serve largely redundant functions (Figure S3). In agreement with our previous study (16), knocking out the AckA-Pta pathway (the energy-conserving step of the metabolism) had a larger consequence upon survival (Figure 4C). Interestingly, increasing PCN concentrations resulted in increased survival of the Δ*phz1/2* Δ*ackA-pta* mutant, albeit at significantly lower levels (Figure 4C). We hypothesized that this alternative mode of phenazine-dependent survival might also rely on the NADH dehydrogenases, and therefore tested a Δ*phz1/2* Δ*nuoF* Δ*nqrF* Δ*ackA-pta* mutant. Though this strain's survival was lower than the Δ*phz1/2* Δ*ackA-pta* mutant, it still improved up to 75 μM PCN yet the improvement in survival was lost at higher concentrations of PCN, indicating that the NADH dehydrogenase complexes play a significant role at these concentrations (Figure 4C). Overall, our data are consistent with substrate-level phosphorylation being the primary energy conserving mechanism under these conditions (Figure 1B) but also suggest the existence of an alternative PCN-dependent metabolic pathway that supports much lower levels of survival.

We also measured the long-term current generated as a function of PCN concentration and found the two were largely correlated (Figure 4D). As with the large reactors, we observed an early spike in current generation dependent on the phenazine concentration provided that then subsided to a lower, more stable current, though the decay happened at a slower rate than in the large reactors (Figure 4D, Figure 2A). The one exception was at 750 μM PCN, which produced highly variable initial currents despite stable currents later on (Figure 4D). By integrating the current generated between days one and five (i.e. after the initial current spike), we calculated the average PCN reduction rate across PCN concentrations and found it saturated above 75 μM (Figure 4E). At 375 μM PCN, the current measured on days 1-5 was below what the electrode was capable of oxidizing, exemplified by the initial high current spike (Figure 4D). What might cause this saturation? We hypothesized that either PCN oxidation at the electrode was limiting due to biofouling, or PCN reduction was limiting due to the cells themselves.

To distinguish between these scenarios, we used scanning electron microscopy to visualize cells on the electrodes, finding that the electrodes were mostly clear with a sparse monolayer of cells present on the working electrode surface, with the densest cell monolayer found in the 375 μM PCN condition (Figure S4A). While the absence of biofilms on the electrode suggested that biofouling was unlikely to explain the observed reduction rate plateau, we sought a more direct test of whether the cells or the electrode was limiting. Accordingly, on day 5 of the survival assay, we pooled Δ*phz1/2* cells from multiple technical replicate wells in the 375 μM PCN condition, pelleted them, resuspended them in a small volume and added them to other wells containing Δ*phz1/2* cells and 375 μM PCN such that the total cell concentration was approximately doubled. We observed a 1.5x increase in

current generation following the imposed cell doubling that was sustained for at least 10 hours (Figure S4B), demonstrating that the electrode was not limiting. Our results suggest that after about one day in anaerobic conditions, the cellular reduction rate above a certain PCN concentration becomes attenuated. What explains this attenuation is a worthy subject for future studies, especially given that 375 μM is near to the concentration of PCN found in *P. aeruginosa* biofilms(24).

Finally, we sought to determine whether the power output of the PCN facilitated fermentation was at or above the minimum necessary for maintenance metabolism. We reasoned that we would observe a relatively constant cell-specific metabolic rate over the PCN concentration range if this were true, as that would indicate that surviving cells require the same metabolic rate. Indeed, this is what we observed (Figure 3F). The cell-specific metabolic rate measured at 75 μM PCN was 3.0×10^3 electrons sec^{-1} $cell^{-1}$ at 25˚C, slightly higher than the rate measured in the large electrochemical reactors. Given the PCN concentration limits survival between 0.75 and 75 μM (Figure 3C), this consistent metabolic rate suggests that PCN limitation imposes an energy limitation, reducing the populations' viability in a PCN-dependent manner. While a fraction of cells may be in the VBNC state that are not accounted for in this analysis, particularly at lower PCN concentrations, such cells would be expected to make a minor contribution to the overall current measured (6). We therefore conclude that the culturable cells are operating near their minimum maintenance requirement under these conditions.

Discussion

Basic curiosity about the minimum power requirement of cells has inspired researchers over the past century to construct sophisticated methods and models aiming to capture what could not be determined directly (4,38,39). The primary contribution of this work is the measurement of the minimum metabolic rate necessary to fuel the anaerobic survival of the bacterium *Pseudomonas aeruginosa*, and the placement of this rate among the lowest reported across the tree of life. By studying a non-growth metabolism that is sustained by electrochemical cycling of a low-potential extracellular electron shuttle, we were able to quantify energy flux directly. We elucidated the key bioenergetic enzymes required to power a hybrid respiratory-fermentative metabolism that supports cellular maintenance. Our results also highlight the extraordinary range of power output that a single bacterial species can use to support its metabolism.

When surviving anaerobically via PCN cycling, *P. aeruginosa* cellular integrity and metabolic activity is sustained at the cell-specific metabolic rate of 1.6×10^3 electrons sec^{-1} $cell^{-1}$ at 25 ˚C. The term basal power requirement (BPR) has been introduced to define the minimum bioenergetic power per unit biomass required to sustain metabolic activity(5). In our system, cell survival is limited by the cell-specific metabolic rate (Figure 4F) making this rate the BPR for *P. aeruginosa* under these conditions. Recently, multiple environmental measurements of microbial cell-specific metabolic rates under energy-limitation have also been made or modeled(40), adding to a short list of BPR estimates. Measurements of oxygen consumption below the seafloor of the North Pacific Gyre were found to reach an asymptote at depth around 25 electrons sec^{-1} $cell^{-1}$, with the temperature unreported but presumably cold(41). The cell-specific metabolic rate of anaerobic sulfate-reducing bacteria found below

the seafloor at multiple sites were measured to reach an asymptote at depth to about 2.8 x 10^2 electrons sec^{-1} $cell^{-1}$ at temperatures around 5˚C(42). Bacteria residing beneath permafrost in the cryopeg brines of Utqiaġvik, Alaska have been modeled to sustain metabolic rates between 18 and 1.7 x 10^3 electrons sec^{-1} $cell^{-1}$ at subzero temperatures(43). Our measurement of the cell-specific metabolic rate not only occupies the lower end of endogenous metabolic rates measured made in the lab (Figure 2B), but it is also surprisingly close to environmental measurements made at much lower temperatures. Thus, it may be that our lab measurement and true environmental BPRs converge on the fundamental limit of what is needed to power bacterial survival, if such a universal value exists.

We also elucidated the key metabolic enzymes supporting this BPR. While we previously established that the AckA-Pta enzymes are necessary for phenazine facilitated fermentation(16), our work here further demonstrates that either of the NADH dehydrogenases Nuo and Nqr are additionally necessary to support full survival of cells via PCN facilitated fermentation (Figure 4C). This may only apply to the phenazine PCN, as we have shown that it is the only derivative made by *P. aeruginosa* that is predominantly reduced at the membrane(35). Indeed, phenazines are known to promiscuously react with many metabolic flavoproteins in the cytosol(36,37). This promiscuity likely explains our finding that increasing concentrations of PCN correlated with increasing survival in the Δ*phz1/2* Δ*nuoF* Δ*nqrF* mutant tested (Figure 4C). We speculate that the benefit the NADH dehydrogenases provide is a direct coupling to the NADH pool and, by extension, pyruvate oxidation. While other flavoproteins can dissipate reducing equivalents onto the PCN pool in the absence of the NADH dehydrogenases, the reductants involved may not be as directly coupled to the NADH pool and be wasted energetically. The PCN-dependent compensation

of the Δ*phz1/2* Δ*ackA-pta* mutant (Figure 4C) is more difficult to explain and suggests the participation of unidentified alternative energy-conserving pathways. These pathways may still be NADH-coupled, which could explain the loss of enhanced survival in the Δ*phz1/2* Δ*ackA-pta* mutant at high PCN concentrations in the Δ*phz1/2* Δ*nuoF* Δ*nqrF* Δ*ackA-pta* mutant (Figure 4C). Future metabolomic experiments will shed light on the nature of these PCN-dependent compensations.

In their normal function during respiratory growth, the Nuo and Nqr complexes chemiosmotically pump protons across the cytosolic membrane with $H^+/2e^-$ of 4 and 2, respectively(44,45). This is driven by a large ΔE°' of 420 mV between the NADH and ubiquinone pools. For PCN reduction by NADH, ΔE°' is less than half that value at 180 mV, corresponding to a ΔG°' of -34.7 kJ/mol. Previous work has estimated the minimum biological energy quantum (the translocation of one proton across the cytoplasmic membrane) to be -20 kJ/mol(46). These values may shift some amount relative to the concentrations of reactants and substrates and the PMF level but provide a useful quantitative baseline. From them, we infer that PCN reduction by an NADH dehydrogenase theoretically provides only enough free energy to translocate one proton, less than the normal proton coupling of Nuo and Nqr, thus we think it is unlikely that these complexes are translocating protons during PCN reduction. Nonetheless, metabolisms operating near the thermodynamic limit are known to occur(47) so further studies using purified Nuo and Nqr using phenazine substrate are needed to determine if this mechanism of energy conservation is plausible.

It is generally believed that organisms in the environment metabolizing at low rates are growing, albeit slowly; indeed, environmental doubling times on the order of days to 1000s of years have been estimated by multiple studies(48). Accordingly, anticipating that

PCN EET would power slow growth, we were surprised that cell growth was not detectable using our HADA assay (Figure 3). It may be that we simply did not wait enough time to observe slow growth in the lab and/or that estimates of slow growth in the environment are inexact. To parse this discrepancy, we note that it has been estimated that the energetic cost of aerobic division for a bacterial cell is approximately 4×10^9 ATP per division(49). Based on the dominant ATP-generating pathway used under these conditions (i.e. oxidation of glucose to acetate coupled to substrate-level phosphorylation, Figure 1B), we estimate that *P. aeruginosa's* ATP output is about 8.0×10^2 ATP sec^{-1} $cell^{-1}$. We can then estimate that if division were possible under PCN facilitated fermentation, cells would be doubling at a rate of once every two months, and perhaps even faster because biosynthetic costs are thought to be less under anoxic conditions(50) and the fraction of energy lost to maintenance processes is presumed to be less during slow growth(51). Yet given the cells are operating at their BPR (Figure 4F), it seems more likely this ATP output is the maintenance energy requirement. Together, these findings prompt us to question whether microbes are capable of doubling on exceedingly-long time scales, or if they instead undergo long-term survival, opportunistically waiting for punctuated bursts of local nutrients to fuel relatively fast growth as has been suggested recently(52). In this way, the classic "feast-famine cycle" may apply to more than just enteric bacteria(53), which would carry implications for biogeochemical modeling(54). Future studies of the growth associated with extremely slow metabolic rates are needed to determine which model is more accurate.

Outside of its fundamental interest to cell biology, understanding the minimal energy requirements and physiology of cells in a non- or slow-growth state has important practical implications. Despite the fact that estimated microbial doubling times in nature typically are

on the order of days to weeks to years(55–58), the vast majority of microbial physiology studies in pure culture have been conducted using model species grown with doubling times under an hour. The consequences of this lab-to-nature metabolic rate mismatch has resulted in our inability to control slow-growing microbes in nature and disease. For example, drugs used to treat chronic infections often fail because they target machinery that is absent or insignificant in growth-arrested organisms(59). A better understanding of slow-growth or maintenance physiology is thus essential to develop more effective therapeutics to treat chronic infections. Similarly, synthetic biologists aiming to catalyze desirable changes in natural settings, such as applying pro-biotics to the rhizosphere to stimulate the growth of crops, lack a basic understanding of how cells survive periods of growth arrest due to desiccation or nutrient limitation; yet such knowledge is essential if designed bacteria are to be successful when deployed in the field (60,61). Perhaps most pressing is that climate scientists' predictions of the contribution of microbial metabolism to the global carbon cycle do not incorporate realistic bacterial metabolic rates into their models(62). In all these cases, an understanding of life "in the slow lane", is needed(52). Our PCN-cycling system opens the door to quantitative mechanistic studies of a maintenance state that comes much closer to approximating real-world metabolisms than the typical growth conditions used in the lab.

Finally, while bioenergetic comparisons often rely on thermodynamic arguments to compare the energy conservation efficiency of different metabolisms, our results highlight the importance of kinetics in explaining the remarkable plasticity of microbial metabolism. To wit: per glucose molecule, fermentation generates roughly 10 times less ATP than aerobic respiration, yet the cell-specific metabolic rate during facilitated fermentation we measure is 1,000 times slower than *P. aeruginosa*'s fast aerobic growth. In terms of power, this disparity

is dominated not by differences in energy conservation efficiency but by differences in rates. Indeed, it seems likely that slow kinetics may dominate the bioenergetic reality of maintenance metabolism near the limits of life. If, how, and when metabolic rate is controlled at the molecular level or limited by the environment are important questions to be addressed in future research and key to an understanding of the dominant pace of microbial life on the planet.

Methods

Bacterial growth conditions

All *Pseudomonas aeruginosa* UCBPP-PA14 strains were plated on LB agar from -80˚C glycerol stocks and grown overnight at 37˚C. Plates were stored at 4˚C for up to a week and were used to inoculate liquid cultures. Initial liquid cultures were grown in 7 mL of LB medium in glass culture tubes (VWR #47729-583) in an orbital shaker (New Brunswick, Innova 44) at 37˚C shaking at 250 rpm on a slant for 20 hours (final OD_{500nm} ~6).

Bacterial survival conditions in large electrochemical reactors

Initial cultures were used to inoculate a large 250 mL LB culture to an initial OD_{500nm} of 0.06. This large culture was grown under the same conditions as the initial culture for 5.5 hours to an OD_{500nm} of 3.0±0.2. These cells were pelleted (10 min, 6800 x*g*) and washed twice in a minimal medium (100 mM MOPS pH 7.2 with NaOH, 43 mM NaCl, 93 mM NH_4Cl, 3.7 mM KH_2PO_4, 1 mM $MgSO_4$), then resuspended to an OD of 75 and transferred into an MBraun nitrogen-only atmosphere glove box (Unilab model) containing the prepared glass reaction vessels (custom made) and held at 33˚C. 1 mL of the concentrated culture was

then diluted into the main chamber of the large reaction vessels containing 99 mL of N_2-sparged minimal medium with 20 mM D-glucose and 3.6 μM $FeSO_4$ added (hereafter referred to as glucose minimal medium), along with 75 μM PCN in the relevant samples. This culture was connected to a potentiostat (Gamry Reference 600 model) via a graphite rod working electrode (Alfa Aesar #14738), platinum mesh counter electrode (custom-made using Alfa Aesar platinum gauze #10283), and Ag/AgCl reference electrode (Basi #MW-2030). The counter electrode was held in a small side-chamber separated from the main by a glass frit containing 9 mL minimal medium and 75 μM PCN. The working electrode was poised at a constant 0 mV vs. Ag/AgCl and the cultures were incubated with stirring using a stir rod in the vessel. 100 μL samples were removed periodically via a port over the main chamber of the vessel for CFU counting.

Bacterial survival conditions in 96-potentiostat electrochemical plate

Initial cultures were pelleted and washed twice in minimal medium, resuspended to an OD of 15, and transferred into an anerobic Coy Chamber held at 33˚C and 2-3% H_2 containing the prepared 96-well electrochemical plate (custom-made as previously described(21)) with a screen-printed carbon working electrode and counter electrode, and Ag/AgCl reference electrode. 10 μL of the concentrated culture was then diluted into each well of the plate containing 190 μL of N_2-sparged glucose minimal medium. The plate was sealed using both a slit-seal cover (BioChromato #R80.120.00) and an aluminum seal cover (DiversifiedBiotech #ALUM-1000) to prevent evaporation of the cultures between sampling. The plate was incubated at 33˚C without shaking in a custom 96-potentiostat system originally developed at the National Institute for Material Science, Japan. Every wells'

working electrode was held at a constant 0 mV vs. Ag/AgCl. On days 1, 3, and 5 of the incubation, the aluminum seal was removed and the well contents were mixed by pipetting a 150 µL volume. 10 µL was then removed for CFU dilution counting (20 µL on Day 5 to capture the lowest CFU concentrations). The plate was resealed with a fresh aluminum seal and then placed back in the 96-potentiostat system until the next CFU sampling.

Mutant strain construction and complementation

All plasmids used in this work are listed in the Key Resources Table. Primers were synthesized by Integrated DNA Technologies and are also listed in the Key Resources Table. For all molecular cloning, plasmids were constructed using Gibson assembly reactions (NEB). Plasmids were chemically transformed into *E. coli* strain S17 and then conjugated into *P. aeruginosa* PA14. Mutants were constructed using standard homologous recombination using 1 kb regions flanking the gene(s) of interest in the pMQ30 plasmid. Genetic complement strains were constructed by reintroducing the deleted gene or operon in *trans* at the *att*Tn7 site downstream of *glmS* in the *P. aeruginosa* genome using the pJM220 plasmid. For each complementation, the gene or operon was designed to have its expression driven by a rhamnose-inducible promoter, and accordingly, complementation survival experiments were conducted using complete MOPS survival medium supplemented with l-rhamnose (0.005% w/v, 305 µM).

CFU counting

Phosphate buffered saline (PBS) was used for diluting cell cultures prior to plating for CFUs. Dilutions spanning 6-7 orders of magnitude were plated on LB agar using 5 µL spots and

incubated at 37˚C overnight. Colonies were counted with the aid of a dissection microscope (Nikon SMZ800). The furthest dilution spot containing at least 10 colonies was counted. Plates were kept for at least another 48 hours at room temp to check for delayed colony appearance; counts were updated when this rarely occurred.

High-performance liquid chromatography

Samples were collected by centrifuging 1 mL of sample and passing the supernatant through a 0.22 μm filter. Samples were stored at -80˚C until analysis. Acetate and succinate were quantified using a Waters e2695 Separations Module equipped with a 2998 PDA Detector and run through an Aminex HPX-87H column (Bio-Rad) held at room temperature at a flow rate of 0.5 mL min^{-1} for 25 mins. The mobile phase used was 5 mM H_2SO_4. Retention times for analytes were validated with single species standards. For each analyte, standards ranging from 0 to 20 mM were used to calibrate peak area against a known concentration.

Cell dry weight measurements

On day 5 of the anaerobic survival in the large electrochemical reaction vessels, 2 mL samples of +PCN/pot culture were collected into pre-weighed tubes. The cultures were pelleted and resuspended twice in deionized water, then pelleted again. The supernatant was removed, and the pellet was dried overnight in a 55˚C drying oven. The dried pellets were then weighed on a microbalance, and the weight was divided by 2 * CFU / mL counts for that day to estimate the grams cell dry weight per cell.

Propidium Iodide staining and imaging

Samples of culture from the large electrochemical reaction vessels were collected on day 5 of anaerobic incubation. The cells were pelleted and washed twice in anoxic PBS, then stained with 70 μM propidium iodide (Invitrogen) for 20 minutes in anoxic conditions. The cell suspension was then brought out of the MBraun chamber and spotted onto 1% (w/v) agar pads and imaged on a Nikon Eclipse Ti-2 inverted microscope using an ORCA-Flash4.0 V3 camera. Excitation light (555 nm) was supplied through a SpectraX LED light engine for a 200-ms exposure, and emission light was passed through a standard TRITC filter cube (Semrock) with the excitation filter removed. Identical LUTs were applied across all fluorescence images for comparison. The number of cells stained was counted by eye with these LUTs applied; cell husks (those with no discernable phase-dark aspect) were excluded.

HADA single-cell growth measurements

250 mL LB cultures of cells were grown as described in the *Experimental Model* with 60 μM HADA label. Excess HADA at the end of growth was washed away and the cells were inoculated into the anaerobic electrochemical reaction vessels as described above. For the nitrate control, smaller LB cell cultures containing HADA were used (7 mL) and washed identically before being inoculated into N_2-sparged balch tubes containing 10 mL of glucose minimal medium with 0.05% casamino acids and with or without 40 mM KNO_3 added. The balch tubes were incubated at room temperature in the dark to ensure a slow growth over approximately the same time scale as the electrochemical survival experiment. On each day of either incubation (balch or echem), 0.5 mL of cells were sampled, pelleted, and resuspended in oxic PBS. On later days, the -PCN/pot samples were resuspended in smaller

volumes of PBS to normalize cell density. 1 μL of the suspension was spotted onto 1% (w/v) agar pads and imaged on a Nikon microscope as described in *Propidium Iodide staining and imaging*, using a 395 nm excitation, 200-ms exposure time, and a standard DAPI filter cube (Semrock) with the excitation filter removed. Due to global loss of fluorescence brightness at later timepoints, fluorescence LUTs were adjusted independently for each day to maximize visualization of cell body vs. pole staining. LUTs were set the same across images from the same day. The number of fluorescent poles vs. total poles was counted by eye with these LUTs applied.

VBNC resuscitation

On days 3, 5, and 7 of the large reactor anaerobic incubation, samples of -PCN/pot culture from the vessels were pelleted and resuspended twice in oxic PBS of equal volume. A sample of this cell suspension was immediately plated for CFUs while another sample was diluted 1:10 in PBS in culture tubes and incubated at 33˚C aerobically without shaking. A sample of this aerobic resuscitation suspension was plated for CFUs after 1, 2, and 3 days of incubation.

ATP quantification assay

ATP was quantified using a Promega BacTiter-Glo kit according to the manufacturer's protocol. On day 7 of the large reactor anaerobic incubation, samples of culture from the vessels were pelleted and resuspended twice in anoxic PBS. Cells from the +PCN/pot condition were resuspended at a final concentration of 1x, while the -PCN/pot condition were resuspended at a 10x concentration to acquire sufficient luminescence from the assay. ATP

quantification was divided by the CFUs for that day; resuscitated CFUs were used for the -PCN/pot condition.

Scanning electron microscopy

At the end of day 2 of the 96-potentiostat electrochemical plate survival experiment, after current had already subsided following the initial spike in the 375 μM PCN condition, samples were gently mixed by pipetting a 150 μL volume, then removed from the wells. 2.5% glutaraldehyde in PBS was added to each well and incubated for 10 min at 25˚C. The samples were carefully rinsed three times with PBS, then dehydrated by an ethanol wash gradient with 5 min incubations. The dehydrated samples were then washed with *t*-butanol twice for 5 minutes. The electrochemical board on the bottom of the plate was removed, and freeze-dried in *t*-butanol under vacuum for 2 days. The board was then platinum coated and observed by a Keyence VE-9800 microscope at 10 or 20 kV.

Quantification and statistical analysis

For all experiments, Prism 10 was used for analysis except for integration of current, which was done in Origin 10. Technical replicates were averaged to generate single biological replicates before statistical analysis; therefore, all error ranges reported represent variation from biological replicates. Since CFUs were counted in log space, geometric means were used as a summary statistic. Any reported values that incorporated CFU counts (such as cell-specific metabolic rates) are also reported as a geometric mean. Otherwise, replicates were averaged using a linear mean.

To calculate an average PCN reduction rate in the 96-potentiostat system, current vs time traces were trimmed by 3 hrs immediately following the times when the plate was removed and returned to the potentiostat: these times following reconnection resulted in spurious, large spikes in current that settled back down to levels prior to removal of the plate. The current between days one and five was integrated, giving values with units nA*hr. This was then converted to units of electrons using standard conversion factors, divided by 90 hrs (4 d minus 6 hrs surrounding times of plate removal), divided by the geometric mean of the day 1-5 CFU $(0.2\ mL)^{-1}$ counts, and reported as units of electrons sec^{-1} $cell^{-1}$.

Reagents

REAGENT or RESOURCE	**SOURCE**	**IDENTIFIER**
Bacterial and Virus Strains		
Pseudomonas aeruginosa UCBPP-PA14 Δ*phz1/2*	(63)Dietrich et al., 2006	N/A
P. aeruginosa UCBPP-PA14 Δ*phz1/2* Δ*nuoF* Δ*nqrF*	(35)Ciemniecki and Newman, 2023	N/A
P. aeruginosa UCBPP-PA14 Δ*phz1/2* Δ*ackA-pta*	(16)Glasser et al., 2014	N/A
P. aeruginosa UCBPP-PA14 Δ*phz1/2* Δ*nuoF* Δ*nqrF* Δ*ackA-pta*	This study	N/A
P. aeruginosa UCBPP-PA14 Δ*phz1/2* Δ*nuoF* Δ*nqrF*, *att*Tn7::*rhaP*$_{BAD}$-*nuoF*	This study	N/A

P. aeruginosa UCBPP-PA14 Δ*phz1/2* Δ*nuoF* Δ*nqrF*, *att*Tn7::*rhaP*$_{BAD}$-*nqrF*	This study	N/A
E. coli S17 (chemically competent for transformation)	ATCC	ATCC-BAA-2428
E. coli SM10/pTNS1 (chromosomal insertion helper strain)	(64)Choi and Schweizer, 2006	N/A
Chemicals, peptides, and recombinant proteins		
Difco LB Broth	BD	Cat#244620
Difco LB AGAR	BD	Cat#244520
MOPS	Sigma-Aldrich	Cat#RDD003
Sodium Chloride	Fisher	Cat#BP358-212
Ammonium Chloride	Fisher	Cat#A649-500
Potassium Phosphate Monobasic	Fisher	Cat#P382-500
Magnesium Sulphate Heptahydrate	Fisher	Cat#M63-500
D-Glucose	Fisher	Cat#D16-500
Iron(II) Sulphate Heptahydrate	Fluka	Cat#44970
Phenazine-1-carboxamide	ChemScene	Cat#CS-W022931
Sodium Acetate Trihydrate	Fisher	Cat#S209-500
Sodium Succinate Dibasic Hexahydrate	Sigma-Aldrich	Cat#S2378
Potassium Nitrate	Fisher	Cat#P263-500
HADA	Tocris	Cat#6647
Propidium Iodide	Invitrogen	Cat#P1304MP
Oligonucleotides (5'-3')		

ackA-pta upstream forward: ACGACGGCCAGTGCCAAGCTTTCAGGCTGCAGAAGGACTG	This study	N/A
ackA-pta upstream reverse: GCCCACTGGGCGGCGTTCCTTCACTGCTCCTTGGTCTGCT	This study	N/A
ackA-pta downstream forward: AGCAGACCAAGGAGCAGTGAAGGAACCCCGCCCAGTGGGC	This study	N/A
ackA-pta downstream reverse: CATGATTACGAATTCGAGCTTACTGATCGCGGCCTGGAAGAAAAAGC	This study	N/A
Recombinant DNA		
pMQ30	(65)Shanks et al., 2006	N/A
pJM220	(66)Jeske and Altenbuchner, 2010	N/A
pMQ30 Δ*ackA-pta*	This study	N/A
pJM220 *rhaP*$_{BAD}$-*nuoF*	(35)Ciemniecki and Newman, 2023	N/A
pJM220 *rhaP*$_{BAD}$-*nqrF*	(35)Ciemniecki and Newman, 2023	N/A

Software and Algorithms		
GraphPad Prism 10 v10.1.1		https://www.graphpad.com/
Origin 10 v10.1		https://www.originlab.com

Figures

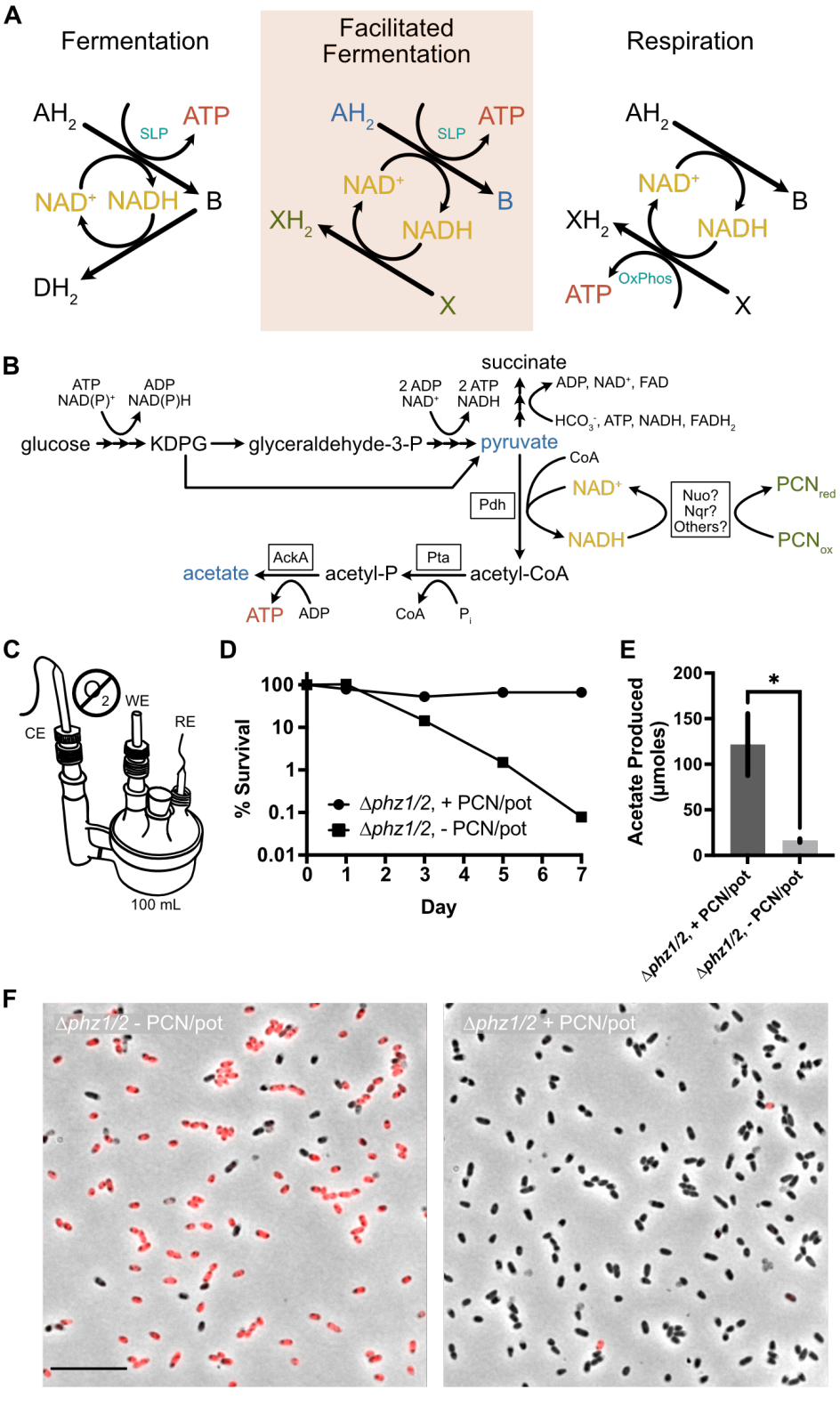
A
Fermentation
Facilitated Fermentation
Respiration
AH2
ATP
SLP
NAD+
NADH
B
DH2
XH2
X
OxPhos
B
succinate
ATP
NAD(P)+
ADP
NAD(P)H
2 ADP
NAD+
2 ATP
NADH
ADP, NAD+, FAD
HCO3-, ATP, NADH, FADH2
glucose
KDPG
glyceraldehyde-3-P
pyruvate
CoA
Pdh
Nuo?
Nqr?
Others?
PCNred
PCNox
AckA
Pta
acetate
acetyl-P
acetyl-CoA
ATP
ADP
CoA
Pi
C
CE
WE
RE
2
100 mL
D
% Survival
100
10
1
0.1
0.01
0
1
2
3
4
5
6
7
Day
Δphz1/2, + PCN/pot
Δphz1/2, - PCN/pot
E
Acetate Produced (μmoles)
200
150
100
50
0
*
Δphz1/2, + PCN/pot
Δphz1/2, - PCN/pot
F
Δphz1/2 - PCN/pot
Δphz1/2 + PCN/pot

Figure 1. PCN redox-cycling promotes anaerobic energy conservation and survival via a facilitated fermentation. (A) Simplified schema of heterotrophic metabolisms and their predominant mode of energy conservation, exemplifying how facilitated fermentation is a fermentation-respiration hybrid. SLP – substrate level phosphorylation, OxPhos – oxidative phosphorylation. (B) Working model of the active metabolic pathways catabolizing glucose during PCN facilitated fermentation. The NADH dehydrogenases Nuo and Nqr are putatively involved in the metabolism because of their previously established function as key PCN reductases (31). (C) Schematic of large glass electrochemical reactors used in this study to continuously re-oxidize PCN anaerobically reduced by the cell culture. A stir bar in the main chamber kept the culture well-mixed. CE – counter-electrode, WE – working electrode, RE – reference electrode. (D) Anaerobic survival of Δ*phz1/2* strain in glucose minimal medium with or without 75 μM PCN and an oxidizing potential. 100% survival represents approximately 8 x 10^8 CFU mL^{-1}. Data are representative of 2 biological replicates. (E) Quantification of acetate production after 7 days of culture incubation. Data are averaged across 2 biological replicates, error bars represent the standard deviation. Welch's t-test was used to compare samples, *$p<0.05$. (F) Propidium iodide staining of anaerobic cultures on day 5 of survival imaged on a fluorescence microscope. Images are representative of 2 biological replicates. Scale bar is 10 μm.

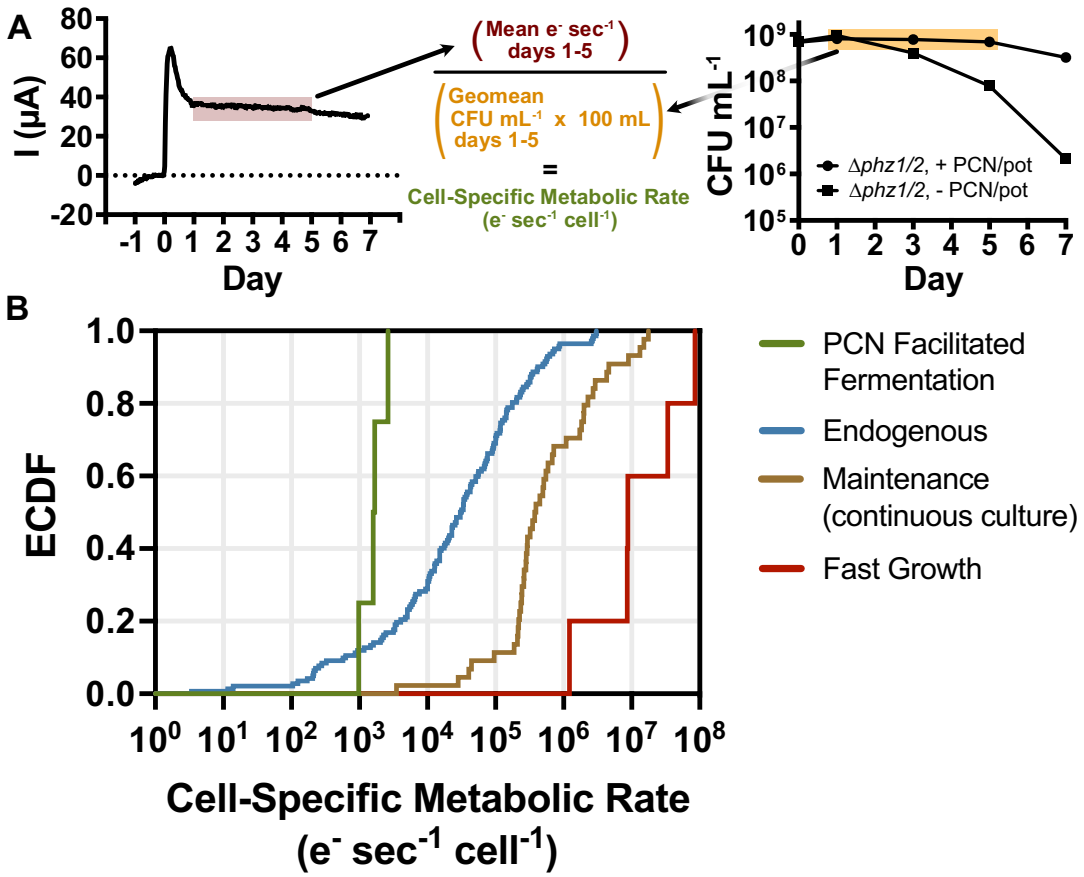

Figure 2. The metabolic rate of PCN facilitated fermentation is extremely low. (A) Cell-specific metabolic rate during PCN facilitated fermentation was quantified from large electrochemical reactor experiments. Cells are added on day 0. The mean current generated by the culture across days 1 to 5 was averaged and divided by the geometric mean of CFUs across the same period. Data are representative of 4 biological replicates. (B) Empirical cumulative distribution functions of lab-measured bacterial metabolic rates collated previously by Hoehler et al. (27), with units transformed to electrons sec^{-1} $cell^{-1}$ at 25°C. Fast growth includes bacteria growing at or near their maximum growth rate. Maintenance includes inferred maintenance energy metabolic rates (i.e. during zero growth) extrapolated from slow-growing continuous culture studies. Endogenous includes metabolic rates measured in the absence of any exogenous electron donor, thereby using endogenous stores of donors instead. Each data point is an independent experimental measurement. The dataset encompasses 90 species and 198 measurements.

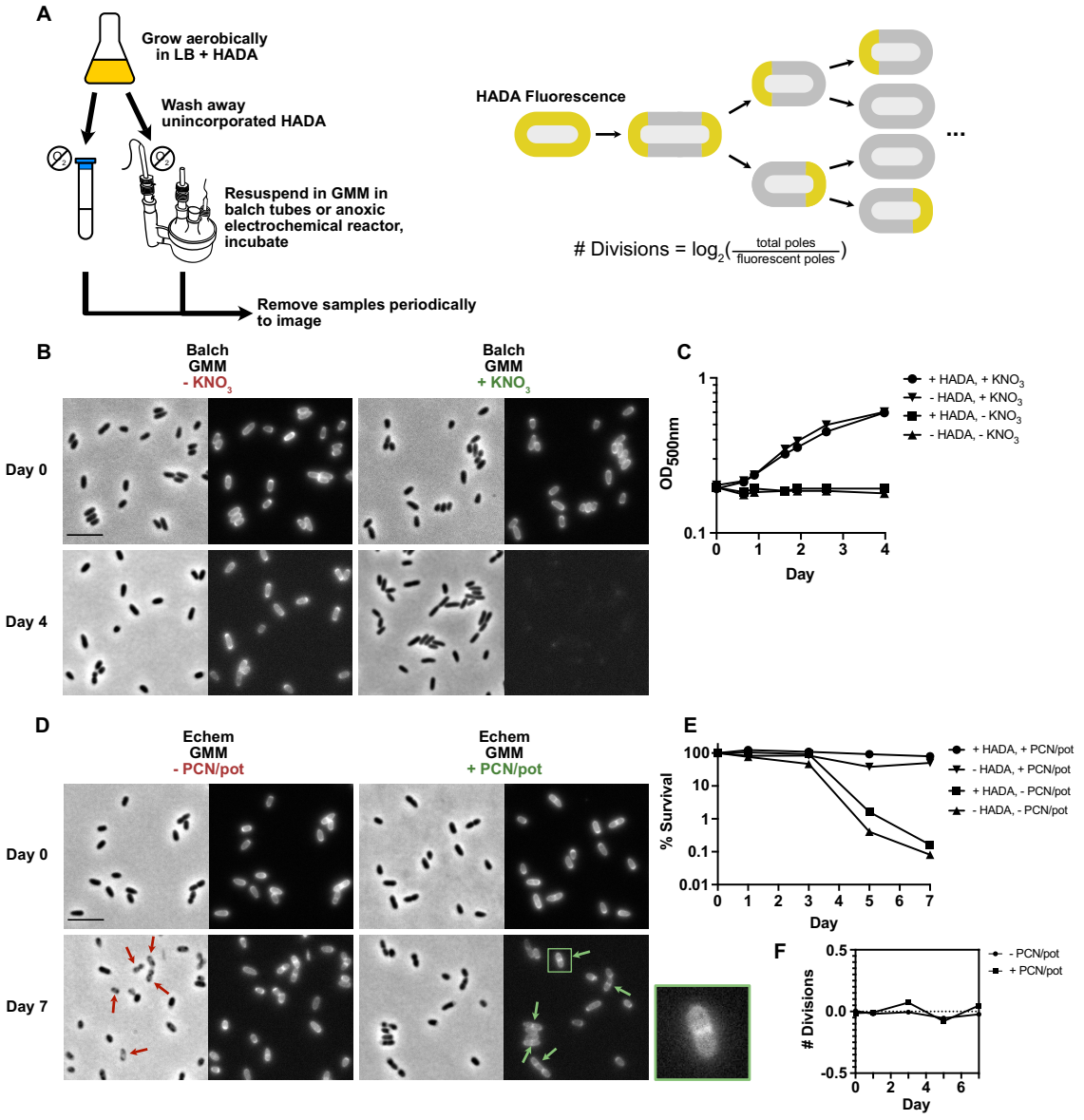

Figure 3. Single cells do not grow during anaerobic survival via PCN facilitated fermentation. (A) Experimental design and expected topological dilution of HADA cell wall stain during cell division. (B) HADA fluorescence imaging of cells during anaerobic growth on glucose and nitrate in sparged balch tubes. GMM – glucose minimal media. Scale bar is 5 µm. (C) Anaerobic growth of cultures imaged in (B) compared to cultures not that were not stained with HADA. (D) HADA fluorescence imaging of cells during anaerobic survival on glucose, PCN, and an oxidizing potential in large electrochemical reactors. Scale bar is 5 µm. Red arrows indicate phase-dark granules that accumulate in cells that are not provided with PCN and an oxidizing potential. Green arrows indicate HADA-labeled septa that remained intact over the week-long incubation; inset is a zoomed example,

each edge is 3.75 μm. (E) Anaerobic survival of cultures imaged in (D) compared to cultures that were not stained with HADA. (F) Estimated number of divisions of the +PCN/pot culture imaged in (D) via manual counting of fluorescent vs total cell poles and the equation in (A). Each datapoint is n≥400 cells. All data in figure are representative of two biological replicates.

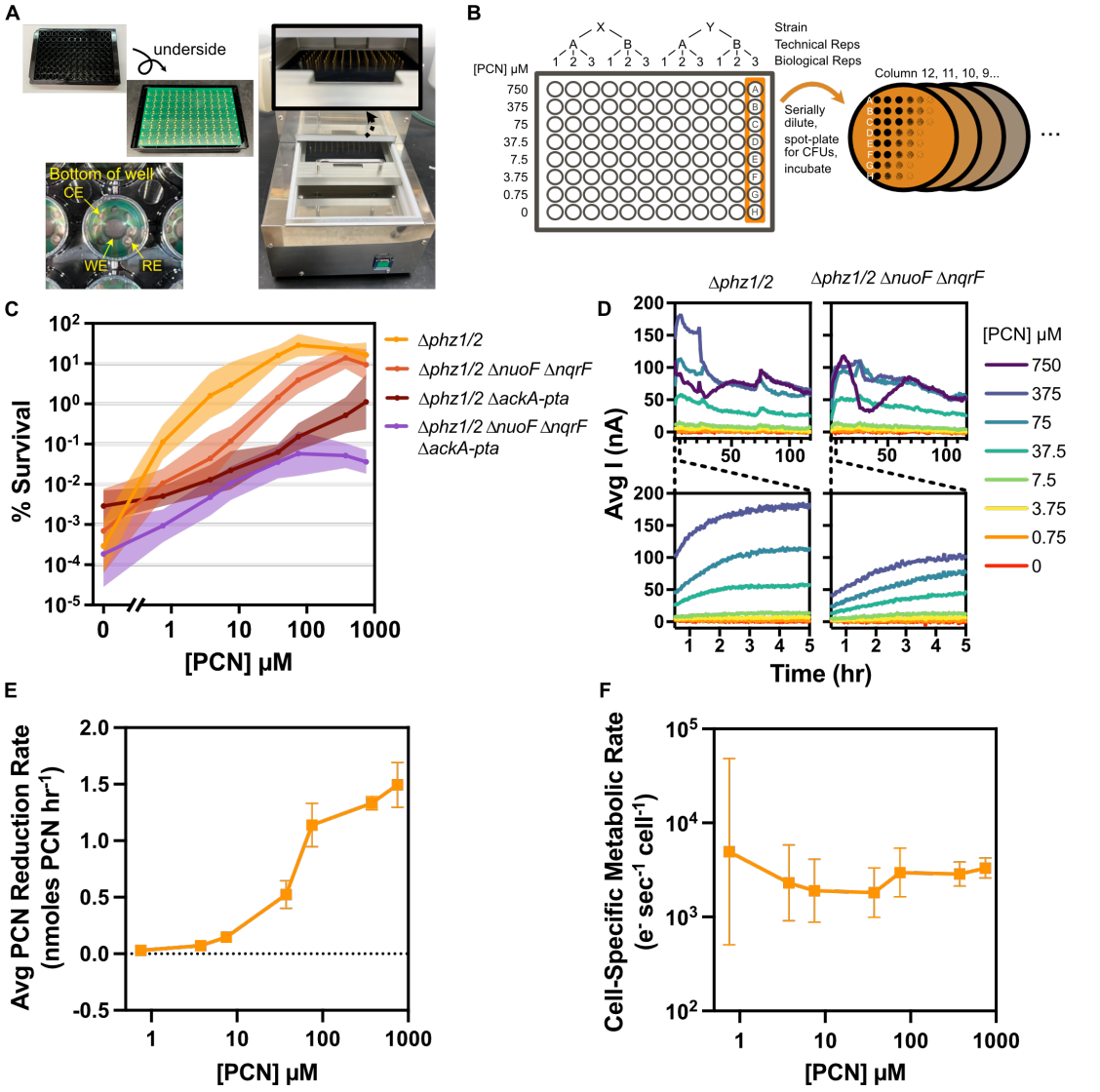

Figure 4. High-throughput PCN EET experiments reveal a dependence on NADH dehydrogenases and survival near the minimum maintenance requirement. (A) 96-poteniostat plate reader used for experiments. Each well of the plate is outfitted with an independent working electrode (WE), counter electrode (CE), and reference electrode (RE) that are connected to the pins of the potentiostats via contacts on the bottom of the plate. (B) Example experimental design of high-throughput PCN redox-cycling survival experiments. (C) Survival of Δ*phz1/2* and metabolic mutant strains after 5 days of anaerobic incubation in a glucose minimal medium across various concentrations of PCN. Each datapoint is the geometric mean of at least 5 biological replicates. Shaded regions represent 95% confidence intervals. 100% survival represents approximately 8 x 10^8 CFU mL^{-1}. (D) Average current produced by Δ*phz1/2* and Δ*phz1/2* Δ*nuoF* Δ*nqrF* strains over the

course of 5 days, with zoom-ins on the initial 5 hours of current production. Averages (E) PCN reduction rate of Δ*phz1/2* cultures over days 1 to 5 of the anaerobic incubation. Each data point is the average of 5 biological replicates and error bars represent the 95% confidence interval. (F) Cell-specific metabolic rate of Δ*phz1/2* cells during days 1 to 5 of the anaerobic incubation across various concentrations of PCN. Each data point is the geometric mean of 5 biological replicates and error bars represent the 95% confidence interval.

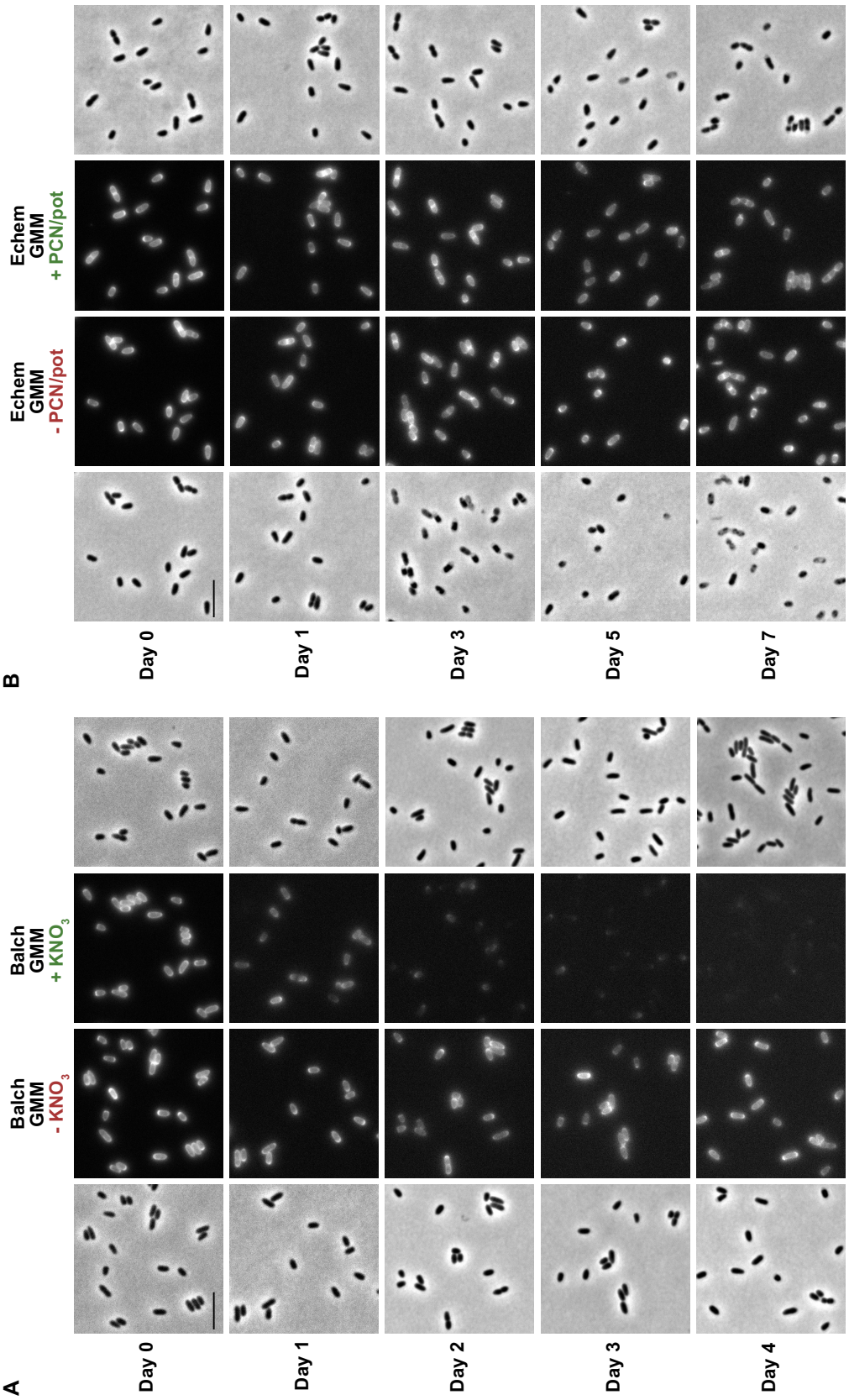
A
Balch GMM - KNO3
Balch GMM + KNO3
Day 0
Day 1
Day 2
Day 3
Day 4
B
Echem GMM - PCN/pot
Echem GMM + PCN/pot
Day 0
Day 1
Day 3
Day 5
Day 7

Figure S1. Full dataset showing single-cells do not grow during PCN facilitated fermentation. (A) HADA fluorescence during anaerobic growth on glucose and nitrate. Expansion of the dataset in Figure 3B across each day of data collection. (B) HADA fluorescence during anaerobic survival on glucose, PCN, and an oxidizing potenial. Expansion of the dataset in Figure 3D. Scale bar is 5 μm.

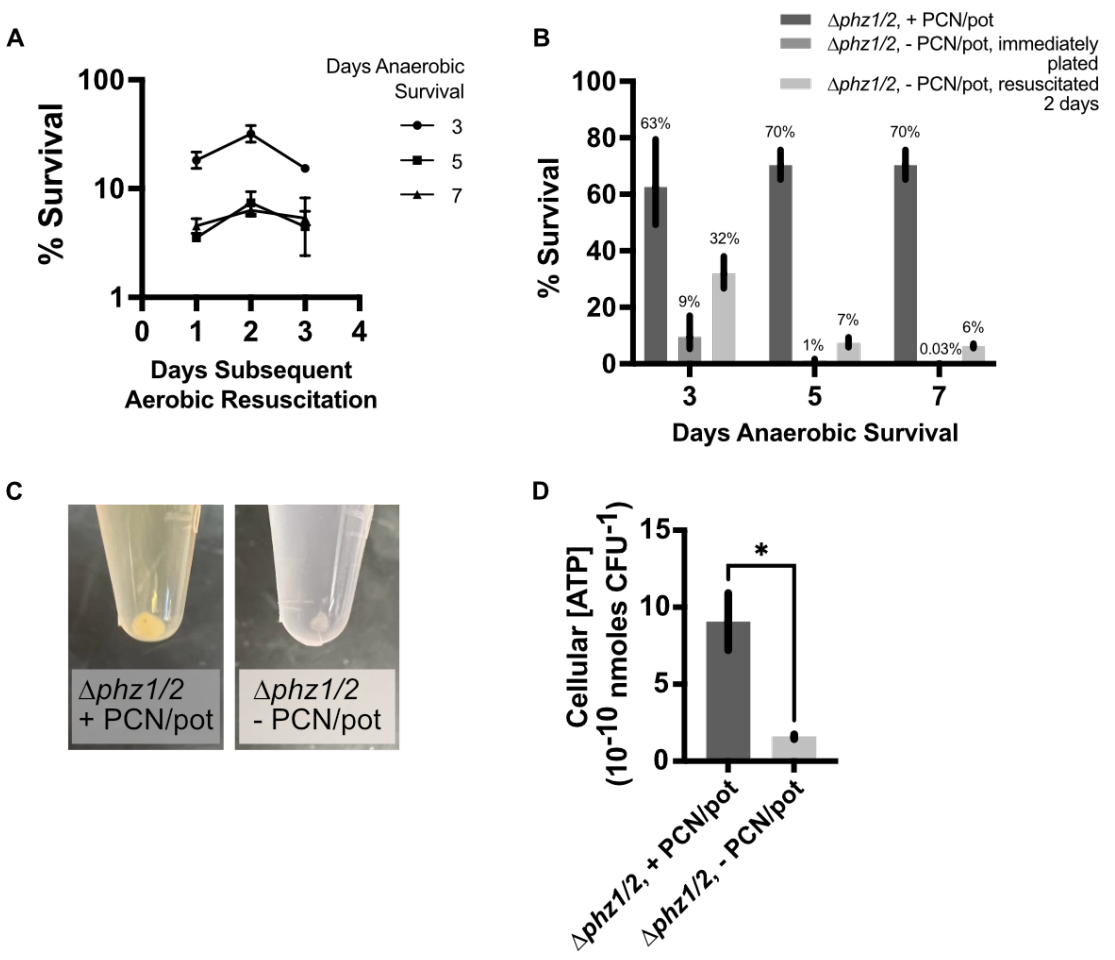

Figure S2. The major cause of anaerobic CFU loss is death. (A) Aerobic resuscitation of Δ*phz1/2* as a function of incubation time in oxic PBS after removal from anaerobic -PCN/pot condition. See methods for details. Each data point is the geometric mean of two biological replicates. Error bars represent the standard deviation. (B) Survival of Δ*phz1/2* -PCN/pot cells before and after maximum resuscitation. (C) Pellets of 1 mL of cell culture after 7 days anaerobic incubation. (D) Cell ATP levels after 7 days of anaerobic incubation. Data are averaged across 2 biological replicates, error bars represent the standard deviation. Welch's t-test was used to compare samples, *$p<0.05$.

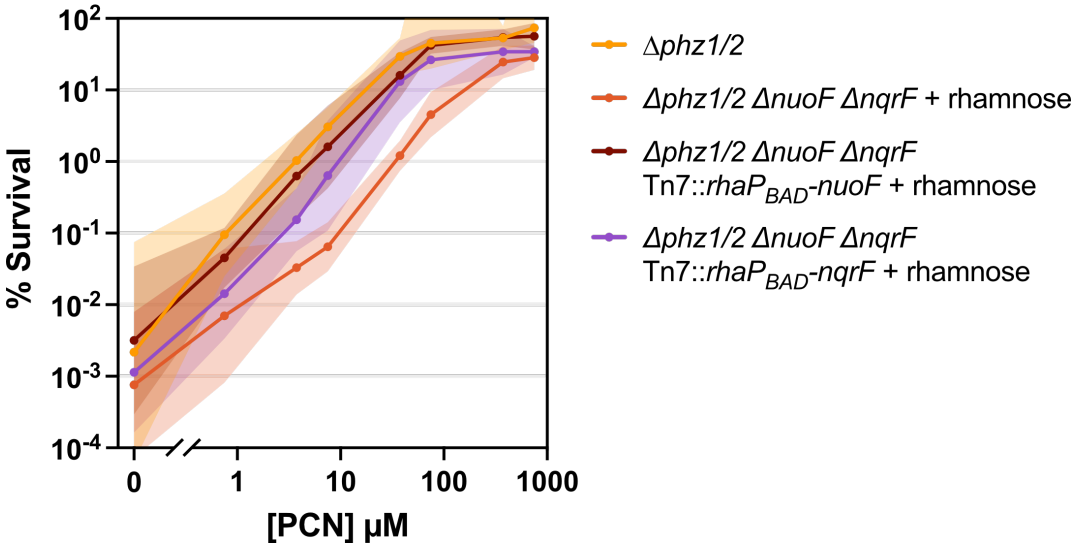

Figure S3. Nuo and Nqr are each sufficient to complement survival at most PCN concentrations. The *nqrF* or *nuoF* gene were each complemented in *trans* into the Δ*phz1/2* Δ*nuoF* Δ*nqrF* mutant under a rhamnose-inducible promoter. Survival of these strains are shown after 5 days of anaerobic incubation in a glucose minimal medium with or without 0.005% (w/v) rhamnose added as indicated. Each datapoint is the geometric mean of at least 3 biological replicates. Shaded regions represent 95% confidence intervals. 100% survival represents approximately 8 x 10^8 CFU mL^{-1}.

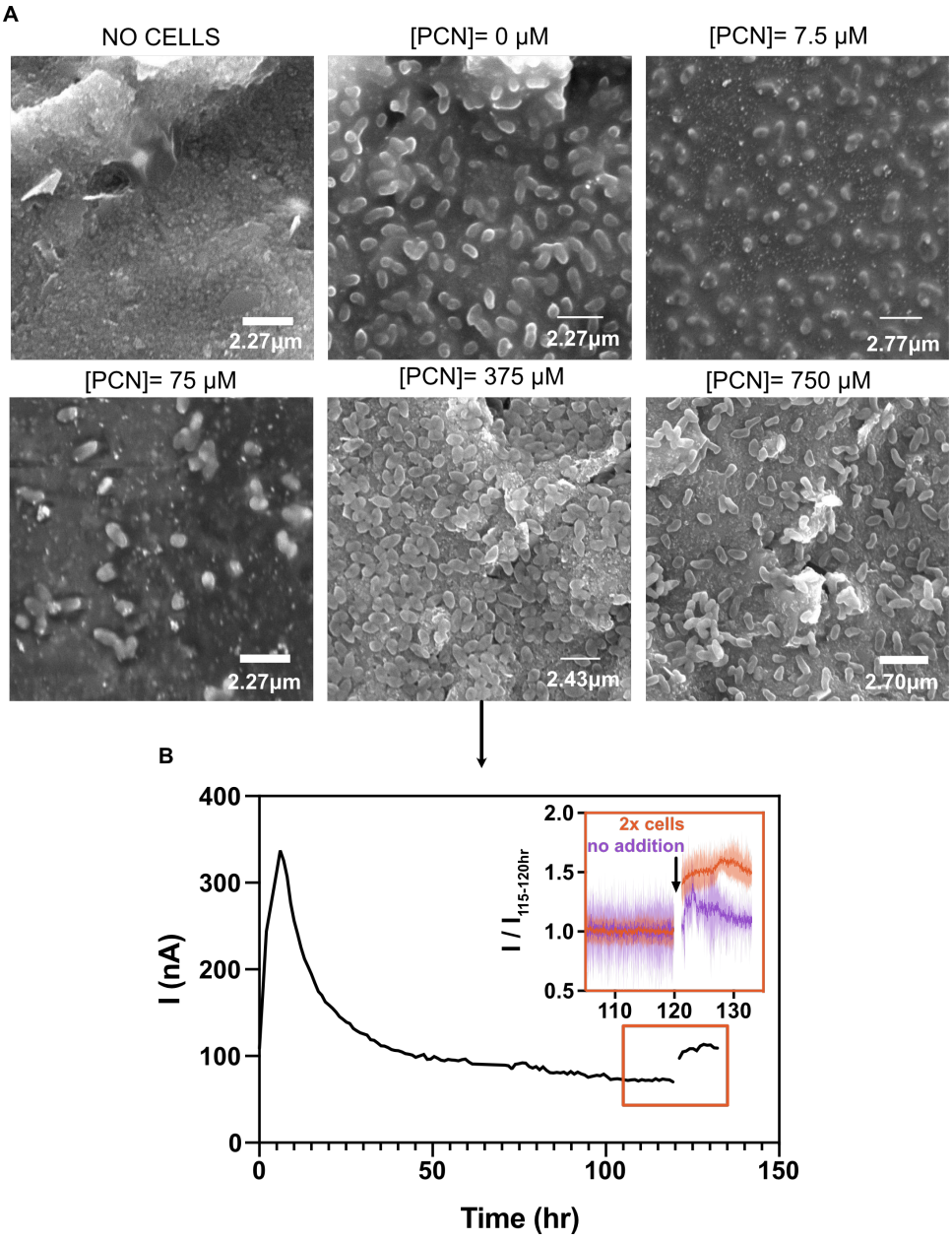

Figure S4. The electrode is not limiting current production at later time points of anaerobic survival at high concentrations of PCN. (A) SEM of the working electrode surface after 2 days of Δ*phz1/2* anaerobic incubation at various concentrations of PCN. (B) Average current produced by Δ*phz1/2* cells in 375 µM PCN. Inset – after five days, cells from other wells identically incubated were concentrated and added to the wells. A concomitant increase in the culture's current production was measured. Current is averaged across 4 biological replicates and shaded regions represents the 95% confidence interval.

Supplemental Information

Analysis of bacterial metabolic rate data from Hoehler et al. 2023, PNAS

Hoehler at al.(27) recently presented a compendium of metabolic rate measurements across kingdoms of life to estimate the metabolic rate of the total biosphere. Here, we aimed to use a subset of this dataset to contextualize our measurement of the extremely slow metabolic rate of PCN facilitated fermentation in *P. aeruginosa*, particularly the bacterial metabolic rate measurements that were classified as Endogenous metabolism ("Endogenous"), maintenance from continuous culture studies ("Maintenance"), and fast growth ("Fast Growth"). Below we discuss and justify our analysis of this dataset.

Justification of electrons sec^{-1} units

The power units reported in the Hoehler et al. data table are Watts. However, the original primary measurements are almost all in units of **[amount O_2] [unit time]$^{-1}$ [unit biomass]$^{-1}$**. To convert to Watts, the assumption used is a conversion factor of 20 J (mL O_2)$^{-1}$, which was also used previously by the prior metabolic rate meta-studies they cite (67,68). This value is well-established in studies of human and animals as the energy transformation for oxygen. The value is derived from the joules released per volume oxygen consumed by combusting carbohydrates in a bomb calorimeter, and while that is a reasonable source for quantifying the biochemical energy conserved plus heat produced in an animal due to respiration, we are interested instead solely in the ATP generated in a bacterium per amount O_2 consumed. Cells cannot conserve all the energy released by a combustion (what a

calorimeter measures) into useful biochemical energy (i.e. ATP); if they did, overall $\Delta G=0$ and there would be no metabolic driving force.

This is exemplified by the following, where a typical value of 32 ATP generated glucose^{-1} conserves less than half of the total energy of glucose combustion (69):

$C_6H_{12}O_6 + 6\ O_2 \rightarrow 6\ CO_2 + 6\ H_2O$ $\Delta G^{\circ\prime} = -2866$ kJ/mol
$32 \times (ADP + P_i \rightarrow ATP$ $\Delta G^{\circ\prime} = 33.5$ kJ/mol)
Overall $\Delta G^{\circ\prime} = -1794$ kJ/mol (lost as heat)

We therefore sought an alternative unit of metabolic rate that would hold higher fidelity and intuition to the underlying bioenergetics of ATP production in bacteria. *We present below that for the glucose metabolisms and aerobic respiration rates that compose the majority of this dataset, units of electrons have a surprising approximate equivalency to units of ATP.*

We begin with glucose catabolized via aerobic respiration, the metabolism that predominates the measurements within the Hoehler et al. dataset. In *Pseudomonas aeruginosa*, this reaction at the substrate level has the equation:

$C_6H_{12}O_6 + 3\ ADP + 6\ O_2 + 3\ P_i$
$\rightarrow 6\ CO_2 + 3\ ATP + 6\ H_2O$

Which includes 1 net ATP from glycolysis and 2 from the TCA cycle. In this process the metabolism also reduces and oxidizes 10 $NAD(P)^+$ molecules and 2 ubiquinone (UQ) molecules. To convert the NAD(P)H and UQH_2 intermediates into ATP units, we assume a maximum energy conservation efficiency of the aerobic electron transport chain(44,70) (ETC):

10 $H^{+}_{\rightarrow out}$/NADH ($4H^{+}/2e^{-}$ from Nuo/NDH-1 NADH dehydrogenase, $2H^{+}/2e^{-}$ from bc_1 complex, $4H^{+}/2e^{-}$ from cbb_3 cytochrome oxidase)

6 $H^{+}_{\rightarrow out}/UQH_2$ ($2H^{+}/2e^{-}$ from bc_1 complex, $4H^{+}/2e^{-}$ from cbb_3 cytochrome oxidase)

4 $H^{+}_{\rightarrow in}$/ATP (from ATP synthase)

This results in ATP ratios of:

2.5 ATP / NAD(P)H

1.5 ATP / UQH_2

We can now convert our overall reaction to units of ATP:

3 ATP from SLP

+

10 NAD(P)H == 25 ATP from Oxphos

+

2 UQH_2 == 3 ATP from OxPhos

=

31 ATP $glucose^{-1}$.

If glucose is completely oxidized, 24 electrons are ultimately transferred from the glucose molecule to oxygen.

$$\frac{31 \text{ ATP glucose}^{-1}}{24 \text{ electrons glucose}^{-1}} = \mathbf{1.3}\,\frac{\mathbf{ATP}}{\mathbf{electron}}$$

Note that in deriving this value, the maximum ETC energy conservation efficiency and complete oxidation of glucose was assumed. The real *in vivo* value is therefore likely less than this estimate.

As another example, in *E. coli*, the overall reaction is the same but there is no net ATP produced via glycolysis and the ETC energy conservation efficiency is different. In *E. coli*:

8 $H^+_{\rightarrow out}$/NADH ($4H^+/2e^-$ from Nuo/NDH-1 NADH dehydrogenase, $4H^+/2e^-$ from *bo* oxidase)

4 $H^+_{\rightarrow out}/UQH_2$ (from *bo* oxidase)

4 $H^+_{\rightarrow in}$/ATP (from ATP synthase)

This results in ATP ratios of:

2 ATP / NAD(P)H

1 ATP / UQH_2

We can now convert our overall reaction to units of ATP.

2 ATP from SLP

+

10 NAD(P)H == 20 ATP from Oxphos

+

2 UQH_2 == 2 ATP from OxPhos

=

24 ATP $glucose^{-1}$.

and therefore 1.0 ATP $electron^{-1}$ in *E. coli*.

Now we turn to compare this to the PCN facilitated fermentation metabolism (Figure 1B). This metabolism has an upstream glycolytic arm with the equation:

$C_6H_{12}O_6 + 2\ NAD(P)^+ + ADP + P_i$
$\rightarrow 2\ C_3H_3O_3^- + 2\ NAD(P)H + ATP + 4\ H^+$

This reaction is presumed to be redox-balanced by a succinate-producing pathway. Even though the known redox intermediates include a $FADH_2$ electron donor, we assume it is reducing-equivalent interchangeable because NADH has a lower standard midpoint potential than $FADH_2$. This balancing reaction has the equation:

$C_3H_3O_3^- + HCO_3^- + ATP + NADH + FADH_2 + H^+$
$\rightarrow C_4H_4O_4^{-2} + NAD^+ + FAD + ADP + P_i + 2\ H_2O$

These two pathways so far produce no net ATP and no net reducing equivalents while producing one pyruvate to be oxidized by the acetate-producing pathway, which has the equation:

$C_3H_3O_3^- + NAD^+ + ADP + P_i + 2\ H_2O$
$\rightarrow C_2H_3O_2^- + NADH + ATP + HCO_3^- + 2\ H^+$

Lastly, the reducing equivalent produced by this acetate-producing pathway is oxidized by PCN:

$NADH + PCN + H^+$
$\rightarrow NAD^+ + PCNH_2$

Adding up all the reactions above (again, assuming reducing equivalent interchangeability), we have a net reaction of:

$C_6H_{12}O_6 + ADP + P_i + PCN$
$\rightarrow C_4H_4O_4^{-2} + C_2H_3O_2^- + ATP + PCNH_2 + 3\ H^+$

During this reaction, 2 electrons are ultimately transferred from the glucose molecule to PCN. Therefore:

$$\frac{1\ \text{ATP glucose}^{-1}}{2\ \text{electrons glucose}^{-1}} = \mathbf{0.5}\,\frac{\mathbf{ATP}}{\mathbf{electron}}$$

While we do not observe measurable cell growth during this facilitated fermentation in our survival assay (Figure 3D, F), anabolic pathways may still be active to replace damaged molecules during maintenance. This value is likely therefore an overestimate that approaches the real value.

We conclude that across bioenergetically disparate metabolisms relevant to this study, metabolic rates in units of electrons have an approximate equivalency to units of ATP. In this dataset, this conclusion carries an ATP error discrepancy between PCN facilitated fermentation and oxygen respiration measurements of about 2-3x.

While reporting metabolic rates in units of ATP sec^{-1} $cell^{-1}$ would lower the metabolic rate measured for the PCN facilitated fermentation and raise the metabolic rates for most of the measurements in the Hoehler et al. dataset, we choose to instead report the metabolic rate in units of electrons because it is the most transparent value that carries the least assumptions across all the measurements.

Justification of $cell^{-1}$ units

The goal of our analysis was to use the already-curated list of bacterial metabolic rate publications from the Hoehler et al. dataset and, using the primary publication's reported values and units, convert to units of **electrons sec^{-1} $cell^{-1}$** and **electrons sec^{-1} (g cell dry weight)$^{-1}$**. Normalizing by gCDW is sensical: metabolic rate is known to scale with the total biomass (i.e. enzymes) carrying it out. This value has the further benefit of usually being directly measured in the studies. However, implicit in this normalization is the assumption that the total abundance of enzymes is rate limiting, which may not be the case for a starved or slow-growing cell; one can reasonably imagine a significant subset of total enzyme present regulated to be inactive, aggregated, or operating below their V_{max} because of substrate limitations that may vary study to study. Since we cannot confidently and sufficiently know the physiological state of the cells in all measurements reported, the more intuitively interpretable **electrons sec^{-1} $cell^{-1}$** is preferred in this analysis and reported as such in the main text.

However, use of $cell^{-1}$ units becomes weaker when considering bacterial cells of an unusually large size (e.g. *Thiomargarita namibiensis*) where a sizable fraction of their overall metabolic

capability would need to be inactive for values normalized by gCDW to approach those normalized per cell. We therefore chose to omit these few datapoints of very large species in the Hoehler et al. dataset (gCDW $cell^{-1} > 10^{-11}$ g, n=4) as outliers from our analysis.

We also note that variation in a bacterial species' cell size across conditions is typically less than an order of magnitude (7). Cell dry weight values, if not reported in the original publication, were estimated from other sources that measured those cells in similar conditions. Otherwise, cell sizes from a reference source such as Bergey's Manual were used. Given most measurements of bacterial size are usually taken while the cell is in a growth state (i.e. the state associated with its largest sizes) these values likely lean toward being overestimates relative to non-growth conditions, the state relevant to our analysis. This would therefore lead to underestimations of the true **electrons sec^{-1} $cell^{-1}$**. Given our claim is that phenazine metabolism is extremely slow, we note that having the comparisons lean as underestimates has the benefit of minimizing the likelihood of errors compromising our conclusion.

Conversion factors

The temperature and mass conversion factors remained the same between the Hoehler et al. analysis and our analysis.

Temperature Conversion

The data were normalized to a standard 25˚C using a Q_{10} conversion:

$$W(25°\text{C}) = W(T) * Q_{10}^{(25^{\circ}\text{C-T})/10^{\circ}\text{C}}$$

Where W is the metabolic rate, Q_{10} is the fold-change in metabolic rate for a 10°C temperature increase, and T is the temperature of measurement. We use a Q_{10} value of 2.0 for the bacterial measurements here.

Mass Conversion

To convert from protein weight to cell dry weight a protein-to-dry weight ratio of 0.5 was used.

To convert cell nitrogen weight to cell dry weight a nitrogen-to-dry weight ratio of 0.1 was used.

To convert from wet mass to dry mass, a dry-wet ratio of 0.3, or 70% water content, was used.

To convert carbon in biomass to cell dry weight, a carbon-to-dry weight ratio of 0.5 was used.

Conversion to units of electrons

To convert mL O_2 to electrons, the ideal gas law was used to assume 1 mol O_2 = 22.4 L O_2. Therefore, 4.46×10^{-5} mol O_2 (mL O_2)$^{-1}$.

Multiplying by avogadro's number, we get 2.69×10^{19} molecules O_2 (mL O_2)$^{-1}$.

Multiplying by 4 electrons per oxygen molecule reduced to water, we get 1.08×10^{20} electrons $(mL\ O_2)^{-1}$.

For measurements of C consumption, 4 electrons per C atom oxidized was assumed.

For measurements of S consumption, 8 electrons per S atom oxidized was assumed.

Notes on Collation

During the analysis, some duplicate values were found in the dataset and removed as erroneous.

In the case of multiple measurements reported in a single publication for a single species (e.g., different strains), the lowest reported value was collated.

In the case where both carbon consumption rate and oxygen consumption rate are reported in maintenance energies from Tijhuis (1993), oxygen consumption was preferentially used when available. This matches the majority of endogenous metabolism measurements and incorporates the possibility of endogenous electron donor contributions to the metabolism.

In the case where metabolic rates were found to be derived from a model instead of directly measured, they were excluded.

One metabolic rate was added to the Hoehler et al. collection: the metabolic rate of *Pseudomonas aeruginosa* during fast aerobic growth in continuous culture, which was 1.5 x 10^6 electrons sec^{-1} $cell^{-1}$ at 25˚C (28).

ΔG˚' of PCN Facilitated Fermentation

Here we estimate the ΔG˚' for PCN facilitated fermentation. As described above and shown in Figure 1E, PCN is only (or otherwise predominantly) involved in redox-balancing the acetate-producing portion of the fermentation. Therefore, to consider how much energy can be conserved from PCN reduction, only the oxidation of pyruvate to acetyl-CoA is considered (22,71):

pyruvate + CoA → acetyl-CoA + CO_2 + H^+ + 2 e^-	E˚' = -480 mV
PCN_{ox} + 2 H^+ + 2 e^- → PCN_{red}	E˚' = -140 mV
pyruvate + CoA + PCN_{ox} + H^+ → acetyl-CoA + PCN_{red} + CO_2	ΔE˚' = +340 mV

We then use the equation:

$\Delta G^{\circ\prime} = -\Delta E^{\circ\prime} n_e F$ where n_e is the number of electrons transferred and F is Faraday's constant.

$$\Delta G^{\circ\prime} = -(0.340\ V) * 2 * 96{,}500\ C\ mol^{-1} = \mathbf{-65.6\ kJ\ mol^{-1}}$$

Using this ΔG˚', Avogadro's number, and n_e we derive the conversion value:

$$65.6\ \frac{kJ}{mol} * \frac{mol\ PCN}{6.02\ x\ 10^{23} molecules\ PCN} * \frac{molecule\ PCN}{2\ e^-} = 5.45\ x\ 10^{-20}\ J\ (e^-)^{-1}$$

This conversion value and our gCDW cell^{-1} measurement (2.0 x 10^{-13}) can then be used to convert our cell-specific metabolic rate to units of W (g C)$^{-1}$:

$$1.6\ x\ 10^3 \frac{e^-}{\sec * cell} * 5.45\ x\ 10^{-20} \frac{J}{e^-} * \frac{cell}{2.0\ x\ 10^{-13} gCDW} * \frac{gCDW}{0.5\ g\ C}$$

$$= \mathbf{8.7\ x\ 10^{-4}\ W\ (g\ C)^{-1}}$$

References

1. Bergkessel M, Basta DW, Newman DK. The physiology of growth arrest: uniting molecular and environmental microbiology. Nat Rev Microbiol. 2016 Aug 11;14(9):549–62.

2. Morita RY. Bioavailability of energy and its relationship to growth and starvation in nature. Can J Microbiol. 1988;34:436–41.

3. LaRowe DE, Amend JP. Power limits for microbial life. Front Microbiol. 2015 Jul 15;6:718.

4. Tijhuis L, Van Loosdrecht MC, Heijnen JJ. A thermodynamically based correlation for maintenance gibbs energy requirements in aerobic and anaerobic chemotrophic growth. Biotechnol Bioeng. 1993 Aug 5;42(4):509–19.

5. Hoehler TM, Jørgensen BB. Microbial life under extreme energy limitation. Nat Rev Microbiol. 2013 Feb;11(2):83–94.

6. Jin X, Zhang X, Ding X, Tian T, Tseng C-K, Luo X, et al. Sensitive bacterial Vm sensors revealed the excitability of bacterial Vm and its role in antibiotic tolerance. Proc Natl Acad Sci USA. 2023 Jan 17;120(3):e2208348120.

7. Lever MA, Rogers KL, Lloyd KG, Overmann J, Schink B, Thauer RK, et al. Life under extreme energy limitation: a synthesis of laboratory- and field-based investigations. FEMS Microbiol Rev. 2015 Sep;39(5):688–728.

8. Yin L, Ma H, Fones EM, Morris DR, Harwood CS. ATP is a major determinant of phototrophic bacterial longevity in growth arrest. MBio. 2023 Apr 25;14(2):e0360922.

9. Robador A, Amend JP, Finkel SE. Nanocalorimetry Reveals the Growth Dynamics of *Escherichia coli* Cells Undergoing Adaptive Evolution during Long-Term Stationary Phase. Appl Environ Microbiol. 2019 Aug 1;85(15).

10. Riedel TE, Berelson WM, Nealson KH, Finkel SE. Oxygen consumption rates of bacteria under nutrient-limited conditions. Appl Environ Microbiol. 2013 Aug;79(16):4921–31.

11. Glasser NR, Saunders SH, Newman DK. The colorful world of extracellular electron shuttles. Annu Rev Microbiol. 2017 Sep 8;71:731–51.

12. Schiessl KT, Hu F, Jo J, Nazia SZ, Wang B, Price-Whelan A, et al. Phenazine production promotes antibiotic tolerance and metabolic heterogeneity in *Pseudomonas aeruginosa* biofilms. Nat Commun. 2019 Feb 15;10(1):762.

13. VanDrisse CM, Lipsh-Sokolik R, Khersonsky O, Fleishman SJ, Newman DK. Computationally designed pyocyanin demethylase acts synergistically with tobramycin to kill recalcitrant *Pseudomonas aeruginosa* biofilms. Proc Natl Acad Sci USA. 2021 Mar 23;118(12).

14. Wang Y, Kern SE, Newman DK. Endogenous phenazine antibiotics promote anaerobic survival of *Pseudomonas aeruginosa* via extracellular electron transfer. J Bacteriol. 2010 Jan;192(1):365–9.

15. Eschbach M, Schreiber K, Trunk K, Buer J, Jahn D, Schobert M. Long-term anaerobic survival of the opportunistic pathogen *Pseudomonas aeruginosa* via pyruvate fermentation. J Bacteriol. 2004 Jul;186(14):4596–604.

16. Glasser NR, Kern SE, Newman DK. Phenazine redox cycling enhances anaerobic survival in *Pseudomonas aeruginosa* by facilitating generation of ATP and a proton-motive force. Mol Microbiol. 2014 Apr;92(2):399–412.

17. Hunt KA, Flynn JM, Naranjo B, Shikhare ID, Gralnick JA. Substrate-level phosphorylation is the primary source of energy conservation during anaerobic respiration of Shewanella oneidensis strain MR-1. J Bacteriol. 2010 Jul;192(13):3345–51.

18. Benz M, Schink B, Brune A. Humic acid reduction by propionibacterium freudenreichii and other fermenting bacteria. Appl Environ Microbiol. 1998 Nov;64(11):4507–12.

19. Flynn JM, Ross DE, Hunt KA, Bond DR, Gralnick JA. Enabling unbalanced fermentations by using engineered electrode-interfaced bacteria. MBio. 2010 Nov 2;1(5).

20. Tejedor-Sanz S, Stevens ET, Li S, Finnegan P, Nelson J, Knoesen A, et al. Extracellular electron transfer increases fermentation in lactic acid bacteria via a hybrid metabolism. eLife. 2022 Feb 11;11.

21. Miran W, Huang W, Long X, Imamura G, Okamoto A. Multivariate landscapes constructed by Bayesian estimation over five hundred microbial electrochemical time profiles. Patterns (N Y). 2022 Nov 11;3(11):100610.

22. Wang Y, Newman DK. Redox reactions of phenazine antibiotics with ferric (hydr)oxides and molecular oxygen. Environ Sci Technol. 2008 Apr 1;42(7):2380–6.

23. Jo J, Price-Whelan A, Cornell WC, Dietrich LEP. Interdependency of Respiratory Metabolism and Phenazine-Associated Physiology in *Pseudomonas aeruginosa* PA14. J Bacteriol. 2020 Jan 29;202(4).

24. Saunders SH, Tse ECM, Yates MD, Otero FJ, Trammell SA, Stemp EDA, et al. Extracellular DNA promotes efficient extracellular electron transfer by pyocyanin in *Pseudomonas aeruginosa* biofilms. Cell. 2020 Aug 20;182(4):919-932.e19.

25. Amy PS, Morita RY. Starvation-survival patterns of sixteen freshly isolated open-ocean bacteria. Appl Environ Microbiol. 1983 Mar;45(3):1109–15.

26. Bratbak G, Dundas I. Bacterial dry matter content and biomass estimations. Appl Environ Microbiol. 1984 Oct;48(4):755–7.

27. Hoehler TM, Mankel DJ, Girguis PR, McCollom TM, Kiang NY, Jørgensen BB. The metabolic rate of the biosphere and its components. Proc Natl Acad Sci USA. 2023 Jun 20;120(25):e2303764120.

28. Chen SN. Growth Kinetics of *Pseudomonas aeruginosa* [Internet] [Master thesis]. Montana State University; 2001 [cited 2024 Feb 16]. Available from: https://scholarworks.montana.edu/xmlui/handle/1/8162

29. Geckil H, Stark BC, Webster DA. Cell growth and oxygen uptake of *Escherichia coli* and *Pseudomonas aeruginosa* are differently effected by the genetically engineered *Vitreoscilla* hemoglobin gene. J Biotechnol. 2001 Jan 23;85(1):57–66.

30. Finkel SE, Kolter R. Evolution of microbial diversity during prolonged starvation. Proc Natl Acad Sci USA. 1999 Mar 30;96(7):4023–7.

31. Yakhnina AA, McManus HR, Bernhardt TG. The cell wall amidase AmiB is essential for *Pseudomonas aeruginosa* cell division, drug resistance and viability. Mol Microbiol. 2015 Sep;97(5):957–73.

32. Navarro PP, Vettiger A, Ananda VY, Llopis PM, Allolio C, Bernhardt TG, et al. Cell wall synthesis and remodelling dynamics determine division site architecture and cell shape in *Escherichia coli.* Nat Microbiol. 2022 Oct;7(10):1621–34.

33. Arai H. Regulation and Function of Versatile Aerobic and Anaerobic Respiratory Metabolism in *Pseudomonas aeruginosa*. Front Microbiol. 2011 May 5;2:103.

34. Pu Y, Li Y, Jin X, Tian T, Ma Q, Zhao Z, et al. ATP-Dependent Dynamic Protein Aggregation Regulates Bacterial Dormancy Depth Critical for Antibiotic Tolerance. Mol Cell. 2019 Jan 3;73(1):143-156.e4.

35. Ciemniecki JA, Newman DK. NADH dehydrogenases are the predominant phenazine reductases in the electron transport chain of *Pseudomonas aeruginosa.* Mol Microbiol. 2023 May;119(5):560–73.

36. Imlay JA. The molecular mechanisms and physiological consequences of oxidative stress: lessons from a model bacterium. Nat Rev Microbiol. 2013 Jul;11(7):443–54.

37. Glasser NR, Wang BX, Hoy JA, Newman DK. The Pyruvate and α-Ketoglutarate Dehydrogenase Complexes of *Pseudomonas aeruginosa* Catalyze Pyocyanin and Phenazine-1-carboxylic Acid Reduction via the Subunit Dihydrolipoamide Dehydrogenase. J Biol Chem. 2017 Mar 31;292(13):5593–607.

38. Pirt SJ. The maintenance energy of bacteria in growing cultures. Proc R Soc Lond B Biol Sci. 1965 Dec 10;163(991):224–31.

39. Kempes CP, van Bodegom PM, Wolpert D, Libby E, Amend J, Hoehler T. Drivers of bacterial maintenance and minimal energy requirements. Front Microbiol. 2017 Jan 31;8:31.

40. Hoehler TM, Amend JP, Jørgensen BB, Orphan VJ, Lever MA. Editorial: Studies on life at the energetic edge – from laboratory experiments to field-based investigations, volume II. Front Microbiol. 2024 Jan 4;14.

41. Røy H, Kallmeyer J, Adhikari RR, Pockalny R, Jørgensen BB, D'Hondt S. Aerobic microbial respiration in 86-million-year-old deep-sea red clay. Science. 2012 May 18;336(6083):922–5.

42. Jaussi M, Jørgensen BB, Kjeldsen KU, Lomstein BA, Pearce C, Seidenkantz M-S, et al. Cell-specific rates of sulfate reduction and fermentation in the sub-seafloor biosphere. Front Microbiol. 2023 Jul 24;14:1198664.

43. Kanaan G, Hoehler TM, Iwahana G, Deming JW. Modeled energetics of bacterial communities in ancient subzero brines. Front Microbiol. 2023 Jul 26;14:1206641.

44. Kaila VRI, Wikström M. Architecture of bacterial respiratory chains. Nat Rev Microbiol. 2021 May;19(5):319–30.

45. Raba DA, Rosas-Lemus M, Menzer WM, Li C, Fang X, Liang P, et al. Characterization of the *Pseudomonas aeruginosa* NQR complex, a bacterial proton pump with roles in autopoisoning resistance. J Biol Chem. 2018 Oct 5;293(40):15664–77.

46. Schink B. Energetics of syntrophic cooperation in methanogenic degradation. Microbiol Mol Biol Rev. 1997 Jun;61(2):262–80.

47. Jackson BE, McInerney MJ. Anaerobic microbial metabolism can proceed close to thermodynamic limits. Nature. 2002 Jan 24;415(6870):454–6.

48. Price PB, Sowers T. Temperature dependence of metabolic rates for microbial growth, maintenance, and survival. Proc Natl Acad Sci USA. 2004 Mar 30;101(13):4631–6.

49. Stouthamer AH. A theoretical study on the amount of ATP required for synthesis of microbial cell material. Antonie Van Leeuwenhoek. 1973 Dec;39:545–65.

50. Mccollom TM, Amend JP. A thermodynamic assessment of energy requirements for biomass synthesis by chemolithoautotrophic micro-organisms in oxic and anoxic environments. Geobiology. 2005 Apr;3(2):135–44.

51. van Bodegom P. Microbial maintenance: a critical review on its quantification. Microb Ecol. 2007 May;53(4):513–23.

52. Walker RM, Sanabria VC, Youk H. Microbial life in slow and stopped lanes. Trends Microbiol. 2023 Dec 19;

53. Koch AL. The Adaptive Responses of *Escherichia coli* to a Feast and Famine Existence. Adv Microb Physiol. 1971;6:147–217.

54. Rothman DH. Slow closure of Earth's carbon cycle. Proc Natl Acad Sci USA. 2024 Jan 23;121(4):e2310998121.

55. Caro TA, McFarlin J, Jech S, Fierer N, Kopf S. Hydrogen stable isotope probing of lipids demonstrates slow rates of microbial growth in soil. Proc Natl Acad Sci USA. 2023 Apr 18;120(16):e2211625120.

56. Coskun ÖK, Özen V, Wankel SD, Orsi WD. Quantifying population-specific growth in benthic bacterial communities under low oxygen using H218O. ISME J. 2019 Jun;13(6):1546–59.

57. Blazewicz SJ, Hungate BA, Koch BJ, Nuccio EE, Morrissey E, Brodie EL, et al. Taxon-specific microbial growth and mortality patterns reveal distinct temporal population responses to rewetting in a California grassland soil. ISME J. 2020 Jun;14(6):1520–32.

58. Kirchman DL. Growth rates of microbes in the oceans. Ann Rev Mar Sci. 2016;8:285–309.

59. Perry EK, Meirelles LA, Newman DK. From the soil to the clinic: the impact of microbial secondary metabolites on antibiotic tolerance and resistance. Nat Rev Microbiol. 2022 Mar;20(3):129–42.

60. Jones EM, Marken JP, Silver PA. Synthetic microbiology in sustainability applications. Nat Rev Microbiol. 2024 Jan 22;

61. Jaishankar J, Srivastava P. Molecular basis of stationary phase survival and applications. Front Microbiol. 2017 Oct 16;8:2000.

62. Shi Z, Crowell S, Luo Y, Moore B. Model structures amplify uncertainty in predicted soil carbon responses to climate change. Nat Commun. 2018 Jun 4;9(1):2171.

63. Dietrich LE, Price-Whelan A, Petersen A, Whiteley M, Newman DK. The phenazine pyocyanin is a terminal signalling factor in the quorum sensing network of *Pseudomonas aeruginosa*. Mol Microbiol. 2006 Sep;61(5):1308–21.

64. Choi K-H, Schweizer HP. mini-Tn7 insertion in bacteria with single *att*Tn7 sites: example *Pseudomonas aeruginosa*. Nat Protoc. 2006;1(1):153–61.

65. Shanks RMQ, Caiazza NC, Hinsa SM, Toutain CM, O'Toole GA. *Saccharomyces cerevisiae*-based molecular tool kit for manipulation of genes from gram-negative bacteria. Appl Environ Microbiol. 2006 Jul;72(7):5027–36.

66. Jeske M, Altenbuchner J. The *Escherichia coli* rhamnose promoter $rhaP_{BAD}$ is in *Pseudomonas putida* KT2440 independent of Crp–cAMP activation. Appl Microbiol Biotechnol. 2010 Feb;85(6):1923–33.

67. Makarieva AM, Gorshkov VG, Li B-L. Energetics of the smallest: Do bacteria breathe at the same rate as whales? Proc Biol Sci. 2005 Oct 22;272(1577):2219–24.

68. Makarieva AM, Gorshkov VG, Li B-L, Chown SL, Reich PB, Gavrilov VM. Mean mass-specific metabolic rates are strikingly similar across life's major domains: Evidence for life's metabolic optimum. Proc Natl Acad Sci USA. 2008 Nov 4;105(44):16994–9.

69. Harold FM. The Metabolic Web. The Vital Force: A Study of Bioenergetics. W.H. Freeman and Company; 1986.

70. Arai H, Kawakami T, Osamura T, Hirai T, Sakai Y, Ishii M. Enzymatic characterization and in vivo function of five terminal oxidases in *Pseudomonas aeruginosa*. J Bacteriol. 2014 Dec;196(24):4206–15.

71. Beber ME, Gollub MG, Mozaffari D, Shebek KM, Flamholz AI, Milo R, et al. eQuilibrator 3.0: a database solution for thermodynamic constant estimation. Nucleic Acids Res. 2022 Jan 7;50(D1):D603–9.

Chapter 6

CONCLUSIONS AND FUTURE DIRECTIONS

Throughout nature, microbes frequently subsist with limited energy for extended periods, yet the metabolic underpinnings of this survival are only vaguely understood. In the opportunistic pathogen *Pseudomonas aeruginosa*, anaerobic phenazine redox-cycling and the facilitated fermentation it supports are an experimentally tractable metabolism seemingly dedicated to powering survival without growth. This metabolism therefore represents a rare experimental foothold toward direct investigation of cell maintenance, a state that was before only accessible through extrapolation, modeling, and inference (1). While the major energy conserving step of the facilitated fermentation powering maintenance had been identified before this work began, there were many unanswered questions and hurdles that remained: for example, not knowing where in the cell phenazines were reduced and the extremely low throughput of survival experiments. The main scientific contribution of this thesis is the elucidation of the genes and enzymes involved as phenazine reductases in the electron transport chain (ETC) (Chapter 3), the characterization of phenazine interactions with the ETC and the bioenergetic consequences (Chapter 3 and 4), the development of a high-throughput assay to study phenazine redox-cycling and cell maintenance (Chapter 5), the confirmation that this metabolism does not power growth (Chapter 5), and the quantification and contextualization of this maintenance

metabolism's rate among the lowest across the biosphere (Chapter 5). The key specific biological findings include:

1) Identifying the main subcellular location of the two phenazines retained in the highest amount by *P. aeruginosa* biofilms (2): pyocyanin in the cytosol and phenazine-1-carboxamide at the inner membrane.
2) Identifying the main phenazine reductases of phenazine-1-carboxamide (PCN), the phenazine made and retained in the highest amount in biofilms (2), to be the NADH dehydrogenases Nuo and Nqr. Either are sufficient to power anaerobic survival via phenazine redox-cycling.
3) Showing that phenazines are oxidized by the quinone pool and constitute a redox-loop between the NADH and quinone pools, in agreement with parallel work conducted in the Newman lab in *Citrobacter* (3) and previous work in *E. coli* (4).
4) Showing that under aerobic conditions, all phenazines can short-circuit normal electron flow through the electron transport chain and lower the H^+/O ratio, or energy conservation efficiency, of respiration.
5) Quantifying the cell-specific metabolic rate associated with cell maintenance during anaerobic PCN facilitated fermentation to be 1.6 x 10^3 electrons sec^{-1} $cell^{-1}$, equivalent to 10 times lower than the average basal metabolic rate across the biosphere, 100 times lower than previous estimates of maintenance metabolic rate found in studies using chemostats, and 1,000 times lower than when *P. aeruginosa* is growing aerobically.
6) Showing that this rate is near the minimum necessary for survival and equates to an approximate cell-specific ATP consumption rate of 800 ATP sec^{-1} $cell^{-1}$, which

to my knowledge, is the first estimate of a maintenance energy requirement made from direct measurement of non-growing cells.

The clear future directions that stem from these findings can be found in each chapter's respective discussion section. In this chapter, I will discuss more speculative ideas stemming from a holistic overview of the thesis work. Each of the sections below introduce new terms to describe concepts I have not previously found in the literature, but which could serve as intellectual frameworks or hypotheses for future studies.

Metabolic frustration

One of the major questions posed in Chapter 2 was how phenazines can be efficiently coupled to NAD^+ production, and by extension substrate-level phosphorylation, during anaerobic redox-cycling. Phenazines' promiscuity with various metabolic flavoproteins is well-characterized and is a key aspect of their toxicity in multiple species (5). How does *P. aeruginosa* deal with them then? The first layer of protection comes from an extensive efflux pump system that keeps intracellular concentrations of phenazines low and presumably manageable (6). This also has the added benefit of keeping phenazine ROS production predominantly extracellular, where it has a much lower impact on cell health (7). But a second layer of protection may come from enzymatic specificity in the form of NADH dehydrogenases for PCN. By keeping the sub-cellular location of reduction and reductases limited, flux through the metabolic web is controlled in a way that keeps it net ATP-productive. Otherwise, the cell will waste the relatively slow phenazine reduction reaction events (Chapter 5) and lose ATP production efficiency. If this happens and ATP

levels drop, the cell would be predicted to increase its global metabolic rate through both energy-coupled *and* non-energy-coupled pathways in an inefficient effort to maintain ATP levels (8). I refer to this state of increased metabolic rate in response to energetically wasted reductive power as *metabolic frustration*. (For example, the short-circuiting hypothesis presented in Chapter 4 could be thought of as one type of metabolic frustration if it were shown that phenazines increase the total metabolic rate under aerobic conditions). I hypothesize avoiding metabolic frustration is a major metabolic priority for cells surviving in an energy-limited state. Indeed, this idea is just a reciprocal reframing of the axiom that metabolism as a system is made possible by the miracle of enzyme specificity (9). Without that, life becomes frustrating.

It was therefore very satisfying to identify the NADH dehydrogenases as the predominant phenazine reductases in the ETC of *P. aeruginosa* (Chapter 3), a direct coupling of phenazine reduction to the NADH pool and substrate-level phosphorylation. This satisfaction was expanded when finding mutants in the NADH dehydrogenases had significant survival deficits under PCN facilitated fermentation (Chapter 5). However, the NADH dehydrogenase mutant was surprisingly *not* deficient in current generation during latter time points in the assay and its survival was also compensated by high concentrations of PCN (Chapter 5). Given the mutant's survival was lower than the Δ*phz1/2* strain but current production was about the same, the cell-specific metabolic rate was higher, consistent with metabolic frustration. After removing the major site of phenazine reduction that facilitates productive metabolic flux (the NADH dehydrogenases), how the cell reorganizes metabolic fluxes may resemble how other cytoplasmic-localized phenazines like pyocyanin (Chapter 3) are processed.

I therefore propose that investigating the mechanism of the NADH dehydrogenase mutant's survival during PCN redox cycling and comparing it to the wild-type offers a unique foothold to grow our understanding of how phenazines alter electron flux through the metabolic web. This will likely require metabolomics studies to map fluxes. But another approach could be to additionally knock out previously-identified cytoplasmic phenazine reductase subunits of the TCA cycle enzymes pyruvate and alpha-ketogluterate dehydrogenase, assuming they are not essential (10). Finally, a Tn-seq survival assay, where a library of mutants is assayed together as a population and each gene knockout's survival tallied via sequencing, could be performed in the NADH dehydrogenase knockout background to identify suppressors and/or alternative metabolic nodes important during facilitated fermentation. Identified mutants, either of the TCA cycle phenazine reductases or Tn-seq hits, could then be further investigated for their role in managing intracellular electron flux during cell maintenance and explore under which conditions their absence/presence results in measurable metabolic frustration. Overall, investments in the development of this concept will, I believe, provide an intellectual framework through which we will better understand the metabolic redundancies and systems-level mechanisms that underly astounding feats of microbial survival and resiliency.

Phenazines as a bioenergetic buffer

P. aeruginosa is, from a metabolic standpoint, particularly susceptible to low-oxygen conditions. It cannot grow fermentatively, and the only other anaerobic respiration it can perform is denitrification (11). Yet it survives exceptionally well in energy-depleted environments, particularly those associated with humans (12). One of the ways in which

stress can be induced on any microbe is by depletion of terminal oxidant; some places where *P. aeruginosa* might experience this include in the core of ubiquitous biofilms (13), in the sputum of an infected patient (14), and in water-logged soils (15). The production of phenazines therefore represent a bioenergetic lifeline, whereby slow metabolic activity can be maintained via extracellular electron shuttling to distal oxidants, preventing the onset of death.

However, phenazines also lower the bioenergetic efficiency of the cells' metabolism under aerobic conditions (Chapter 4). In Chapter 4's discussion, I speculated how this could be adaptive; a low-energy state protects cells from the risks of fast growth, mainly intracellular ROS production and antagonistic antibiotics. Phenazines are furthermore only made under quorum-sensing conditions (16), when mostly all the local electron donors have been consumed and a rapid growth state is impossible. Under such conditions, the presence of phenazines will lower the bioenergetic state, but they will not kill the cells until a few days to weeks in starvation has elapsed, depending on the phenazine being tested (17). Therefore, the production of phenazines rapidly drops the cells' bioenergetic state without killing them and begins a slow "countdown" to death, assuming oxygenation of the environment remains constant and electron donors absent. If even scarce amounts of electron donors return, survival is prolonged (17). If oxygenation drop to zero, phenazines' presence will keep the bioenergetic state higher than it would be in their absence (Chapter 5).

Altogether then, phenazines are predicted to stabilize a low-energy state in non- or slow-growing cells against changing electron donor and acceptor conditions. I call this hypothesized characteristic a *bioenergetic buffer* or more specifically, a *low-power*

bioenergetic buffer. One straightforward way to test this hypothesis is to investigate the effects phenazines have on the PMF, the physiological integrator of a cell's energy state (18). Investigation into this topic has already occurred and evidence pointing toward the bioenergetic buffer conclusion is already being advanced in the Newman lab (see Horak, Ciemniecki, and Newman under published content and contributions). One further experiment that has not been done would be to capture timelapse images of starved cells labeled with fluorescent indicators of the PMF and switch them between aerobic and anaerobic conditions with and without phenazines present: the amplitude of the imposed PMF oscillations in the presence of phenazine are predicted to be smaller. Another test of this would be to take the labelled cells and compare aerobic vs. anaerobic and phenazine vs. no phenazine conditions. If measured on a flow cytometer, the distribution of PMF levels from cells in anaerobic+phenazine and aerobic+phenazine conditions would be predicted to heavily overlap, with the PMF of cells in the aerobic no phenazine condition being significantly higher and anaerobic no phenazines significantly lower. One preliminary experiment showed this to be the case (data not shown) but more are needed to confirm.

Coupled with analogous experiments in other RAM-producing organisms like *Burkholderia glumae* and *Dyella japonica*, such work would help to inform the overarching question of why bacteria make RAMs; while there are likely multiple reasons that include the molecules' toxic effects on competitors (5), functioning as a bioenergetic buffer under non-growth conditions could be another. Such a finding could also be leveraged in combination with fitness or evolution experiments to answer important questions about the impact survival plays, as opposed to fast growth, in microbial fitness.

The maintenance economy

Having achieved the development of a high-throughput assay of cells in a pure maintenance state (Chapter 5), the door to investigations of maintenance physiology is opened. Furthermore, this assay is in a model organism wherein powerful genetic and biochemical tools are available. As such, there are numerous questions one can imagine pursuing. In this thesis, I have explored energy conservation (i.e. ATP/PMF generation), but another aspect of how the cell manages energy is its use – together, these two aspects compose an economy, built up by strands of production and expenditure that mesh together to support cell viability. While questions remain about the mechanisms of energy conservation explored in this thesis, the next major question to ask is: what do cells spend their limited energy on to maintain viability? What is the structure of the maintenance economy?

One approach toward conceptualizing this economy is to first break it down into a sequence of events. Cells must enter a maintenance state, carry out maintenance, and then exit a maintenance state for their survival to be successful and measurable. The functions energy is spent on will likely shift according to the stage. The work I presented on survival (Chapter 5) is specifically about carrying out maintenance, as viability is not initially lost during the assay (i.e. entrance) and anaerobic cells deprived of PCN and an oxidizing potential lyse / accumulate propidium iodide stain prior to re-entry into aerobic conditions (i.e. during the maintenance state). But just as important are the other stages: prior work in the Newman lab has confirmed the role of the sigma factor *rpoS* in regulating a programmed entry into a survival state and discovered a role for the protease *ftsH* in this process (19), presumably to help turn over the proteome without relying on new amino acid

synthesis. Still lacking from this model is an understanding of how other energy-intensive processes shift:

- Does the cell remodel or replace its membranes / cell walls? In the HADA experiments I conducted to show a lack of cell growth during PCN facilitated fermentation (Chapter 5), there was no topological change in HADA distribution over the cell wall, but the overall fluorescence of cells did decrease toward a lower asymptote over the course of the experiment. This suggests that during the initial stages of survival, cell wall components are globally replaced without growth. This finding merits follow-up, as cell wall structure is known to have a strong effect on the survival of various stresses (20).
- Does the cell store carbon in polymers like poly-hydroxyalkoanates (21) or in its own lipids to use as electron donor reserves? Previous work has identified beta-oxidation complexes involved in lipid catabolism are important to anaerobic survival in the absence of phenazines (22), and clues in organic acid HPLC traces from long-term anaerobic survival cultures hint toward this possibility (23). Clarity on which carbon source the cell uses during anaerobic survival is of basic interest, and knocking out the required genes could be a useful tool for controlling carbon flux during experiments.
- How are transcription and translation regulated to ensure thrift? Previous work in the Newman lab has elucidated the RNA-polymerase binding protein SutA which appears to be involved in management of transcription during long-term survival (24,25). Given transcription / translation are the most energetically-expensive tasks

the cell can undertake during growth (26,27), an understanding of how they are regulated during survival to ensure thrift is an important avenue of research and potentially of utmost importance to the maintenance economy.

- What is the role of Universal Stress Proteins (USPs)? These genes are consistently found to be important for survival in various species across the kingdom of life (28), and were found to be necessary for anaerobic survival in *P. aeruginosa* (22,29). Their mechanistic function has remained enigmatic, but their importance is undeniable given the stark phenotypes displayed by knockouts and their conservation across kingdoms. Projects investigating their biochemistry and effects on phenazine-dependent anaerobic survival would be highly challenging because of a lack of background information, but accordingly of great general interest.

The maintenance economy is almost certainly complex, riddled with redundancies that protect cells against any single, errant mutations that would destroy their legacy upon the inevitable nutrient stress. Tackling this new physiology therefore requires direct, reductionist approaches; while a survival screen like Tn-seq is undoubtedly useful, it will also miss many important things because it can only screen single knockouts. The importance of the NADH dehydrogenases in PCN facilitated fermentation stands as an example of this; that discovery was fully dependent on a deductive approach and would have never come up in a single-knockout Tn-seq screen because of the redundancy of Nuo and Nqr. Furthermore, even after both NADH dehydrogenases are removed, other reductases step up in their stead to support lower levels of survival (Chapter 5). Clearly,

the cell is not willing to give up so easily. If we wish to gain enough understanding to exert control over the organism—whether that be fully eliminating them in a clinical setting (30) or engineering them for some useful purpose in the field or in industry (31,32)—we must understand as many of the connective strands of the maintenance economy as possible, redundancies and all.

Finally, I will end on a look to the future and acknowledge that as powerful as the assay for anaerobic survival via phenazine-cycling is, it cannot be the only avenue through which maintenance is investigated. Microbes are known for their metabolic diversity, and other species will of course have evolved other ways to survive. Yet all life is unified by key aspects of biochemistry. All cells use ATP, NADH, and a PMF for energy transduction; all cells use DNA for their genetic material and ribosomes for protein synthesis. These molecules compose living matter, regardless of the organism, and are the avenues through which energy and information flow. If we want to understand similarly universal macromolecules and principles underlying the maintenance economy, comparative physiology is required. It may be that there are no truly universal aspects, that every cell survives in its own way. But if commonalities do exist, they are central to a full understanding of life's lower limits, the edges that separate it from non-living matter. Therefore, comparative studies of different species' maintenance economy are yet another way biologists can delve into the perennial question of what it means to be alive.

References

1. Hoehler TM, Jørgensen BB. Microbial life under extreme energy limitation. Nat Rev Microbiol. 2013 Feb;11(2):83–94.

2. Saunders SH, Tse ECM, Yates MD, Otero FJ, Trammell SA, Stemp EDA, et al. Extracellular DNA promotes efficient extracellular electron transfer by pyocyanin in *Pseudomonas aeruginosa* biofilms. Cell. 2020 Aug 20;182(4):919-932.e19.

3. Tsypin LM. The Discovery and Biological Mechanisms of a Widespread Phenazine's Oxidation [Doctoral dissertation]. California Institute of Technology; 2023.

4. Harrington TD, Tran VN, Mohamed A, Renslow R, Biria S, Orfe L, et al. The mechanism of neutral red-mediated microbial electrosynthesis in *Escherichia coli*: menaquinone reduction. Bioresour Technol. 2015 Sep;192:689–95.

5. Hassan HM, Fridovich I. Mechanism of the antibiotic action of pyocyanine. J Bacteriol. 1980;141.

6. Meirelles LA, Perry EK, Bergkessel M, Newman DK. Bacterial defenses against a natural antibiotic promote collateral resilience to clinical antibiotics. PLoS Biol. 2021 Mar 10;19(3):e3001093.

7. Imlay JA. Diagnosing oxidative stress in bacteria: not as easy as you might think. Curr Opin Microbiol. 2015 Apr;24:124–31.

8. Marchetti P, Fovez Q, Germain N, Khamari R, Kluza J. Mitochondrial spare respiratory capacity: Mechanisms, regulation, and significance in non-transformed and cancer cells. FASEB J. 2020 Oct;34(10):13106–24.

9. Harold FM. The Metabolic Web. The Vital Force: A Study of Bioenergetics. W.H. Freeman and Company; 1986.

10. Glasser NR, Wang BX, Hoy JA, Newman DK. The Pyruvate and α-Ketoglutarate Dehydrogenase Complexes of *Pseudomonas aeruginosa* Catalyze Pyocyanin and Phenazine-1-carboxylic Acid Reduction via the Subunit Dihydrolipoamide Dehydrogenase. J Biol Chem. 2017 Mar 31;292(13):5593–607.

11. Arai H. Regulation and Function of Versatile Aerobic and Anaerobic Respiratory Metabolism in *Pseudomonas aeruginosa*. Front Microbiol. 2011 May 5;2:103.

12. Crone S, Vives-Flórez M, Kvich L, Saunders AM, Malone M, Nicolaisen MH, et al. The environmental occurrence of *Pseudomonas aeruginosa*. APMIS. 2020 Mar;128(3):220–31.

13. Dietrich LEP, Okegbe C, Price-Whelan A, Sakhtah H, Hunter RC, Newman DK. Bacterial community morphogenesis is intimately linked to the intracellular redox state. J Bacteriol. 2013 Apr;195(7):1371–80.

14. Cowley ES, Kopf SH, LaRiviere A, Ziebis W, Newman DK. Pediatric cystic fibrosis sputum can be chemically dynamic, anoxic, and extremely reduced due to hydrogen sulfide formation. MBio. 2015 Jul 28;6(4):e00767.

15. Silver WL, Lugo AE, Keller M. Soil oxygen availability and biogeochemistry along rainfall and topographic gradients in upland wet tropical forest soils. Biogeochemistry. 1999 Mar;44(3):301–28.

16. Dietrich LE, Price-Whelan A, Petersen A, Whiteley M, Newman DK. The phenazine pyocyanin is a terminal signalling factor in the quorum sensing network of *Pseudomonas aeruginosa*. Mol Microbiol. 2006 Sep;61(5):1308–21.

17. Meirelles LA, Newman DK. Both toxic and beneficial effects of pyocyanin contribute to the lifecycle of *Pseudomonas aeruginosa*. Mol Microbiol. 2018 Dec;110(6):995–1010.

18. Choe M, Titov DV. Genetically encoded tool for manipulation of ΔΨm identifies the latter as the driver of integrative stress response induced by ATP Synthase dysfunction. BioRxiv. 2023 Dec 27;

19. Basta DW, Angeles-Albores D, Spero MA, Ciemniecki JA, Newman DK. Heat-shock proteases promote survival of *Pseudomonas aeruginosa* during growth arrest. Proc Natl Acad Sci USA. 2020 Feb 25;117(8):4358–67.

20. Mueller EA, Levin PA. Bacterial Cell Wall Quality Control during Environmental Stress. MBio. 2020 Oct 13;11(5).

21. Hoffmann N, Rehm BHA. Regulation of polyhydroxyalkanoate biosynthesis in *Pseudomonas putida* and *Pseudomonas aeruginosa*. FEMS Microbiol Lett. 2004 Aug 1;237(1):1–7.

22. Basta DW, Bergkessel M, Newman DK. Identification of fitness determinants during energy-limited growth arrest in *Pseudomonas aeruginosa*. MBio. 2017 Nov 28;8(6):e01170-17.

23. Glasser NR. Physiological and Biochemical Mechanisms of Phenazine-Mediated Survival in *Pseudomonas aeruginosa*. California Institute of Technology. 2017;

24. Babin BM, Bergkessel M, Sweredoski MJ, Moradian A, Hess S, Newman DK, et al. SutA is a bacterial transcription factor expressed during slow growth in *Pseudomonas aeruginosa*. Proc Natl Acad Sci USA. 2016 Feb 2;113(5):E597-605.

25. Bergkessel M, Babin BM, VanderVelde D, Sweredoski MJ, Moradian A, Eggleston-Rangel R, et al. The dormancy-specific regulator, SutA, is intrinsically disordered and modulates transcription initiation in Pseudomonas aeruginosa. Mol Microbiol. 2019 Sep;112(3):992–1009.

26. Stouthamer AH. A theoretical study on the amount of ATP required for synthesis of microbial cell material. Antonie Van Leeuwenhoek. 1973 Dec;39:545–65.

27. Belliveau NM, Chure G, Hueschen CL, Garcia HG, Kondev J, Fisher DS, et al. Fundamental limits on the rate of bacterial growth and their influence on proteomic composition. Cell Syst. 2021 Sep 22;12(9):924-944.e2.

28. Kvint K, Nachin L, Diez A, Nyström T. The bacterial universal stress protein: function and regulation. Curr Opin Microbiol. 2003 Apr;6(2):140–5.

29. Schreiber K, Boes N, Eschbach M, Jaensch L, Wehland J, Bjarnsholt T, et al. Anaerobic survival of *Pseudomonas aeruginosa* by pyruvate fermentation requires an Usp-type stress protein. J Bacteriol. 2006 Jan;188(2):659–68.

30. Balaban NQ, Helaine S, Lewis K, Ackermann M, Aldridge B, Andersson DI, et al. Definitions and guidelines for research on antibiotic persistence. Nat Rev Microbiol. 2019 Jul;17(7):441–8.

31. Jones EM, Marken JP, Silver PA. Synthetic microbiology in sustainability applications. Nat Rev Microbiol. 2024 Jan 22;

32. Jaishankar J, Srivastava P. Molecular basis of stationary phase survival and applications. Front Microbiol. 2017 Oct 16;8:2000.